CONTRACT No. N00014-67-A-0438-0010
PROJECT No. NR-064-457

PERMEABILITY OF GASES THROUGH FILLED AND UNFILLED RUBBER MEMBRANES

by

G. Y. Lei and F. R. Eirich

POLYTECHNIC INSTITUTE OF BROOKLYN

DEPARTMENT
of
AEROSPACE ENGINEERING
and
APPLIED MECHANICS
and
DEPARTMENT OF CHEMISTRY

OCTOBER 1970

PIBAL REPORT No. 70-44

Contract No. N00014-67-A-0438-0010
Project No. NR-064-457

PERMEABILITY OF GASES THROUGH FILLED AND UNFILLED RUBBER MEMBRANES

by

G. Y. Lei and F. R. Eirich

Polytechnic Institute of Brooklyn

Departments of

Aerospace Engineering and Applied Mechanics

and

Chemistry

OCTOBER 1970

Pibal Report No. 70-44

ABSTRACT

The purpose of this investigation was to study, by way of permeation experiments, structural differences between synthetic poly-cis 1,4-isoprene (SNR) and natural rubber (NR), as well as differences resulting from filling with carbon black. The study aimed further at testing Frisch's theory of isotope effects in activated diffusion and on the unit size of the free volume in rubbers.

The rubber samples consisted of thin crosslinked sheets of NR and SNR. The carbon content (N330 HAF black of about 300Å particles diameter) in the filled samples was 16% by volume.

The permeation rate of H_2 and D_2 through filled and unfilled NR and SNR were measured by the time-lag method as a function of temperature and pressure (40-85°C and 1-55 cm of Hg). The permeability coefficient, P, diffusion coefficient, D, and solubility, S, thus deduced were further used to evaluate the energies of activation for permeation and for diffusion, E_p and E_d, and the heat of solution, ΔH_s according to the Arrhenius equation.

The results show that H_2 has generally a higher permeability and diffusivity than D_2, and that the permeabilities or diffusivities are markedly reduced by the presence of the filler. On the other hand, the solubilities in the filled rubbers were found to be almost double

that of the unfilled samples.

The diffusivities and the activation energies for diffusion and permeation are largely independent of the gas pressure. The heats of solution, ΔH_s, for both gases in the unfilled samples are all positive, but in the filled samples, ΔH_s is positive for D_2, and negative for H_2. These signs of ΔH_s are consistent with their solubilities.

A qualitative analysis of the heat of solution permits one to estimate the heat of adsorption on NR to be approximately 800 cal/mole; the overall heat of solution further allows the estimation of 2 kcal/mole for the energy of hole formation in the rubber.

The solubilities (adsorption) of H_2 and D_2 were found to be low in both rubbers and on the carbon. The adsorption of H_2 on the rubber is about 3.2×10^{-6} g./g. of rubber, and 8×10^{-6} g./g. of carbon. The latter is probably completely wetted by rubber.

Based on the quantum mechanical treatment of diffusion suggested by H. L. Frisch, the unit free volume in the unfilled rubbers is calculated from the value of $\delta\Delta H_s$, i.e., the difference of ΔH_s for D_2 and H_2 in the same medium to be 51 and 64 Å^3 respectively for NR and SNR. However, Frisch's equation can not be applied to calculate the free volumes in the filled samples since ΔH_s was found to be positive for this case.

The jump length, λ, of H_2 in NR and in SNR are found, according to the absolute rate theory, to be almost the same (about 21 Å) in both rubbers, whereas, λ, for D_2 is about 26 A° in NR and 30 Å in SNR.

A semi-quantitative analysis of the diffusion mechanism in the filled samples shows that the data of P, D, and S for the filled samples

can be related to those of the unfilled samples accounting for the reduction of the cross section of the filler, the imposed tortuosity of the diffusion path, and the increase in the viscosity of the rubber due to the presence of the filler particles.

TABLE OF CONTENTS

TABLE OF CONTENTS (Cont'd)

TABLE OF CONTENTS (Cont'd)

LIST OF FIGURES

LIST OF FIGURES (Cont'd)

LIST OF TABLES

LIST OF TABLES (Cone'd)

I. INTRODUCTION

A. Introduction and Purpose of the Thesis

The permeation of small molecules through a polymer is a process of mass transport. The measurement of permeability may be utilized to characterize the molecular or physical structure of a polymer and even reflect on mechanical responses.

The mechanism of the movement of a gas through a polymer is usually conceived as an initial sorption and dissolution of the gas in a very thin surface layer, followed by diffusion of gas molecules under a concentration gradient, and eventually evaporation into the gaseous space at the other surface. In the case of vapors the step prior to the dissolution will be a process of condensation rather than of adsorption. The situation will then be complicated by such facts as: their solubilities are not directly proportional to the pressures and the diffusion coefficients often become highly dependent on the concentration of the penetrants in the polymer. Furthermore, vapors in the polymer also act as plasticizers or swelling agents, lower the glass transition temperature and loosen the segmental motions of the polymer.

By contrast, the situation is usually much less complicated for the permeation of non-condensing gases. In most cases Henry's law is obeyed and the diffusion coefficients are independent of the concentration. For these reasons gases are

preferred for studies into the mechanism of transport via sorption and diffusion, and for the information derived therefrom on polymer structure, morphology, and other features. Although information obtained from the studies of the effect of polymer-penetrant interaction on the transport process, using vapors, is of great value to general membrane studies, it will be treated here only tangentially.

The quantities obtainable from gas transport studies are, depending on the theories of mechanism applied, permeability, diffusivity, solubility, activation energies, jump distance and the free volume in the polymer. The magnitude of these quantities characterizes the penetrant-polymer system and is affected by the polarity or size of the penetrant and the nature of the polymer (i.e., polar or side groups along the chain, double bonds in the chain backbone, degree of cross-linking, degree of crystallinity, plasticizers, and fillers). Any change in the morphology or structure of the polymer will cause changes in these quantities.

It is the purpose of this study to evaluate all these quantities for four rubber samples, namely filled and unfilled natural rubber and synthetic poly-cis-isoprene, as a function of pressure and temperature, using H_2 gas and its isotope, D_2, as penetrants. The isotope effect that will be shown by the permeation data will then be utilized to evaluate the free volumes[1], and the effects of p and T on the penetration rates will be evaluated in terms of the other quantities mentioned. All rubber samples were prepared under

the same conditions and have practically the same chemical composition, i.e., poly(cis 1,4-isoprene), but were selected because synthetic and natural rubber have been found to show significant differences in their tensile strength, elongation and modulus. The filled rubbers contained carbon black and were designed for study of the effect of the filler on the transport process.

The information gained from this study will be interpreted in terms of rubber structure and rubber-filler interaction and should be of obvious theoretical and practical importance.

B. Basic Equations of Permeability of Gases through Polymeric Membranes

According to Fick's first law of diffusion, mass transport or the flow rate, Q in $ml^{-2}t^{-1}$, of a substance in a medium is proportional to its gradient of concentration:

$$Q = -D\frac{dc}{dx} \qquad (1)$$

The proportionality factor, D, is called the diffusion coefficient. However, this equation gives only the steady-state condition for diffusion in dilute systems. If the concentration changes with time as, for instance, during the transient period of flow, the formalism of the equation has to be changed.

Consider a region of unit cross-section and of length dx, extending from x to x+dx, as shown in Fig. 1.

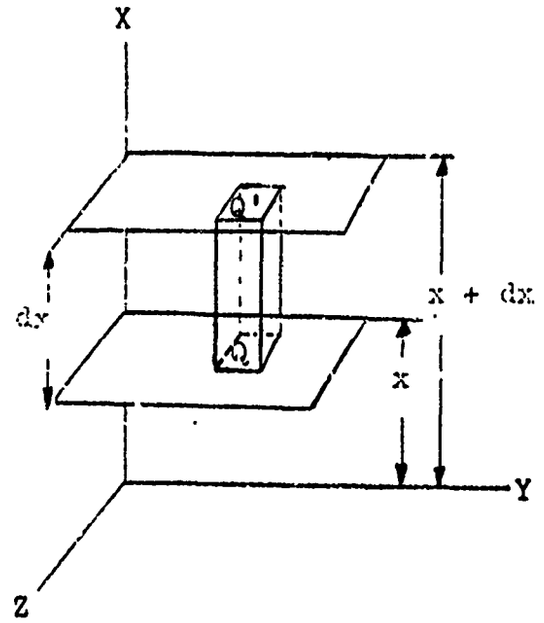

Fig. 1 Diagram of transient flow

The increase in concentration within this region in unit time divided by the volume dx, is the excess of material diffusing into the region over that diffusing out,

$$\frac{\partial c}{\partial t} = \frac{1}{dx}\left[- D\left(\frac{\partial c}{\partial x}\right)_x + D\left(\frac{\partial c}{\partial x}\right)_{x+dx}\right]$$

but

$$\left(\frac{\partial c}{\partial x}\right)_{x+dx} = \left(\frac{\partial c}{\partial x}\right)_x + \frac{\partial}{\partial x}\left(\frac{\partial c}{\partial x}\right)dx$$

therefore,

$$\frac{\partial c}{\partial t} = D\left(\frac{\partial^2 c}{\partial x^2}\right) \qquad (2)$$

This equation is Fick's second law of diffusion in one dimension. For three dimensions, it takes the form of

$$\frac{\partial c}{\partial t} = D\left(\frac{\partial^2 c}{\partial x^2} + \frac{\partial^2 c}{\partial y^2} + \frac{\partial^2 c}{\partial z^2}\right) = D\nabla^2 c \qquad (3)$$

providing D is a constant. However, in many systems D depends markedly on the concentration. In that case, one has to write equations (2) and (3) as

$$\frac{\partial c}{\partial t} = \frac{\partial}{\partial x}\left(D\,\frac{\partial^2 c}{\partial x^2}\right) \qquad (4)$$

and

$$\frac{\partial c}{\partial t} = \frac{\partial}{\partial x}\left(D\,\frac{\partial c}{\partial x}\right) + \frac{\partial}{\partial y}\left(D\,\frac{\partial c}{\partial y}\right) + \frac{\partial}{\partial z}\left(D\,\frac{\partial c}{\partial z}\right) \qquad (5)$$

where D is now a function of x, y, z and c. The above equations have to be solved explicitly, under the experimental conditions, to obtain D.

C. Methods for Solutions to the Equations

1. Steady-State Condition

Consider a substance flowing through a membrane of thickness, L, where the concentrations c_1 and c_2 of the substance at the inlet and outlet surfaces of the membrane are

kept constant. In the steady state, the concentrations of all sections of the membrane remain unchanged, provided the diffusion coefficient, D, is constant. The diffusion equation (2) becomes then

$$\frac{\partial c}{\partial t} = D \frac{d^2c}{dx^2} = 0 , \quad \text{or} \quad \frac{d^2c}{dx^2} = 0 \qquad (6)$$

On integrating the equation twice with respect to x, and introducing the conditions that at $x = 0$, $c = c_1$, and at $x = L$, $c = c_2$, one obtains

$$\frac{c - c_1}{c_2 - c_1} = \frac{x}{L} \qquad (7)$$

Clearly, the concentration changes linearly from c_1 to c_2 through the membrane as long as the membrane is uniform.

Since the flow rate of the substance is constant at the steady-state, equation (1) can also be integrated to give

$$Q_s = \frac{D(c_1 - c_2)}{L} \qquad (8)$$

as long as D remains constant. If the thickness, L, and the surface concentrations, c_1 and c_2, are known, D can be determined from a single observation of the flow rate.

If a gas or vapour diffuses through a membrane, and the pressures p_1 and p_2 at the two sides of the membrane are known, the steady-state flow, Q_s, is given by

$$Q_s = \frac{P\,(p_1 - p_2)}{L} \qquad (9)$$

where P is the proportionality constant termed permeability, with units of cm sec^{-1} and Q_s is in units of gm $cm^{-2} sec^{-1}$. Since the gas rarely dissolves to any extent in a membrane and there is a linear relationship between the external gas pressure and the corresponding concentrations within the surface layer of the membrane, it is possible to express the surface concentration by Henry's law,

$$c = Sp \qquad (10)$$

where S is the solubility in cm^{-1}. Substituting the two surface concentrations, $c_1 = Sp_1$, and $c_2 = Sp_2$, into equation (9) and comparing with equation (8), one readily obtains the relation,

$$P = DS \qquad (11)$$

which indicates that the transmission rate is the result of two concurrent processes, namely, dissolution and diffusion, and depends on the product of the factors describing these processes.

Now let us consider the case where the diffusion coefficient varies with the concentration. Fick's first law may still be considered to hold if one permits D to be a mean value deduced from the measurement of the steady-state flow rate. Integrating the equation between the two surface concentration, c_1 and c_2, yields then

$$Q_s = -\frac{1}{L}\int_{c_1}^{c_2} Ddc = \frac{\bar{D}\,(c_1-c_2)}{L} \qquad (12)$$

where

$$\bar{D} = \frac{1}{c_1-c_2}\int_{c_2}^{c_2} Ddc \qquad (13)$$

2. Time Lag

The most general solution to Fick's second law is given by a Fourier series. Daynes[2] and Barrer[3] showed, under the correct boundary conditions and with a constant or average D, that the amount of diffusant, Q_t in units of ml^{-2}, which passes through a membrane in time, t, is given by

$$Q_t = \frac{Dc_1}{L}\left(t - \frac{L^2}{6D}\right) - \frac{2Lc_1}{\pi^2}\sum_{n=1}^{\infty}\frac{(-1)^n}{n}\exp\left(\frac{-Dn^2\pi^2 t}{L^2}\right) \qquad (14)$$

When t is sufficiently large, the exponential term becomes negligibly small and the equation reduces to

$$Q_t = \frac{Dc_1}{L}\left(t - \frac{L^2}{6D}\right) \qquad (15)$$

A plot of Q_t versus t will result in a straight line at the longer times which represents the regime of steady state flow. The slope of this gives the constant flow, Q_s in units of $ml^{-2}t^{-1}$ since L is a constant. Extrapolating this line to

the t-axis, the intercept, τ , is given by

$$\tau = \frac{L^2}{6D} \tag{16}$$

from which D can be calculated. Once the two quantities D and P are known, the solubility S follows readily from equation (11). This is a remarkable method to evaluate all three essential quantities.

As mentioned, the foregoing derivation requires a constant D. This is probably the case for the diffusion of small molecules in a polymer. For organic vapors, or water vapour, the diffusion constants are often dependent on the concentration of the penetrant in the membrane. This means that the diffusivities can not be readily obtained from this so called time-lag method.

When D depends on concentration, and $c = c(x,t)$ denotes the concentration of gas in the membrane at a distance x from the membrane surface, on the high pressure side, at time t, Frisch[4] has shown, by solving equation (4) under the conditions:

$$c(x,0) = 0 \quad \text{for } x>0$$
$$c(0,t) = c_0 \quad \text{for } t>0$$
$$c(L,t) = 0 \quad \text{for } t>0$$

where c_0 is the concentration of gas on the high pressure side, that the time lag, τ, is given by

$$\tau = \frac{\int_0^L x\, c_s(x)\,dx}{\int_0^{c_o} D(u)\,du} \qquad (17)$$

The concentration inside the membrane at the steady state, $c_s(x)$, can be found in principle as a solution of the quadrature

$$\int_{c_s}^{c_o} D(u)\,du = \frac{x}{L} \int_0^{c_o} D(u)\,du \qquad (18)$$

where u is a dummy variable, and the relation of the diffusion coefficient and of the concentration must be of a known form, or be assumed to suit the analysis.

The use of equations (17) and (18) can be illustrated for two cases:

In the first and simpler case, where D is constant, i.e., $D(c) = D_o$ = constant, equation (18) becomes

$$c_s(x) = c_o \left(1 - \frac{x}{L}\right)$$

When this is substituted into equation (17) with

$$\int_0^{c_o} D(u)\,du = D_o c_o$$

one obtains the known result

$$\tau = L^2 / 6D_o$$

For the second case, where $D(c) = D_o(1+bc)$, D_o is the diffusivity at zero concentration and b is a constant, Frisch has evaluated $c_s(x)$ from equation (18) through a series of expansion in powers of b. For small values of b, an approximate expression for τ was obtained,

$$\tau \sim \frac{L^2}{6D_o}\left(\frac{1 + \frac{1}{4}bc_o}{1 + \frac{1}{2}bc_o}\right)$$

Obviously, D_o and b must be determined by measuring the time lag at two concentrations.

3. Short-Time Approximation

When the diffusion coefficient is small, it would require an inconveniently long time to establish a steady state of permeation. In this case the diffusivity may be obtained from the intercept of the Q_t versus t plot.

An alternative solution to the diffusion equation (2) at short times, for constant D has been proposed as[5]

$$\frac{dp}{dt} = \frac{2AP_1S}{v}\left(\frac{D}{\pi t}\right)^{\frac{1}{2}} \sum_{m=0}^{\infty} \exp\left[-\frac{L^2}{4Dt}(2m+1)^2\right] \qquad (10)$$

where $\frac{dp}{dt}$ is the rate of increase of pressure on account of the diffusant transport through a membrane of area, A, into an initially evacuated space of volume v; S is the solubility and p_1 is the gas pressure at the inlet surface of the membrane. When t is sufficiently small, only the first term of the summation in equation (19) is important

$$\ln\left(t^{\frac{1}{2}}\frac{dp}{dt}\right) \approx \ln\left[\left(\frac{2ASp_1}{v}\right)\left(\frac{D}{\pi}\right)^{\frac{1}{2}}\right] - \frac{L^2}{4Dt} \qquad (20)$$

A plot of $\ln\left(t^{\frac{1}{2}}\frac{dp}{dt}\right)$ against $1/t$ should be a straight line of slope $\left(-\frac{L^2}{4D}\right)$ from which the value of D is obtained. This method was used by Rogers, Burity and Alpert[5] and has been applied successfully in several quite different systems by Meares[6].

4. Sorption and Desorption

The diffusion coefficients of vapours in polymers are several orders of magnitude lower then those of gases. The estimation of a steady rate of permeation is therefore very time consuming. However, the kinetic study of the sorption and desorption of gases or vapours in polymers can be made into a simple and rapid method for the determination of diffusion coefficients.

The typical apparatus employed by Garret and Park[7] is shown in Fig. 2. A specimen of known shape is suspended from a quartz spiral balance in an atmosphere of the gas or

vapour to be studied at constant pressure and temperature. The rate of increase in weight of the sample is determined from the extension of the spring as a function of time.

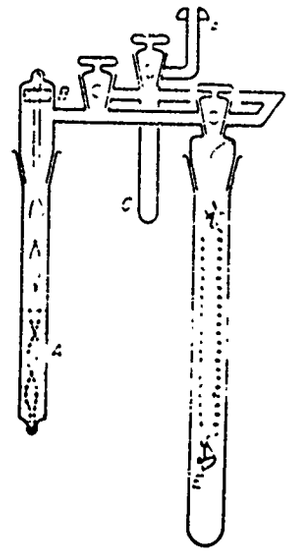

Fig. 2 Quartz spring sorption apparatus. A, Stirred vapour source. B, magnetic stirrer. C, cold thimble for desorption studies. D, quartz spring. E, polymer specimen on glass cradle. F, ball joint to vacuum system.

When D is independent of concentration, the amount of diffusant, Q_t, taken up by a planar sheet in time, t, is[8]

$$\frac{Q_t}{Q_\infty} = 1 - \frac{8}{\pi^2} \sum_{k=0}^{\infty} \frac{\exp\left\{-\left[(2k+1)\,\pi / L\right]^2 Dt\right\}}{(2k+1)^2} \qquad (21)$$

where Q_∞ is the equilibrium sorption attained, theoretically, after infinite time. The same equation holds also for desorption if Q_∞ is the amount desorbed after infinite time and Q_t is the amount lost up to time, t. For long times, equation (21) may be approximated by

$$\frac{Q_t}{Q_\infty} = 1 - \frac{8}{\pi^2} \exp\left(-\frac{\pi^2 Dt}{L^2}\right) \qquad (22)$$

For short times the approximation

$$\frac{Q_t}{Q_\infty} = \frac{4}{L}\left(\frac{Dt}{\pi}\right)^{\frac{1}{2}} \qquad (23)$$

is adequate. A plot of Q_t/Q_∞ against $(t/L^2)^{\frac{1}{2}}$ is initially linear so that D can be evaluated from the slope. Also if $t_{\frac{1}{2}}$ is the time at which $Q_t/Q_\infty = \frac{1}{2}$, then

$$D = \frac{L^2}{64 t_{\frac{1}{2}}} = \frac{4.919 \times 10^{-2}}{(t_{\frac{1}{2}}/L^2)} \qquad (24)$$

When D is a function of concentration, the quantitative relationship between the diffusion coefficient and the concentration can be determined from a series of sorption experiments at different initial concentrations. For each sorption, the Q_t/Q_∞ versus $(t/L^2)^{\frac{1}{2}}$ plot, according to equation (23), gives some mean value, $\bar{D}$, of the variable diffusion coefficient averaged over the range of concentrations, in the membranes.

Calculations have shown that, for any one experiment a reasonable approximation for $\bar{D}$ is given by

$$\bar{D} = 1/c_o \int_0^{c_o} D dc$$

Using this relationship a graph of $\bar{D}c_o$ as a function of c_o can be drawn. Numerical or graphical differentiation with respect to c_o gives a first approximation to the relationship between D and c[8]. In many cases this first approximation is sufficiently accurate. But, it is sometimes possible to obtain a better approximation by the simpler method of using both sorption and desorption data. If $\bar{D}_s$ and $\bar{D}_d$ are calculated from the initial gradients for sorption and desorption, respectively, then $\frac{1}{2}(\bar{D}_s + \bar{D}_d)$ is a better approximation to

$$(1/c_o) \int_0^{c_o} D dc$$

than either $\bar{D}_s$ or $\bar{D}_d$[9].

D. Temperature Dependence

The rate of transport of gases or vapours in a polymer varies with temperature. In most cases, the temperature dependence of P, D, and S follows the Arrhenius equation as a reasonably good approximation. They can then be represented by

$$P = P_o\, e^{-E_p/RT}$$

$$D = D_o\, e^{-E_d/RT} \qquad (25)$$

and $$S = S_o\, e^{-E_s/RT} = S_o\, e^{-\Delta H_s/RT}$$

where P_o, D_o and S_o are constants; E_p, E_d and E_s are experimentally determined activation energies for permeation, diffusion and dissolution. The activation energy of dissolution is customarily referred to as heat of solution, ΔH_s. The above equations may be written in terms of the differentials, obtained from the slopes of the semi-logarithmic graphs, as

$$E_p = \frac{-R\, d \ln P}{d\,(1/T)}$$

$$E_d = \frac{-R\, d \ln D}{d\,(1/T)} \qquad (26)$$

and $$\Delta H_s = \frac{-R\, d \ln S}{d\,(1/T)}$$

The heat of solution can be readily determined from

$$\Delta H_s = E_p - E_d \qquad (27)$$

since $P = DS$.

Thus, the various energies can be obtained from the slope of the plots of the corresponding logarithmic quantities

versus 1/T. The activation energy for diffusion is associated with different meaning in various diffusion theories, as shall be discused in the next section.

E. Theories for Diffusion

There are several theories dealing with the problem of transport of gas through polymer membranes and the role of the activation energy of diffusion. The volume fluctuation theory postulates that diffusional jumps of the penetrants arise from volume fluctuations and that the experimental activation energy is an average value for all fluctuations large enough to allow a jump[10]. The hole formation theory assumes that the polymer molecules have to be pushed far enough apart to form a hole sufficient for the infiltration of the gas molecules, the activation energy in this theory is the energy needed to move the chains apart. The transition state theory postulates that the diffusants must be thermally activated in order to surmount a potential energy barrier encountered in the course of their jumps from one equilibrium position within the membrane to the next. Since the interpretation of our data is based on the transition state theory, we shall examine it in some detail.

The transition state theory as developed by Eyring and co-workers[13] states that, in diffusing in solution (solid or liquid), a molecule of solute and one of solvent are required to slip past one another. Suppose the distance between two successive equilibrium positions is λ.

The change of the standard free energy with distance can then be represented by the curve in Fig. 3.

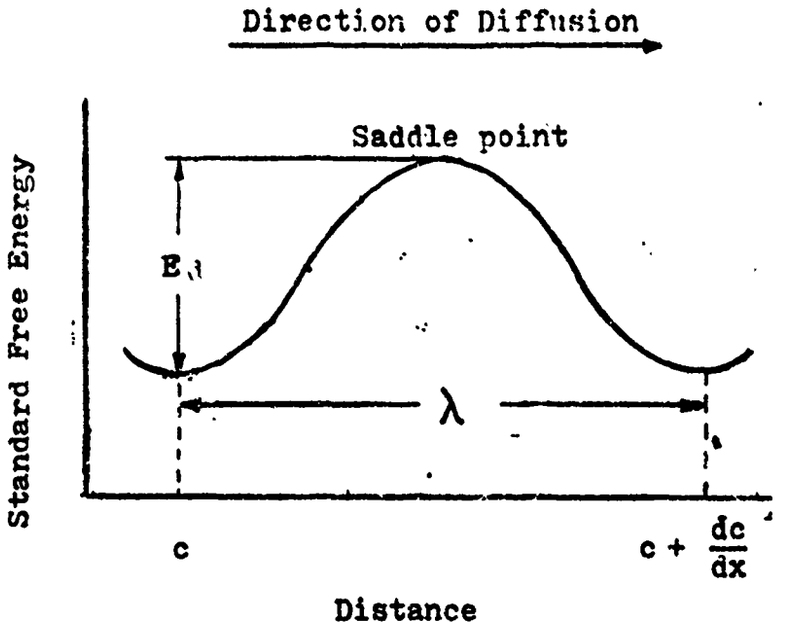

Fig. 3 Energy profile for diffusion

For ideal or highly dilute solutions at rest, the standard free energy is the same in all equilibrium positions. Thus the energy of activation will be the same in the forward and backward direction, the specific rate constant, w, is the same for transport in either direction, and the molecules move at random with no net transport. If there is a concentration gradient, dc/dx, and λ is the distance between the successive equilibrium positions, the concentration in moles per cubic centimer of solute in the initial and final states of diffusion jumps, are c and

$c + \frac{dc}{dx}\lambda$ respectively. The number of moles of solute moving in forward direction, e.g., from left to right, through a unit cross sectional area per second is then given by

$$Q_f = V_f = \lambda c w \quad \text{moles-cm}^{-2}\text{-sec}^{-1}$$

where w, expressed in terms of concentrations, is the specific reaction rate for diffusion, i.e., the number of moles of solute molecules moving from one position to the next per unit time. Similarily, the rate of movement in the backward direction, is

$$Q_b = V_b = \lambda (c + \lambda \frac{dc}{dx}) w \quad \text{mole-cm}^{-2}\text{-sec}^{-1}$$

The resultant flow from left to right is therefore

$$Q = V = - \lambda^2 w \frac{dc}{dx} \quad \text{moles-cm}^{-2}\text{-sec}^{-1}$$

On applying Fick's first law,

$$Q = - D \frac{dc}{dx} \quad \text{moles-cm}^{-2}\text{-sec}^{-1}$$

it follows that

$$D = w\lambda^2 \tag{28}$$

The specific rate constant for diffusion is then given by

$$w = \frac{kT}{h} K_c^{\ddagger}$$

where k and h are the Boltzmann and Planck constants, and $K_c^{\ddagger}$ is the concentration equilibrium constant for the formation of the activated species.

Introducing the standard free energy

$$\Delta F^{o\ddagger} = -RT \ln K_c^{\ddagger}$$

it follows that

$$w = \frac{kT}{h} e^{-\Delta F^{o\ddagger}/RT} = \frac{kT}{h} e^{\Delta S^{o\ddagger}/R} e^{-\Delta H^{o\ddagger}/RT} \qquad (29)$$

since $\Delta F^{o\ddagger} = \Delta H^{o\ddagger} - T\Delta S^{o\ddagger}$. The standard state may be chosen to be the state of unit concentration because rate constants are usually expressed in terms of concentrations. The quantities $\Delta F^{o\ddagger}$, $\Delta S^{o\ddagger}$ and $\Delta H^{o\ddagger}$ are called the free energy, the entropy and the enthalpy of activation respectively.

The experimental activation energy for diffusion, E_d, is obtained from the Arrhenius equation,

$$\frac{d \ln w}{dT} = \frac{E_d}{RT^2}$$

Comparison with equation (29) shows that

$$E_d = RT + \Delta H^{o\ddagger} \qquad (30)$$

Accordingly, from equations (28), (29), and (30), the diffusion coefficient may be expressed by

$$D = e\lambda^2 \frac{kT}{h} e^{\Delta S^{o\ddagger}/R} e^{-E_d/RT} \qquad (31)$$

The rate constant, w, can be written in terms of the partition functions of the system in the activated and normal states at 0^oK, and hence equation (28) then becomes

$$D = \lambda^2 w = \lambda^2 \frac{kT}{h} \frac{F^{\ddagger}}{F} e^{-\epsilon_o/kT} \qquad (32)$$

from which the absolute magnitudes of diffusion coefficients can in principle be determined by evaluation of the partition function[14].

If the degrees of the freedom of the diffusional movement are assumed to be translational only, i.e., if the rotational and vibrational contributions in the activated and normal states are taken to be equal, the translational partition function for three degrees of freedom within the free volume, V_f, is given by

$$F_{tr} = \left(\frac{2\pi mkT}{h^3} \right)^{3/2} V_f$$

The activated species has only two degrees of freedom so that its translational partition function is

$$F^{\ddagger}_{tr} = \left(\frac{2\pi mkT}{h^2} \right) V_f^{2/3}$$

Setting $E_d = N\epsilon_o$ and substituting for the ratio $F^{\ddagger}_{tr}/F_{tr}$ in equation (32), one finds for D

$$D = \frac{\lambda^2}{V_f^{1/3}} \left(\frac{kT}{2\pi m}\right)^{\frac{1}{2}} e^{-E_d/RT} \qquad (33)$$

Comparing equations (31) and (33) leads to

$$V_f^{1/3} = h\, e^{-(\Delta S^{o\ddagger}/R+1)/(2\pi mkT)^{\frac{1}{2}}} \qquad (34)$$

This equation can be used to calculate the standard free entropy of activation, if the free volume, V_f, is known. Frisch has developed an innovative method for the estimation of the free volume base on the quantum isotope effect in permeation. This is discussed in the following section.

F. Quantum Isotope Effect in Permeation

Hydrogen and its isotope, deuterium have the same effective molecular volumes notwithstanding the difference in their mass. When such small gas molecules are dissolved in microscopic cavities in the polymer matrix, they may be thought of as free particles confined in a potential energy box in the quantum mechanical sense. If the cavity is approximated by a cube, the quantized translational energy for the particle is given (in three dimensions) by

$$\epsilon_{n,i} = \frac{3\, n^2h^2}{8\, m_i d^2}$$

or

$$\epsilon_i = \frac{3\, h^2}{8\, m_i d^2} \qquad (35)$$

At temperatures not far from room temperature the particle is in its ground state[15] with the principal quantum number, $n = 1$. Equation (35) thus relates the dimension of the cavity, d, and the mass, m_i, to the potential energy, ϵ_i, of the particle. Realizing this, Frisch[1] has proposed a model based on the transition state theory, i.e. a "smoothed potential" energy surface as shown in its diagram of Fig. 4 with the particle in a potential well of barrier height numerically equal to the activation energy of diffusion, E_d, and with the width, d, of the cavity.

The actual diffusion path along the diffusion coordinate proceeds in a plane normal to the potential energy trough which defines the saddle area of width, λ_b. The amount of thermal activation E_d required to allow the penetrant isotope to surmount the potential barrier is $(\epsilon_i^* - \epsilon_i)$, the ϵ_i^* arising from the partition function of the activated complex, Q_i^*, and ϵ_i from the partition function, Q_i, of the penetrant in the cavity. Since ϵ_i^* and ϵ_i decrease with increasing mass m_i, one expects to observe a difference in the measured isotopic activation energies by the amount,

$$\delta E_d = (E_d)_{D_2} - (E_d)_{H_2} = (\epsilon^*_{D_2} - \epsilon_{D_2}) - (\epsilon^*_{H_2} - \epsilon_{H_2})$$

$$= -(\epsilon_{D_2} - \epsilon_{H_2}) + (\epsilon^*_{D_2} - \epsilon^*_{H_2}) = -\delta\epsilon + \delta\epsilon^* \qquad (36)$$

for the diffusion of isotopes H_2 and D_2 in the same medium.

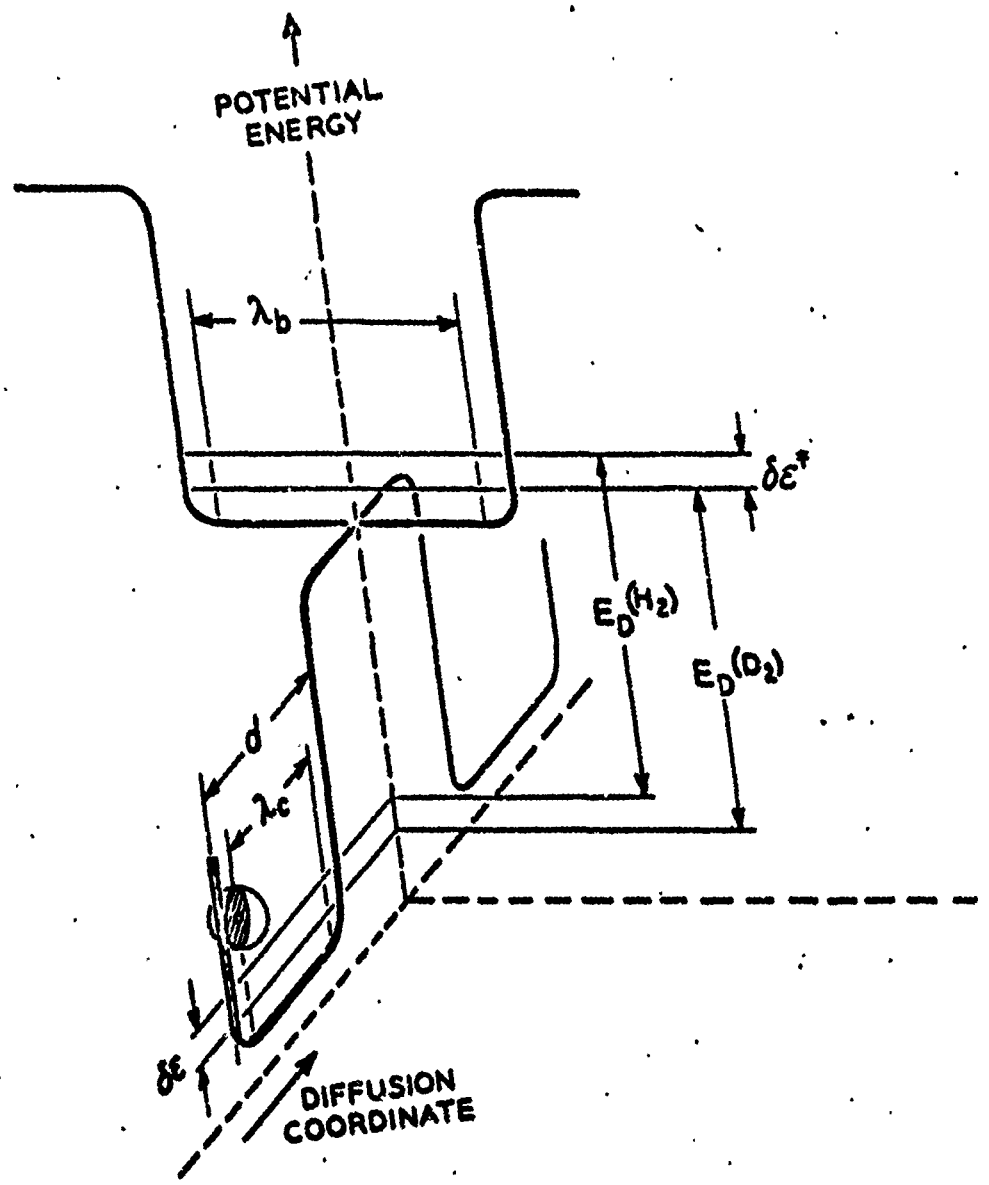

Fig. 4 Energy Diagram - 3 Dimensions

ΔH_s, the heat of solution, is independent of the activated state, but can be derived from Q_i, the partition function of the penetrant in the cavity. The difference of the heat of solution for penetrants D_2 and H_2 in the same medium is

$$\delta \Delta H_s = (\Delta H_s)_{D_2} - (\Delta H_s)_{H_2} = \epsilon_{D_2} - \epsilon_{H_2} = \delta\epsilon \qquad (37)$$

Substitute equation (35) into (37) for a mole of penetrant, it becomes,

$$\delta \Delta H_s = \delta\epsilon = \frac{3 N h^2}{8 \lambda_c^2}\left(\frac{1}{M_{D_2}} - \frac{1}{M_{H_2}}\right)$$

$$= - \frac{3 N h^2}{32 \lambda_c^2} \qquad (38)$$

Since the H_2 and D_2 gas particles possess the same molecular diameter, σ, the boundary condition for the wave equation goes in both cases from $\frac{1}{2}\sigma$ to $(d - \frac{1}{2}\sigma)$, yielding, λ_c.

Replacing λ_c by $(d - \sigma)$ and equating d with one side of a cube which constitutes the cavity, the incremental free volume, V_f, one gets

$$\delta \Delta H_s = \frac{- 3 N h^2}{32 (V_f^{1/3} - \sigma)^2}$$

or

$$V_f^{1/3} = \frac{18.8}{(-\delta \Delta H_s)^{\frac{1}{2}}} + \sigma \qquad (39)$$

Thus, the average dimension of the free volume can be estimated from the difference in the heat of solution for H_2 and D_2 in the same membrane, if the effective molecular diameters of the isotopes are taken to be equal at 2.93 Å, the quantum mechanically corrected Lennard-Jones potential diameter of H_2[16].

Similarily, we may write

$$\delta E_p = \delta \epsilon^* = - \frac{3 N h^2}{32 \lambda_b^2} \qquad (40)$$

and

$$\delta E_d = \frac{3 N h^2}{32} \left(\frac{1}{\lambda_c^2} - \frac{1}{\lambda_b^2} \right) \qquad (41)$$

since $\delta E_p = \delta E_d + \delta \Delta H_s$. Here, δE_p is the difference in the activation energies for permeation of two isotopic species in the same medium. The cavity dimension, λ_b, for the activated species can then also be estimated.

G. Factors Affecting P, D and S

1. Nature of the Gas

The transmission rate of a penetrant is highly affected by the size of its molecules since larger holes need to be present in the matrix for the diffusion of larger molecules with consequently deeper energy wells. In fact, in the diffusion of bigger molecules lower diffusivities and higher activation energies have been found[17,18,19].

2. The Nature of the Polymer

Because the diffusion is the result of the interplay

of the random motion of the polymer segments with translational mobility of the gas molecules, any factor influencing the polymer segmental mobility is expected to affect the diffusion coefficient. The presence of side groups such as methyls or of polar groups, on the polymer molecule hinders the chain movement and hence should lower the diffusion coefficient and increase the activation energy[20]. On the other hand, the introduction of unsaturation into the polymer backbones should increase the diffusion coefficients as a result of increasing free volume, or internal chain mobility[21], for cis-conformations and reduce them for trans-conformations.

3. Effect of Crystallinity or Crosslinking

Crosslinkings in the polymer matrix restrict the segmental mobilities, while crystallites in the polymer act as impermeable obstacles to the movements of penetrants. Both effects reduce the diffusivity[22,23].

4. Effect of Glass Transition

As the polymer goes from the liquid-like rubber state to the glass state, its segmental mobility and free volume decrease. The lower mobility of the polymer segments below the glass transition temperature, T_g, should be expected to influence the permeation process. In fact, in his studies of the effect of the glass transition on the diffusion of gases in the polymer, Meares[24] found that the Arrhenius plot showed a distinct change of slope at T_g for poly(vinyl acetate). However, Stannett and Williams[25] found no inflection in their Arrhenius plots for poly(ethyl methacrylate).

Kumins and Roteman[18] also found no effect of the glass transition of poly(vinyl chloride-vinyl acetate) copolymer for all gases studied except CO_2. The lack of influence may be connected with the size of the penetrants and the relative extent of the change in the coefficients of isothermal expansion at the glass transition temperature. Kumin and Roteman have suggested that mainly the size of the holes changes above T_g, but not the number. If the penetrant molecules are small enough, the probability that a penetrant molecule encounters a hole of sufficient size could remain roughly the same. With larger penetrant molecules, the size becomes more important and an effect of the glass transition is thus seen[19].

5. Effect of Plasticizers

The addition of a plasticizer to a polymer decreases the frictional forces between the molecular chains resulting in a greater segmental mobility. An expected increase in the diffusion rate has been confirmed by a number of workers[26-29].

6. Effect of the Filler

The permeation rate is considerably reduced when the polymer matrix contains dispersed solid particles. The effect of the filler on diffusivity may be thought to arise primarily from the fact that each filler particle, being impermeable, behaves as a geometric obstruction in the path of the gas through the polymer. The gas molecules must cover a longer distance to pass around the filler particles and the rate of permeation is lowered. The shape of the filler should then have an additional effect in that lamellar fillers may

have a much greater obstructing geometry than spherical particles when the lamellar particles orientate themselves perpendicularly to the main path of the penetrant[30,31].

The purpose of this work then, as mentioned before, was to measure the transmission rate of the penetrants, H_2 or D_2, in four rubber samples (unfilled and filled synthetic and natural rubbers) as a function of temperatures and gas pressures. The transmission rates (or diffusion coefficients) and the activation energies for permeation and diffusion, evaluated from the Arrhenius plot were to be compared in the light of the morphological differences of these elastomers and with respect to the effect of the filler. From the quantum isotope effect in the permeation, the cavity size of the sample was to be estimated, and this information, coupled with the densities of the samples, used to evaluate the differences in physical structures of the unfilled synthetic and natural rubbers.

II. EXPERIMENTAL

A. Apparatus

The diffusion apparatus used in this study consists of three main parts; the gas feeding system, the diffusion cell and the gas measuring system. Figure 5 is a block diagram for the apparatus.

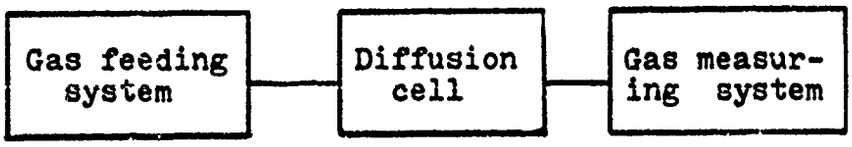

Fig. 5 Block diagram for the apparatus

1. Diffusion Cell and the Constant Temperature Bath

The diffusion cell was developed following the original design of Barrer [32]. It is made of stainless steel and consists of two parts as shown in Fig. 6. The upper part is a cylindrical hollow plunger containing a neoprene rubber O-ring, while the lower part consists of a cylindrical hollow base containing a metal washer and a sintered metal disc. The base is connected

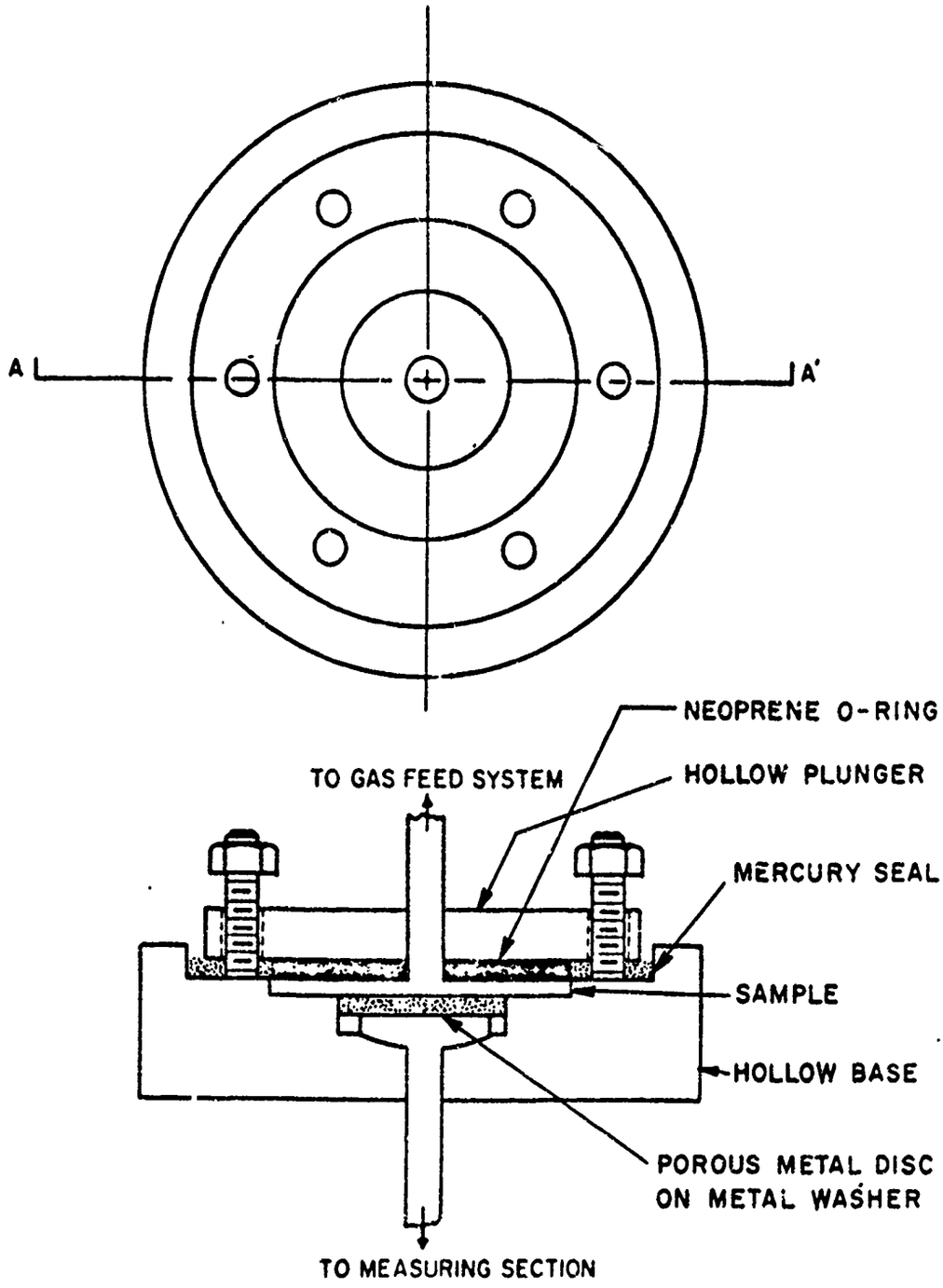

Fig. 6 Schematic of Diffusion Cell

to the gas measuring system via a ¼" Kovar brass to glass seal. The plunger is connected to the gas feeding system through a ¼" flexible brass tubing.

In practice, the specimen is placed at the top of the sintered metal disc in the hollow base which is in turn supported by the metal washer. Therefore, the specimen will not collapse from two unequal pressures at its two surfaces. The O-ring in the plunger assures a vacuum-tight seal of the cell when the plunger is fastened to the base by six sets of steel bolts and screws. The system is further leak proofed by the mercury seal in the void spaces between plunger and base.

The constant temperature bath contains the following items:

1) A fully insulated aluminum bath containing Dow Corning 200 silicone oil.
2) A probe from the Fisher Temperature Control, model 44, with a built-in relay and power supply.
3) A Bodine motor stirrer from Talboys Instrument Corp.
4) A quartz immersion heater, 100w.
5) A Fisher 76mm thermometer, covering a temperature range of -1°C to 110°C.
6) A Fisher thermometer magnifier.
7) A cooling brass coil.

The silicone oil has a viscosity of 50 cp at 25°C. Since its viscosity changes only slightly over a wide temperature range,

it should provide a smooth and efficient circulation for heat exchange. By properly adjusting the speed of the stirrer and the flow rate of the cooling water, the bath temperature can be controlled to better than ±0.05°C over the experimental temperature range, 40-85°C.

2. The Gas Feeding System

The upper part of the diffusion cell is connected to a two liter capacity gas storage flask via a flexible ¼" brass coil and a fast action Nupro gate valve as shown in Fig. 7. The flexible coil is used to reduce the initial surge of gas from the storage flask to the diffusion cell as the gate valve is opened. The storage flask is connected to the compressed H_2 and D_2 gas cylinders through a flexible brass coil and a stopcock. Again, the brass coil is used for reducing the surge of the gas from the gas cylinder. A mercury manometer which records the storage gas pressure is at the left of the flask. The pressure is read out from a meter stick fastened immediately behind the manometer column. With the aid of the magnifier the scale can be read accurately to ±0.1 mm H_g. A vacuum monitor, the thermocouple gauge, is also incorporated in the system so that the vacuum of the system can be checked from time to time. By means of a Welch Duo-Seal oil diffusion pump, model 1400 (not shown in the figure), a vacuum of 10^{-6}cm H_g can be reached for the whole gas feeding system. With the pump action isolated, the leak rate of the system is about one micron per hour. This is considered to be more than

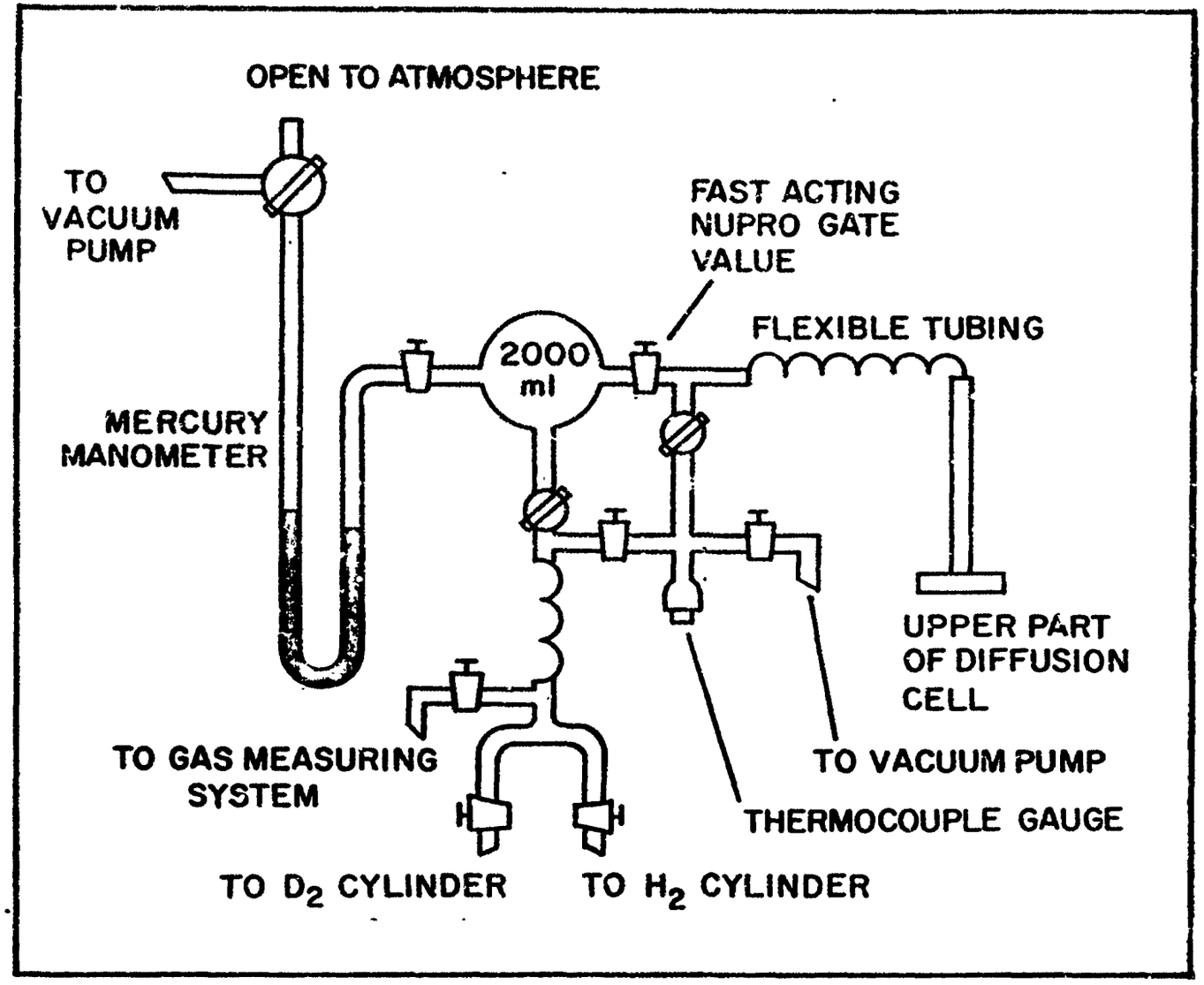

Fig. 7 Gas feeding system

sufficient for the experiment, since the longest runs lasted about three to four hours and the shortest runs only half an hour.

The pressure at the manometer did not change during the course of experimental runs, since all runs were terminated after the gas transported had reached a pressure about 80 microns in the receiver. This corresponds to a pressure change of less than 0.01% in the storage flask for the lowest gas pressure, 1cm H_g, used in the experiment. A manostat was therefore unnecessary.

3. The Gas Measuring System

The base of the diffusion cell is connected to the gas measuring system through a Covar metal to glass seal as shown in Fig. 8. The space between the base of the diffusion cell to the stopcock #1, #2, or #3, #4 and #5 determines the receiver volume V_1, V_2 or V_3. By properly manipulating the stopcocks, the gas transported across the membrane can be routed to one of these receiver volumes and its pressure measured by a Hughes thermocouple vacuum gauge tube, type 6343, in connection with a read-out unit. The schematic diagram of the thermocouple gauge is shown in Fig. 9. The thermocouple (pin 3 and 5) is in close proximity to the tube heater (pin 1 and 7) and provides an output E.M.F. determined by the operating current to the tube's heater and by the heat conductivity of the residual gas in the evacuated system. The thermocouple output is 10 millivolts at hard vacuum, and 0.1

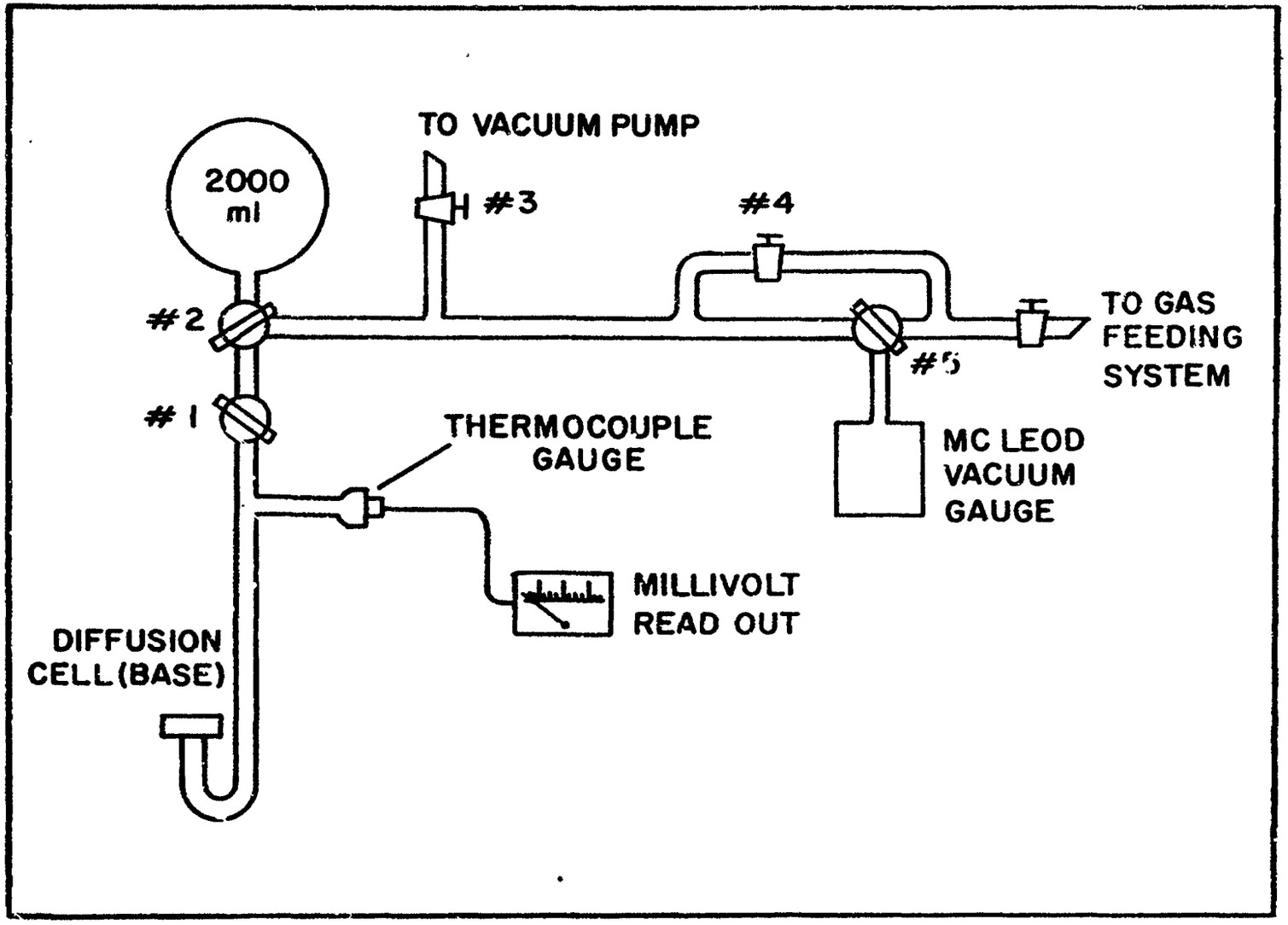

Fig. 8 Gas measuring system

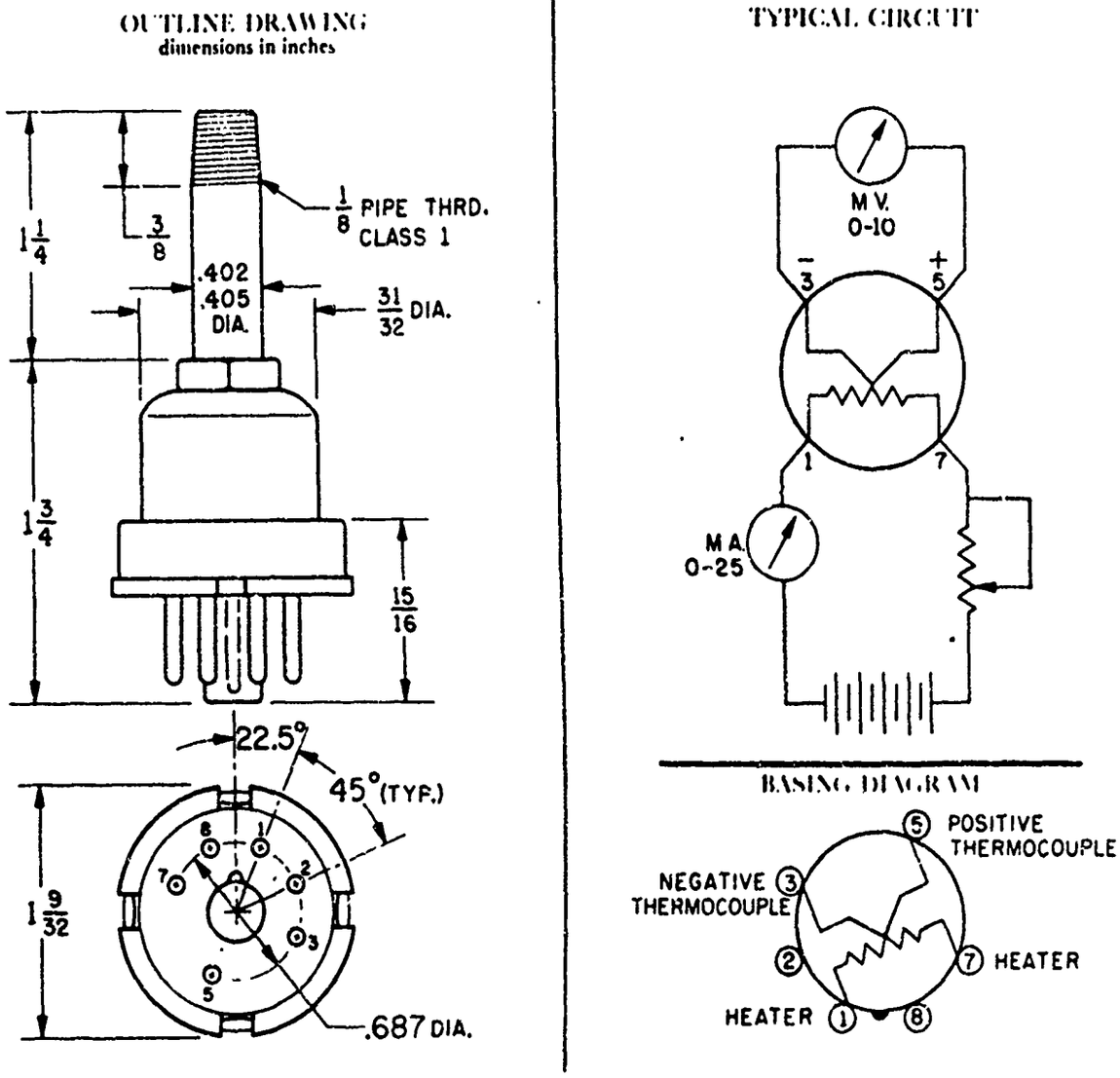

Fig. 9 Thermocouple vacuum gauge tube, Type 6343, Hughes

millivolts at atmospheric pressure (air). Thus, this type of gauge measures the change in output EMF produced by the heat conductivity of the gas in the tube. The gas pressure in the receiver can be derived from the output EMF through the calibration curve. Details of the calibration procedure are described in Sec. II, page 45. An example of calibration curve is shown in Figures 10 and 11.

The magnitude of the receiver volumes was estimated in the following manner. A calibration for the thermocouple gauge with H_2 was established against the McLeod gauge. The volume of the storage flask in Fig. 8 was determined to be 2003 ml before being installed into the system. The pressure of H_2 gas in V_1 and the volume from the diffusion cell to stopcock No. 1, were measured first and then a new pressure reading was taken in V_2 (up to the stopcock No. 2) with the stopcock No. 1 opened. This was repeated with volumes, V_3 and V_4 (V_4 is the sum of V_3 plus the volume of the flask). The following volume ratios were obtained from the gas laws:

$$V_2 / V_1 = 1.08$$

$$V_3 / V_1 = 2.13$$

$$V_4 / V_1 = 56.51$$

Substituting $V_4 = V_3 + 2003$ ml, it follows readily that

$$V_1 = 37.9 \text{ ml}$$

$$V_2 = 40.8 \text{ ml}$$

$$V_3 = 80.73 \text{ ml}$$

to within approximately ± 1% .

The McLeod vacuum gauge, model 2 from Manostat Incorporated, was used primarily to calibrate the thermocouple gauge. By assuming that the gas obeys the ideal gas law, $pv = n RT$, the pressure to be measured is related to the linear length of the McLeod capillary, L, taken from the top of the capillary to the mercury level drawn up into the capillary by,

$$p = 0.02492 L^2$$

where L is in units of mm and p in microns of H_g. Since all the stopcocks were greased with Apiezon N, a high vacuum grease, and treated afterward with moderate heat from an electrical heat gun to release trapped air, the entire gas measuring system, including the base of the diffusion cell, was maintained at a pressure of 1×10^{-6} cm H_g by means of a mercury diffusion pump and a Welch DuoSeal model 1405 fore pump. The leakage rate into the system was no more than 1

micron (10^{-3} Torr) a day when the pump unit was isolated.

B. Materials

1. Membranes

Four membranes made of filled and unfilled synthetic and natural rubber (SNR and NR), were used in this study. They were supplied by the B. F. Goodrich Rubber Co. Akron, Ohio, courtesy of Dr. J. R. Beatty. The unfilled NR and SNR (gum stock) have basically the same chemical compositions, poly-cis-1,4 isoprene, and posses the same low degree of crosslinking, see Table 1. The molecular weight between crosslinks is about 8×10^{-3}, determined by the swelling method. The chemical compositions and the degrees of crosslinking of the filled NR and SNR were basically the same as the corresponding unfilled membranes. The filler used was HAF carbon black.

All the specimens were cut from the large sample sheets, stored in a desiccator and kept in a dark place at a temperature not over 25°C from the time of receipt. The recipe for these materials is presented in Table 1, along with the pertinent specifications and physical properties. The procedure for determining the bulk density of the membranes and the molecular weight between the crosslinks is presented in the section of experimental technique on page 42.

TABLE 1

RECIPES AND SPECIFICATIONS OF THE SAMPLES

Specifications of the unfilled NR and SNR samples*

Nomenclature	Density (g/cm^3)	Crosslinking agent	M.wt. between crosslinks	Physical Property		
				Tensile strength	Elongation	300% modulus
NR (gum stock)** (p.(cis 1,4-isoprene))	0.9281	dicumyl peroxide (~2%)	8.28×10^3 (by swelling method)	900psi	600%	200psi
SNR(gum stock) (Syn. p.(cis 1,4-isoprene))	0.9183	"	8.24×10^3	100	170%	--

*Recipes for the unfilled NR and SNR are identical with the filled samples as shown in the following Table except for the omission of the carbon black and the lower % dicup.

**Pale crepe NR

Recipes for the filled NR and SNR samples (parts/weight)

NR		SNR	
Pale Crepe NR	100.0	Syn. p. isoprene	100.0
Dicup 40 C	5.0	Dicup 40 C	4.25
Antioxidant 2246	1.0	Antioxidant 2246	1.0
Triethanol Amine	0.25	Triethanol Amine	0.25
N 330 Black***	40.0	N 330 Black	40.0

*** N 330 black is an HAF type (high abrasion furnace) of about 300 A particle size.

2. Gases

Hydrogen and deuterium gas were purchased from the Matheson Gas Co. with a purity of 99.95% for H_2 and 99.5% for D_2. The effect of impurities in the gases on the permeation rates was negligible and no further purification of the gases was performed.

C. Experimental Procedures and Techniques

1. Determination of the Bulk Density of the Sample and the Molecular Weight between Crosslinks by Equilibrium Swelling

Theories and treatments regarding the swelling of the amorphous crosslinked polymer in a solvent are found elsewhere(33,34). For the case of a swollen gel in equilibrium with excess solvent the molecular weight, $\bar{M}_c$, between crosslinks is given by(35)

$$\bar{M}_c = \frac{-\rho_p V_1 (S^{1/3} - \frac{1}{2} S)}{\ln (1-S) + \chi S^2 + S}$$

were $S = (1 + Q_m)^{-1}$. The ratio, Q_m(unitless), of the volume of the liquid in the swollen gel to the volume of the dry polymer, is calculated from

$$Q_m = \frac{\rho_p (W_g - W_p)}{\rho_1 W_p}$$

Subscripts, 1, p, and g refer to the solvent, dry polymer and the gel. The densities, ρ (g/cm^3), the weights, W, and the molar volume V, were individually determined. The polymer-solvent interaction parameter, χ, is a dimensionless quantity which is related to the energy of interaction characteristic of a particular polymer-solvent system and may be calculated from Huggin's equation[36]. For the NR (also SNR)-benzene system the value of $\chi = 0.425$ was taken from the literature[37] and used in the calculation of $\bar{M}_c$.

The procedure used for swelling the rubber was the following[38],

1) Determination of W_g: To an amber screwtop bottle containing 0.1g of phenyl naphthylamine(PNA) and 50 ml of benzene, an accurately weighted rubber sample, unfilled NR and SNR, was added (1.5 $\pm$ 0.5 gm, approximately dimensions 0.3 x 0.5 x 2.5 cm). The bottle was placed in a constant temperature water bath kept at 25 $\pm$ 1°C for a week. The sample was removed from the solvent, blotted and rapidly weighed in a tarred weighing bottle. It took about three days for the sample to reach the swelling equilibrium. Duplicate runs were carried out for each sample.

2) Determination of Bulk Density of the Rubber, ρ_p: The bulk density of the dry (unswollen) rubber was determined as follows. Several cubes (each side about 1 mm in length) of the rubber were placed in a beaker containing methanol. Water was then slowly added from a burette while the mixture was stirred to insure uniformity. When the rubber chips were

suspended within the mixture, its density was equal to that of the rubber. The liquid was then transferred to a calibrated pycnometer and weighed. The rubber density was found by subtracting the mass of the empty pycnometer from the total mass, then dividing by the volume of the pycnometer.

3) Determination of the Density of Solvent, ρ_1:

The density of the solvent, benzene, can be established by either using the pycnometer mentioned above or by merely taking literature values from the handbook. Assuming a linear relationship of density and temperature at short temperature intervals, the density of benzene may be readily obtained.

Values of bulk densities and $\bar{M}_c$ for the unfilled NR and SNR, obtained by using the above procedures, are tabulated in Table 1, in the material section on page 41.

2. Sample Preparation for the Permeation Experiment

The rubber sample as supplied by the manufacturer were sheets of 12" x 12" x 0.09". After visual inspection and measurement of thickness with a micrometer this large sheet which found to be a specimen of good appearance (no dent, cracks, scratches, holes or foreign materials) was cut in 1" diameter. The thickness of the specimen was then measured in at least ten different places with a micrometer. An average value of the thickness was recorded which was accurate to within ± 0.001 mm. Care was taken to avoid surface deformation of the specimen caused by excessive thumbscrew pressure when the micrometer was applied.

The specimen was then mounted into the diffusion cell of the apparatus for degassing in a manner described in Sec. II on page 30. The degassing process was enhanced by pumping both sides of the membrane simultaneously, using two diffusion pump units. The mercury diffusion pump located in the gas measuring system pumped the lower side of the membrane while the oil diffusion pump at the gas feeding system pumped the upper side of the membrane. This insured a faster degassing rate and less strain on the membrane. The preliminary degassing was carried out for two hours at room temperature. The diffusion cell was then immersed in a constant temperature oil bath by raising the bath by a laboratory jack. Intense degassing was continued at 85°C (the highest experimental temperature) until the pressure of the residual gas escaping from the sample was no greater than 3 microns in half an hour. This degassing action lasted about three to four weeks for unfilled and filled samples. The need for this long degassing period was thought to arise from the diffusion of residual solvent and monomers which were trapped in the sample during the menufacturing process.

3. Calibration of the Thermocouple Gauge

Upon completion of the degassing, the calibration of the thermocouple gauge against the McLeod gauge was carried out for H_2 and D_2 at room temperature. The procedure for calibration was, first, to evacuate the low pressure side of the diffusion cell, as well as the pathway to the gas storage

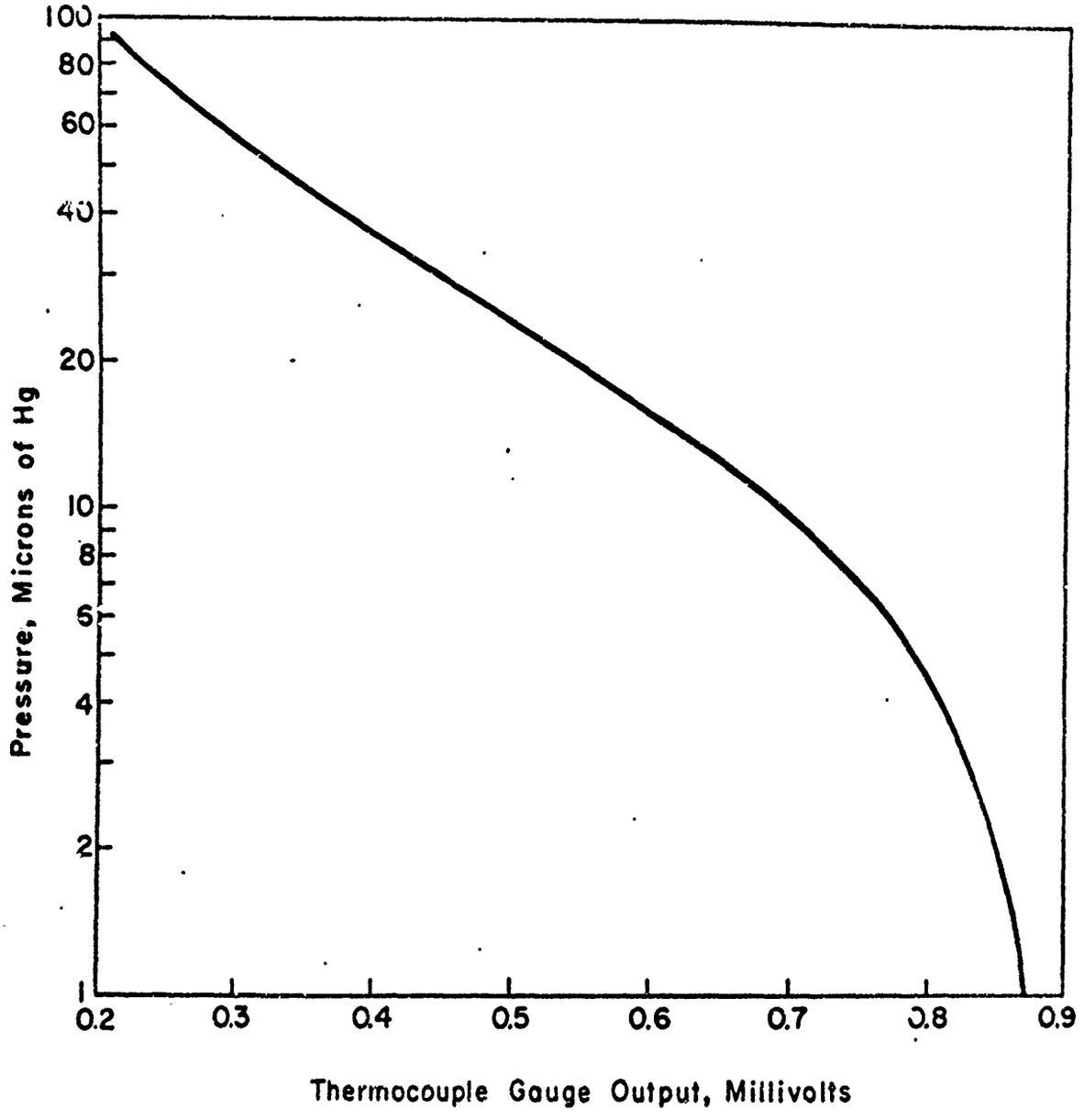

Fig. 10 Thermocouple gauge calibration - H_2

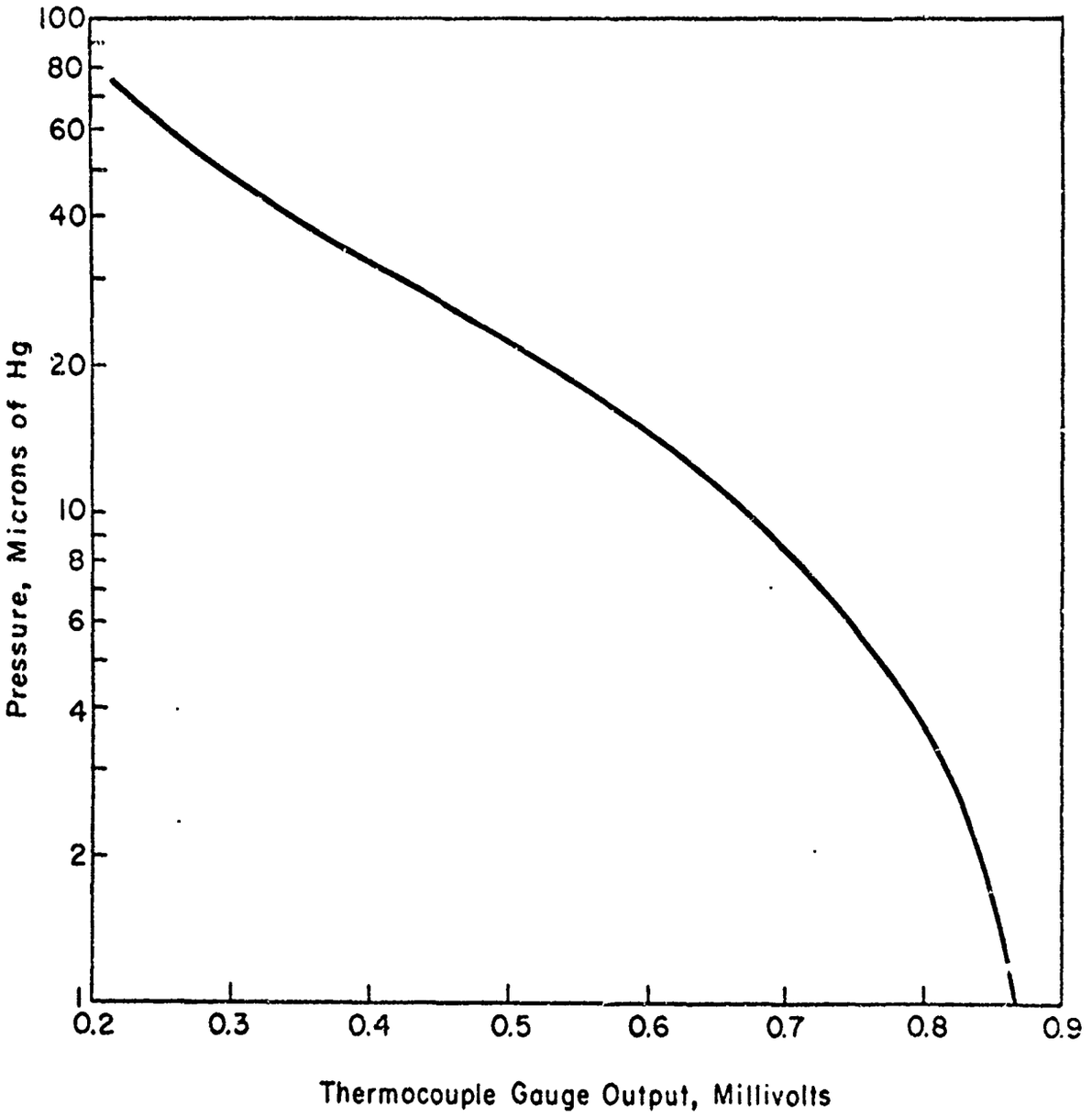

Fig. 11 Thermocouple gauge calibration - D_2

flask, to the highest vacuum, 1 x 10^{-6}cm Hg, and then to feed a small amount of H_2 or D_2 gas from the source into this highly evacuated space to contact with the membrane, thermocouple gauge, and the McLeod gauge. Since the thermocouple gauge is relatively insensitive for pressures above 200 or below 0.1 micron, the calibration was not performed beyond this pressure range. After recording the value of thermocouple gauge output (in millivolts), the absolute pressure was determined by the McLeod gauge. Some of the gas was then allowed to escape from the measuring system and a new set of readings was established. This was repeated for approximately ten micron intervals until the pressure reached the final vacuum. This would give approximately 16 data points for a plot of thermocouple output versus pressure. It is customary to establish the calibration curve by a semi-log plot of the pressure in microns of Hg versus the gauge output in millivolts. Example calibration curves are shown for H_2 and D_2 in Figures 10 and 11. A new calibration was established whenever a new membrane was introduced for an experiment.

4. Collection of Data

After several trial runs, the volume of the receiver, V_1, was found suitable for the experiment. The runs were then carried out in a regular order:

1) Work began with the highest gas pressure at the highest temperature with one kind of gas, say H_2.

2) Keeping the temperature unchanged the gas pressure was varied from the highest to the lowest.

3) The temperature was then changed to the next lower reading and the procedure repeated.

4) The above procedure was then repeated with D_2 gas.

The degassing time after each run depended on the temperature and thickness of the sample. Less time was required for the thinner samples and the higher temperatures. For most experimental condition, about four hours was needed for sufficient degassing. However, in order to insure a thorough degassing, more than four hours were allowed to pass for all runs before the data were collected.

After the completion of the degassing stage, the permeation experiment was proceeded by

1) Adjusting the gas pressure in the storage flask to the proper level by a bleed valve.

2) Recording the time with a stopwatch as soon as the Nupro gate valve was opened. Readings were taken from the thermocouple gauge every half minute for the shortest runs at the highest pressure and temperature, 85°C and 55 cm Hg, and every five minutes for the longest runs at the lowest pressure and temperature, 1 cm. and 40°C. All runs were stopped after the gas transported to the receiver reached a pressure of about 80 micron, since the thermocouple gauge responded best to pressures in the 1 to 75 micron region (see

the calibration curve on pages 46 and 47. This required about 20 minutes for the shortest runs, and five hours for the longer runs.

3) Recording the gas pressure accurately from the monometer with the aid of the 4" magnifier, and isolating the gas source from the diffusion cell by closing the Nupro gate valve.

4) Finally, degassing the membrane for at least four hours before the next run was performed.

5. Calculation of P, D, and S

If the gas obeys the ideal gas law, $pv = n RT$, the pressure in the receiver, V_1, may be treated as proportional to the amount, Q_t, transported. Applying equation (15), a plot of Q_t versus t, was made for each of the permeation runs. The time lag, τ was obtained by extrapolating the linear portion of the plot to the time axis as shown in Figure 12 while the slope of the line gave the flux, Q_s. However, this graphical extrapolation to the time axis is equivalent to evaluating the zero time for the linear pressure rise from the ideal zero value. In order to take into account the small residual pressure in the receiver, V_1, at the beginning of each run, the following analytical method was used to obtain the value of τ rather than merely reading the intercept at the time axis.

The linear portion of the curve in Fig. 12 can be represented by

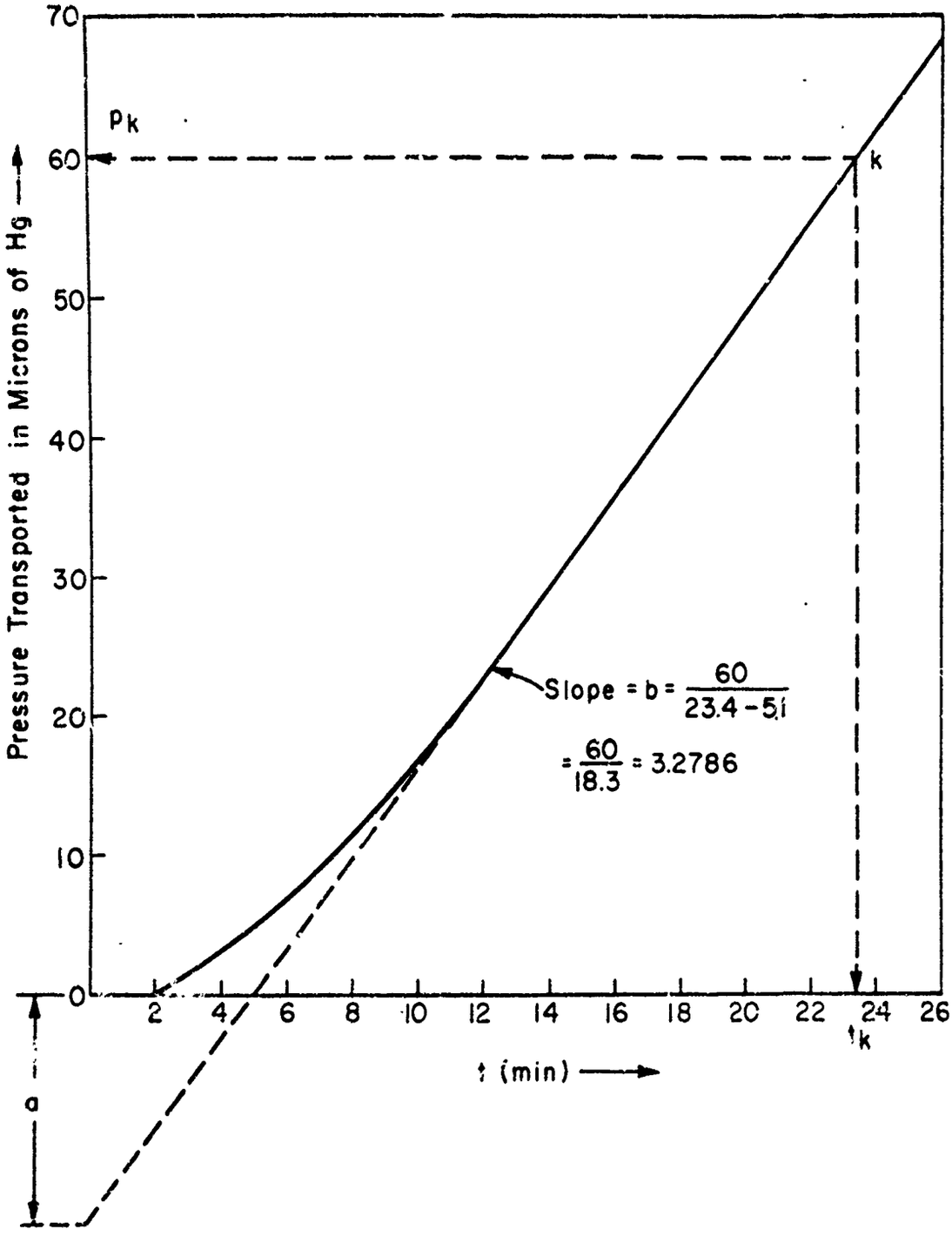

Fig. 12 Typical time lag curve, permeation of D_2 gas through unfilled natural rubber at 70°C and gas pressure of 17.6 cm of Hg.

$$p = a + bt$$

where p is the pressure in microns, b is the slope in micron per minute, t is the time in minutes, and "a" is the intercept in microns. Solving the equation for $t = 0$, at $p = p_o$, one obtains

$$\tau = \frac{p_o - a}{b} \quad \text{min}$$

The diffusion coefficient, D, is calculated from the value of τ as shown in equation (16)

$$D = \frac{L^2}{6\tau} \quad \text{cm}^2/\text{min}$$

or

$$D = \frac{L^2 \times b}{360\,(p_o - a)} \quad \text{cm}^2/\text{sec} \qquad (42)$$

The slope of the line in Fig. 12 represents the steady state flow, Q_s, through a cross sectional area, A. The permeability, P, in equation (9) is then given by

$$P = \frac{Q_s \times L}{A\,\Delta p} \qquad (43)$$

The solubility, S, follows readily according to equation (11), $S = P/D$. A sample calculation of P, D and S is given in Appendix I.

6. Calculation of E_d, E_p, and ΔH_s

The Arrhenius equations (25), quoted on page 16, may be written in the logarithmic form as

$$\log D = \log D_o - \frac{E_d}{2.303\ R}\frac{1}{T} \qquad (44)$$

and

$$\log P = \log P_o - \frac{E_p}{2.303\ R}\frac{1}{T} \qquad (45)$$

where the value of R is 1.987 cal/mole-degree. Thus, a plot of log D or log P against 1/T should give a straight line, the slope of which equals $-E_d/2.303R$ or $-E_p/2.303R$. The activation energy, E_d, or E_p, can thus be evaluated.

However, in order to obtain a best straight line, the graphical method was not used. Instead, the least square method was employed to calculate the slope and the intercept of a best straight line from the data. Since both equations above can be simply represented by

$$y = a + bx \qquad (46)$$

where $y = \log D$ or $\log P$

$a = \log D_o$ or $\log P_o$

$b = E_d/2.303R$ or $E_p/2.303R$

$x = 1/T$

A sample calculation of E_d and E_p is shown in Appendix II. ΔH_s follows as the difference: $(E_p - E_d)$.

III EXPERIMENTAL RESULTS

This section is divided into four parts, devoted to the four types of samples. Values of permeability, P, diffusivity, D and solubility, S at various gas pressures and temperatures studies for each sample are calculated in the same manner as shown in the "sample calculation" in Appendix I and tabulated accordingly. The Tables of P, D, and S are preceeded by a summary of the activation energies for permeation and diffusion, E_p and E_d, the heat of solution, ΔH_s, and the pre-exponential, D_o, at each gas pressure. E_d, E_p and D_o are calculated by the least square method. A sample calculation is given in Appendix II. ΔH_s is the difference of E_p and E_d.

In all cases, the area of the membrane exposed to the penetrant was 2.85 cm^2 cell and a receiver volume, V_1, of 37.9 ml was used. The average thickness of each sample is as the follows:

Sample	Average thickness, cm
Unfilled NR	0.2101
Unfilled SNR	0.2116
Filled NR	0.2097
Filled SNR	0.1926

TABLE 2

ACTIVATION ENERGIES, HEAT OF SOLUTION AND PRE-EXPONENTIAL FOR TRANSPORT OF H_2 OR D_2 GAS THROUGH UNFILLED NATURAL RUBBER AT VARIOUS GAS PRESSURES

gas	Gas Pressure (cm of Hg)	Temp.* Range (°C)	$D_o \times 10^2$ (cm^2/sec.)	E_d (kcal/mole)	E_p (kcal/mole)	ΔH_s (kcal/mole)
H_2	1.1	40 - 85	7.11	5.24	6.34	1.10
"	3.4	"	8.34	5.34	6.28	0.94
"	8.0	"	5.06	5.00	6.32	1.32
"	11.9	"	5.23	5.01	6.27	1.26
"	17.7	"	3.83	4.80	6.34	1.54
"	30.2	"	4.56	4.93	6.23	1.30
"	42.6	"	5.69	5.08	6.15	1.07
"	55.7	"	4.13	4.85	6.26	1.41
D_2	1.0	"	6.11	5.41	6.38	0.97
"	8.1	"	5.92	5.39	6.02	0.63
"	12.0	"	6.61	5.83	6.10	0.27
"	17.6	"	5.27	5.24	6.05	0.81
"	30.2	"	4.92	5.12	5.86	0.74
"	42.7	"	5.79	5.21	5.86	0.65
"	55.7	"	7.36	5.33	5.85	0.52

* The Arrhenius plot is practically linear for the temperature range.

TABLE 3

HYDROGEN GAS TRANSPORT THROUGH UNFILLED NATURAL RUBBER

AT VARIOUS GAS PRESSURES

$\tau = L^2/6D$ $L = 0.2101$ cm

Gas Pressure (cm of Hg)	Temperature (^oC)	Time Lag, τ (min)	D x 10^5 (cm^2/sec)	P x 10^7 (cc gas/sec-atm-cm)	S x 10^2 (cc gas/cm^3-atm)
1.1	40	8.219	1.49	4.29	2.88
	55	4.836	2.54	6.91	2.73
	70	3.860	3.18	10.78	3.39
	85	2.768	4.43	15.96	3.60
3.4	40	8.029	1.53	4.01	2.63
	55	4.947	2.48	6.35	2.56
	70	3.786	3.24	9.91	3.06
	85	2.665	4.60	14.07	3.06

(to be continued)

TABLE 3 (Cont'd)

Gas Pressure (cm of Hg)	Temperature (^{o}C)	Time Lag, τ (min)	D x 10^5 (cm^2/sec)	P x 10^7 (cc gas/sec-atm-cm)	S x 10^2 (cc gas/cm^3-atm)
8.0	40	7.289	1.68	3.75	2.23
	55	5.282	2.32	6.16	2.65
	70	3.841	3.19	9.45	2.96
	85	2.629	4.66	13.31	2.85
11.9	40	7.285	1.68	3.69	2.19
	55	5.027	2.44	5.92	2.43
	70	3.736	3.28	9.20	2.80
	85	2.621	4.68	12.91	2.76
17.7	40	7.306	1.68	3.56	2.12
	55	4.808	2.55	5.73	2.25
	70	3.780	3.24	9.04	2.79
	85	2.718	4.51	12.64	2.80

(to be continued)

TABLE 3 (Cont'd)

Gas Pressure (cm of Hg)	Temperature (^{o}C)	Time Lag, τ (min)	D x 10^5 (cm^2/sec)	P x 10^7 (cc gas/sec-atm-cm)	S x 10^2 (cc gas/cm^3-atm)
30.2	40	7.435	1.65	3.47	2.10
	55	4.908	2.50	5.61	2.25
	70	3.735	3.28	8.75	2.67
	85	2.724	4.50	11.15	2.70
42.6	40	7.426	1.65	3.38	2.54
	55	5.307	2.31	5.61	2.60
	70	3.765	3.26	8.48	2.43
	85	2.665	4.60	11.70	2.05
55.7	40	7.212	1.70	3.30	1.94
	55	4.972	2.47	5.36	2.17
	70	3.764	3.26	8.32	2.56
	85	2.671	4.59	11.55	2.52

TABIE 4

DEUTERIUM GAS TRANSPORT THROUGH UNFILLED NATURAL RUBBER

AT VARIOUS GAS PRESSURES

$\tau = L^2/6D$ L = 0.2101 cm

Gas Pressure (cm of Hg)	Temperature (°C)	Time Lag, τ (min)	D x 10^5 (cm^2/sec)	P x 10^7 (cc gas/sec-atm-cm)	S x 10^2 (cc gas/cm^3-atm)
1.0	40	11.903	1.03	3.94	3.67
	55	8.306	1.48	6.05	4.10
	70	5.488	2.23	9.38	4.20
	85	4.049	3.03	13.57	4.48
8.1	40	7.860	1.04	3.70	3.57
	55	8.136	1.51	5.92	3.93
	70	5.619	2.18	8.85	4.05
	85	4.009	3.06	12.38	4.05

(to be continued)

TABLE 4 (Cont'd)

Gas Pressure (cm of Hg)	Temperature (^{o}C)	Time Lag, τ (min)	D x 10^5 (cm^2/sec)	P x 10^7 (cc gas/sec-atm-cm)	S x 10^2 (cc gas/cm^3-atm)
12.0	40	12.032	1.02	3.65	3.58
	55	8.018	1.53	5.94	3.38
	70	5.508	2.23	8.84	3.97
	85	4.009	3.06	12.50	4.09
17.6	40	10.727	1.14	3.57	3.12
	55	6.919	1.77	5.71	3.22
	70	5.110	2.40	8.51	3.55
	85	3.665	3.35	12.10	3.62
30.2	40	9.512	1.29	3.40	2.64
	55	6.208	1.98	5.43	2.75
	70	4.506	2.72	8.10	2.98
	85	3.353	3.60	11.54	3.16

(to be continued)

TABLE 4 (Cont'd)

Gas Pressure (cm of Hg)	Temperature (°C)	Time Lag, τ (min)	D x 10^5 (cm^2/sec)	P x 10^7 (cc gas/sec-atm-cm)	S x 10^2 (cc gas/cm^3-atm)
42.71	40	9.082	1.35	3.31	2.45
	55	6.208	1.98	5.30	2.68
	70	4.354	2.82	7.80	2.77
	85	3.202	3.83	10.86	2.84
55.7	40	8.808	1.39	3.13	2.25
	55	5.805	2.11	4.92	2.33
	70	4.124	2.97	7.36	2.48
	85	3.005	4.08	10.19	2.50

TABLE 5

ACTIVATION ENERGIES, HEAT OF SOLUTION AND PRE-EXPONENTIAL FOR TRANSPORT OF H_2 OR D_2 GAS THROUGH UNFILLED SYNTHETIC NATURAL RUBBER AT VARIOUS GAS PRESSURES

Gas	Gas Pressure (cm of Hg)	Temp. Range (°C)	$D_o \times 10^2$ (cm^2/sec.)	E_d (kcal/mole)	E_p (kcal/mole)	ΔH_s (kcal/mole)
H_2	1.2	40 - 85	3.87	4.80	5.87	1.07
"	9.1	"	4.06	4.85	5.94	1.09
"	17.5	"	5.96	5.06	5.96	0.90
"	24.8	"	5.07	4.95	5.96	1.01
"	33.5	"	4.62	4.90	5.91	1.01
"	42.7	"	5.65	5.04	5.89	0.85
"	57.8	"	5.40	4.96	6.24	1.28
D_2	1.1	"	11.20	5.42	5.86	0.44
"	8.8	"	7.02	5.77	5.79	0.02
"	17.4	40 - 70	6.49	5.15	6.27	1.12
"	24.7	40 - 85	5.85	5.08	6.14	1.06
"	33.5	"	7.29	5.28	6.19	0.91
"	42.7	"	7.92	5.29	5.83	0.64
"	57.9	"	8.42	5.30	6.14	0.84

TABLE 6

HYDROGEN GAS TRANSPORT THROUGH UNFILLED SYNTHETIC NATURAL RUBBER

AT VARIOUS GAS PRESSURES

$\tau = L^2/6D$ $L = 0.2116$ cm

Gas Pressure (cm of Hg)	Temperature (^{o}C)	Time Lag, τ (min)	D x 10^5 (cm^2/sec)	P x 10^7 (cc gas/sec-atm-cm)	S x 10^2 (cc gas/cm^3-atm)
1.2	40	7.400	1.68	3.97	2.36
	60	4.362	2.85	7.81	2.74
	70	3.592	3.46	9.34	2.70
	85	2.817	4.41	13.18	2.99
9.1	40	7.520	1.65	3.80	2.30
	60	4.707	2.64	7.09	2.68
	70	3.885	3.20	9.00	2.81
	85	2.783	4.47	12.78	2.86

(to be continued)

TABLE 6 (Cont'd)

Gas Pressure (cm of Hg)	Temperature (°C)	Time Lag, τ (min)	D x 10^5 (cm^2/sec)	P x 10^7 (cc gas/sec-atm-cm)	S x 10^2 (cc gas/cm^3-atm)
17.5	40	7.116	1.75	3.90	2.23
	60	4.313	2.88	7.21	2.50
	70	3.553	3.50	8.94	2.55
	--	--	--	--	--
24.8	40	7.312	1.70	3.86	2.27
	60	4.042	3.08	6.97	2.27
	70	3.499	3.55	9.60	2.70
	85	2.901	4.28	12.78	2.98
33.5	40	7.198	1.73	3.82	2.21
	60	4.328	2.87	6.94	2.42
	70	3.522	3.53	9.40	2.66
	85	2.651	4.69	12.50	2.67

(to be continued)

TABLE 6 (Cont'd)

Gas Pressure (cm of Hg)	Temperature (^{o}C)	Time Lag, τ (min)	D x 10^5 (cm^2/sec)	P x 10^7 (cc gas/sec-atm-cm)	S x 10^2 (cc gas/cm^3-atm)
42.7	40	7.534	1.65	3.72	2.25
	60	4.192	2.97	6.30	2.12
	70	3.518	3.53	9.13	2.58
	85	2.702	4.60	12.19	2.65
57.8	40	6.642	1.82	3.24	1.78
	50	5.031	2.47	4.44	1.80
	60	4.053	3.07	6.07	1.98
	70	3.301	3.77	7.98	2.12
	85	2.469	5.03	11.38	2.26

TABLE 7

DEUTERIUM GAS TRANSPORT THROUGH UNFILLED SYNTHETIC NATURAL RUBBER

AT VARIOUS GAS PRESSURES

$\tau = L^2/6D$ $L = 0.2116$ cm

Gas Pressure (cm of Hg)	Temperature (°C)	Time Lag, τ (min)	D x 10^5 (cm^2/sec)	P x 10^7 (cc gas/sec-atm-cm)	S x 10^2 (cc gas/cm^3-atm)
1.1	40	7.779	1.60	4.18	2.62
	50	5.572	2.23	5.83	2.61
	60	3.506	3.55	7.54	2.13
	70	4.322	2.88	11.05	3.84
	85	2.301	5.40	13.00	2.41
8.8	40	8.031	1.55	3.65	2.36
	50	5.547	2.24	4.91	2.19
	60	4.421	2.81	6.66	2.37
	70	3.530	3.52	8.36	2.37
	85	2.762	4.50	11.62	2.58

(to be continued)

TABLE 7 (Cont'd)

Gas Pressure (cm of Hg)	Temperature (°C)	Time Lag, τ (min)	D x 10^5 (cm^2/sec)	P x 10^7 (cc gas/sec-atm-cm)	S x 10^2 (cc gas/cm^3-atm)
17.4	40	7.712	1.61	3.51	2.18
	50	5.914	2.10	4.89	2.33
	60	4.509	2.76	6.61	2.40
	70	3.808	3.26	8.50	2.60
24.7	40	7.707	1.61	3.42	2.12
	50	5.505	2.26	4.68	2.07
	60	4.607	2.70	6.50	2.41
	70	3.703	3.36	8.39	2.50
	85	2.702	4.60	11.59	2.52
33.5	40	7.913	1.57	3.32	2.11
	50	5.806	2.14	4.58	2.14
	60	4.522	2.75	6.24	2.27
	70	3.704	3.36	8.18	2.44
	85	2.714	4.58	11.54	2.52

(to be continued)

TABLE 7 (Cont'd)

Gas Pressure (cm of Hg)	Temperature (°C)	Time Lag, τ (min)	D x 10^5 (cm^2/sec)	P x 10^7 (cc gas/sec-atm-cm)	S x 10^2 (cc gas/cm^3 atm)
42.7	40	7.809	1.59	3.18	2.00
	50	6.005	2.07	4.51	2.18
	60	4.519	2.75	5.97	2.17
	70	3.713	3.35	7.87	2.35
	85	2.676	4.65	10.31	2.22
57.9	40	7.426	1.67	3.09	1.85
	50	5.666	2.19	4.25	1.94
	60	4.425	2.81	5.94	2.12
	70	3.353	3.73	7.41	2.00
	85	2.579	4.82	10.73	2.23

TABLE 8

ACTIVATION ENERGIES, HEAT OF SOLUTION AND PRE-EXPONENTIAL FOR TRANSPORT OF H_2 OR D_2 GAS THROUGH FILLED NATURAL RUBBER AT VARIOUS GAS PRESSURES

Gas	Gas Pressure (cm of Hg)	Temp. Range (°C)	$D_o \times 10$ (cm^2/sec.)	E_d (kcal/mole)	E_p (kcal/mole)	ΔH_s (kcal/mole)
H_2	1.1	40 - 85	2.78	6.96	7.33	0.37
"	3.5	"	3.66	7.20	6.66	-0.54
"	8.1	"	2.14	6.83	6.89	0.06
"	12.0	"	4.09	7.26	6.60	-0.66
"	17.7	"	2.76	6.98	6.52	-0.46
"	30.2	"	3.47	7.08	6.49	-0.59
"	42.7	"	3.91	7.08	6.93	-0.15
"	55.61	"	3.02	6.92	6.64	-0.28
D_2	1.1	"	0.79	6.16	6.61	0.45
"	3.5	"	0.96	6.33	6.90	0.57
"	8.1	"	0.92	6.36	6.63	0.27
"	12.1	"	1.58	6.71	6.81	0.10
"	17.2	"	1.45	6.60	6.88	0.28
"	30.4	"	1.43	6.59	6.53	-0.06
"	42.6	"	1.01	6.47	6.48	0.01
"	55.1	"	1.01	6.41	7.0	0.59

TABLE 9

HYDROGEN GAS TRANSPORT THROUGH FILLED NATURAL RUBBER

AT VARIOUS GAS PRESSURES

$\tau = L^2/6D$ $L = 0.2097$ cm

Gas Pressure (cm of Hg)	Temperature (°C)	Time Lag, τ (min)	D x 10^5 (cm^2/sec)	P x 10^7 (cc gas/sec-atm-cm)	S x 10^2 (cc gas/cm^3-atm)
1.1	40	30.53	0.40	2.57	6.42
	55	20.52	0.60	4.47	7.50
	70	11.62	1.05	7.42	7.06
	85	7.70	1.59	11.22	7.08
3.5	40	34.69	0.35	2.30	6.52
	55	20.80	0.59	3.93	6.69
	70	14.05	0.87	6.05	6.96
	85	7.82	1.56	8.80	5.63

(to be continued)

TABLE 9 (Cont'd)

Gas Pressure (cm of Hg)	Temperature (°C)	Time Lag, τ (min)	D x 10^5 (cm^2/sec)	P x 10^7 (cc gas/sec-atm-cm)	S x 10^2 (cc gas/cm^3-atm)
8.1	40	33.64	0.36	2.04	5.65
	55	20.08	0.61	3.61	6.00
	70	12.75	0.96	5.75	5.94
	85	8.51	1.43	8.11	5.62
12.0	40	35.29	0.35	2.11	6.12
	55	20.84	0.59	3.56	6.07
	70	12.83	0.95	5.50	5.78
	85	8.08	1.51	8.03	5.31
17.7	40	32.22	0.38	1.97	5.20
	55	18.78	0.65	3.30	5.07
	70	12.22	1.00	5.21	5.22
	85	7.83	1.56	7.24	4.65

(to be continued)

TABLE 9 (Cont'd)

Gas Pressure (cm of Hg)	Temperature (°C)	Time Lag, τ (min)	D x 10^5 (cm^2/sec)	P x 10^7 (cc gas/sec-atm-cm)	S x 10^2 (cc gas/cm^3-atm)
30.2	40	31.07	0.39	1.87	4.75
	55	17.52	0.70	3.08	4.42
	70	11.76	1.04	4.38	4.22
	85	7.26	1.68	6.72	4.00
42.7	40	28.00	0.44	1.61	3.70
	55	16.84	0.73	2.84	3.92
	70	11.74	1.04	4.46	3.29
	85	7.04	1.73	6.08	3.51
55.6	40	27.10	0.45	1.57	3.52
	55	16.50	0.74	2.70	3.65
	70	10.00	1.22	4.09	3.36
	85	6.87	1.78	5.99	3.37

TABLE 10

DEUTERIUM GAS TRANSPORT THROUGH FILLED NATURAL RUBBER

AT VARIOUS GAS PRESSURES

$\tau = L^2/6D$ $L = 0.2097$ cm

Gas Pressure (cm of Hg)	Temperature (°C)	Time Lag, τ (min)	D x 10^5 (cm^2/sec)	P x 10^7 (cc gas/sec-atm-cm)	S x 10^2 (cc gas/cm^3-atm)
1.1	40	30.53	0.40	2.61	6.53
	55	20.15	0.61	4.25	5.38
	70	12.33	0.99	6.54	5.33
	85	9.02	2.35	10.12	7.48
3.5	40	34.01	0.36	2.19	6.11
	55	21.31	0.57	3.60	6.28
	70	12.79	0.96	5.68	5.95
	85	9.73	1.26	8.79	7.00

(to be continued)

TABLE 10 (Cont'd)

Gas Pressure (cm of Hg)	Temperature (^{o}C)	Time Lag, τ (min)	D x 10^5 (cm^2/sec)	P x 10^7 (cc gas/sec-atm-cm)	S x 10^2 (cc gas/cm^3-atm)
8.1	40	36.12	0.34	1.98	5.85
	55	23.04	0.53	3.35	6.33
	70	15.02	0.81	5.26	6.46
	85	10.01	1.22	7.50	6.14
12.1	40	37.23	0.33	1.95	5.94
	55	23.04	0.53	3.26	6.15
	70	15.02	0.81	5.06	6.23
	85	9.61	1.27	7.21	5.67
17.2	40	33.64	0.36	1.79	4.92
	55	20.52	0.60	3.01	5.07
	70	13.81	0.88	4.82	5.45
	85	8.72	1.40	7.08	5.05

(to be continued)

TABLE 10 (Cont'd)

Gas Pressure (cm of Hg)	Temperature (^{o}C)	Time Lag, τ (min)	D x 10^5 (cm^2/sec)	P x 10^7 (cc gas/sec-atm-cm)	S x 10^2 (cc gas/cm^3-atm)
30.4	40	34.11	0.36	1.72	4.80
	55	20.52	0.60	2.91	4.89
	70	13.32	0.92	4.42	4.82
	85	9.02	1.35	6.46	4.78
42.6	40	40.03	0.31	1.95	6.38
	55	24.08	0.51	3.37	6.64
	70	15.02	0.81	4.95	6.09
	85	11.00	1.11	7.26	6.54
56.1	40	34.31	0.36	1.64	4.60
	55	18.12	0.67	2.52	3.73
	70	13.83	0.88	4.88	5.53
	85	8.92	1.37	6.32	4.61

TABLE 11

ACTIVATION ENERGIES, HEAT OF SOLUTION AND PRE-EXPONENTIAL FOR TRANSPORT OF H_2 OR D_2 GAS THROUGH FILLED SYNTHETIC NATURAL RUBBER AT VARIOUS GAS PRESSURES

Gas	Gas Pressure (cm of Hg)	Temp. Range (°C)	$D_o \times 10$ (cm^2/sec.)	E_d (kcal/mole)	E_p (kcal/mole)	ΔH_s (kcal/mole)
H_2	1.1	40 - 85	1.69	6.55	6.88	0.33
"	3.5	"	1.67	6.58	6.25	-0.33
"	8.1	"	1.94	6.77	6.09	-0.68
"	12.1	"	2.72	6.94	6.02	-0.92
"	17.7	"	1.63	6.55	6.46*	-0.09
"	30.2	"	1.90	6.58	6.23*	-0.35
"	42.8	"	1.85	6.51	6.12**	-0.39
"	55.0	"		6.38	6.09**	-0.29
D_2	1.2	"	1.44	6.46	6.85	0.39
"	3.5	"	0.67	6.06	6.54	0.48
"	8.0	"	0.58	6.00	6.71	0.71
"	12.0	"	0.67	6.07	6.26	0.19
"	17.7	"	0.55	5.92	6.22	0.30
"	30.1	"	0.57	5.89	6.44*	0.55
"	42.7	"	0.66	5.96	6.03**	0.07
"	56.0	"	0.62	5.89	6.05**	0.16

*For Temperature Range, 50-85°C

**For Temperature Range, 60-85°C

TABLE 12

HYDROGEN GAS TRANSPORT THROUGH FILLED SYNTHETIC NATURAL RUBBER

AT VARIOUS GAS PRESSURES

$\tau = L^2/6D$ L = 0.1926 cm

Gas Pressure (cm of Hg)	Temperature (^{o}C)	Time Lag, τ (min)	D x 10^5 (cm^2/sec)	P x 10^7 (cc gas/sec-atm-cm)	S x 10^2 (cc gas/cm^3-atm)
1.1	40	23.00	0.45	2.88	6.43
	50	16.75	0.62	3.82	6.22
	60	11.21	0.92	5.37	5.84
	70	9.54	1.08	7.43	6.88
	85	6.02	1.71	11.37	6.64
3.5	40	25.13	0.41	2.80	6.84
	50	16.56	0.62	3.78	6.08
	60	13.28	0.78	5.08	6.55
	70	9.13	1.13	6.73	5.97
	85	6.59	1.56	9.90	6.31

(to be continued)

TABLE 12 (Cont'd)

Gas Pressure (cm of Hg)	Temperature (^{o}C)	Time Lag, τ (min)	D x 10^5 (cm^2/sec)	P x 10^7 (cc gas/sec-atm-cm)	S x 10^2 (cc gas/cm^3-atm)
8.1	40	27.55	0.37	2.84	7.60
	50	21.55	0.48	3.93	8.21
	60	14.55	0.71	5.27	7.44
	70	10.10	1.02	6.49	6.36
	85	7.51	1.37	9.90	7.22
12.1	40	27.26	0.38	2.84	7.51
	50	18.27	0.56	3.54	6.28
	60	12.81	0.80	4.92	6.12
	70	9.91	1.04	6.36	6.12
	85	6.71	1.54	9.39	6.11
17.7	40	23.74	0.43	3.07	7.07
	50	17.37	0.59	3.39	5.72
	60	12.53	0.82	4.58	5.57
	70	9.58	1.07	6.16	5.73
	--	--	--	--	--

(to be continued)

TABLE 12 (Cont'd)

Gas Pressure (cm of Hg)	Temperature (°C)	Time Lag, τ (min)	D x 10^5 (cm^2/sec)	P x 10^7 (cc gas/sec-atm-cm)	S x 10^2 (cc gas/cm^3-atm)
30.2	40	20.90	0.49	2.96	5.99
	50	16.23	0.63	3.11	4.90
	60	11.31	0.91	4.22	4.63
	70	8.51	1.21	5.66	4.67
	85	5.61	1.84	7.98	4.34
42.8	40	19.62	0.53	2.78	5.30
	50	13.72	0.75	3.72	4.96
	60	10.63	0.97	3.97	4.10
	70	7.91	1.30	5.12	3.93
	85	5.22	1.97	7.15	3.62
55.0	40	18.43	0.56	2.60	4.66
	--	--	--	--	--
	60	10.22	1.01	3.52	3.49
	--	--	--	--	--
	85	5.00	2.06	6.80	3.30

TABLE 13

DEUTERIUM GAS TRANSPORT THROUGH FILLED SYNTHETIC NATURAL RUBBER AT VARIOUS GAS PRESSURES

$\tau = L^2/6D$ $L = 0.1926$ cm

Gas Pressure (cm of Hg)	Temperature (°C)	Time Lag, τ (min)	D x 10^5 (cm^2/sec)	P x 10^7 (cc gas/sec-atm-cm)	S x 10^2 (cc gas/cm^3-atm)
1.2	40	23.42	0.44	2.50	5.65
	50	16.89	0.61	3.55	5.80
	60	11.98	0.86	4.90	5.67
	70	9.63	1.07	6.61	6.19
	85	6.24	1.65	10.15	6.14
3.5	40	27.11	0.38	2.40	6.28
	50	18.08	0.57	3.26	5.74
	60	15.15	0.68	4.70	6.94
	70	11.32	0.91	6.15	6.74
	85	7.58	1.36	8.89	6.56

(to be continued)

TABLE 13 (Cont'd)

Gas Pressure (cm of Hg)	Temperature (°C)	Time Lag, τ (min)	D x 10^5 (cm^2/sec)	P x 10^7 (cc gas/sec-atm-cm)	S x 10^2 (cc gas/cm^3-atm)
8.0	40	27.85	0.37	2.23	5.97
	50	20.20	0.51	3.23	6.36
	60	14.72	0.70	4.41	6.32
	70	11.71	0.88	5.98	6.80
	85	8.24	1.25	8.66	6.92
12.0	40	25.13	0.41	2.28	5.64
	50	21.03	0.49	3.20	6.51
	--	--	--	--	--
	70	10.62	0.97	5.59	5.78
	85	7.41	1.39	8.12	5.83
17.7	40	23.42	0.44	2.36	5.37
	50	20.61	0.50	3.16	6.34
	60	14.51	0.71	4.19	5.92
	70	11.32	0.91	5.61	6.15
	85	7.41	1.39	8.21	5.91

(to be continued)

TABLE 13 (Cont'd)

Gas Pressure (cm of Hg)	Temperature (°C)	Time Lag, τ (min)	D x 10^5 (cm^2/sec)	P x 10^7 (cc gas/sec-atm-cm)	S x 10^2 (cc gas/cm^3-atm)
30.1	40	22.90	0.45	2.75	6.147
	50	17.46	0.59	2.80	4.78
	60	13.21	0.78	3.86	4.96
	70	10.00	1.03	5.08	4.94
	85	7.15	1.44	7.47	5.18
42.7	40	22.90	0.45	2.79	4.62
	50	16.10	0.64	3.55	4.79
	60	12.72	0.81	3.70	4.58
	70	9.91	1.04	4.99	5.53
	85	6.69	1.54	7.10	6.23
56.0	40	21.46	0.48	2.43	5.05
	50	15.85	0.65	3.69	5.71
	60	12.71	0.81	3.63	4.49
	70	9.12	1.13	4.54	4.02
	85	6.60	1.56	6.93	4.45

IV DISCUSSION OF RESULTS

The experimental results listed in Table 2 through 13 in Section III are discussed in the order of (A), diffusivity, D, solubility, S, and permeability, P; (B), activation energies for diffusion and permeation, E_d and E_p, and heat of solution, ΔH_s and, (C), the free volume of rubber. Except for the free volumes, all the above quantities are treated as a function of gas pressures and in one case as a function of temperature.

A. Diffusivity, D, Solubility, S, and Permeability, P.

1. Diffusivity, D, as a Function of Gas Pressure

The diffusion coefficients evaluated from the time lag τ, according to equation (16), assuming a constant D,

$$\tau = \frac{L^2}{6D}$$

for the transport of hydrogen and deuterium gas through the four samples, are separately plotted against the gas pressure as shown in Figures 13 to 16. In examining these figures, one finds that these diffusivity isotherms are indeed largely independent of the gas pressure at low temperatures, and become slightly pressure dependent at higher temperatures but, in no case, does the difference of the diffusivities through the pressure range, i.e., between 1 and 55 cm of Hg, for any isotherm exceed the unit value ($1 cm^2/sec$) of diffusivity. The average

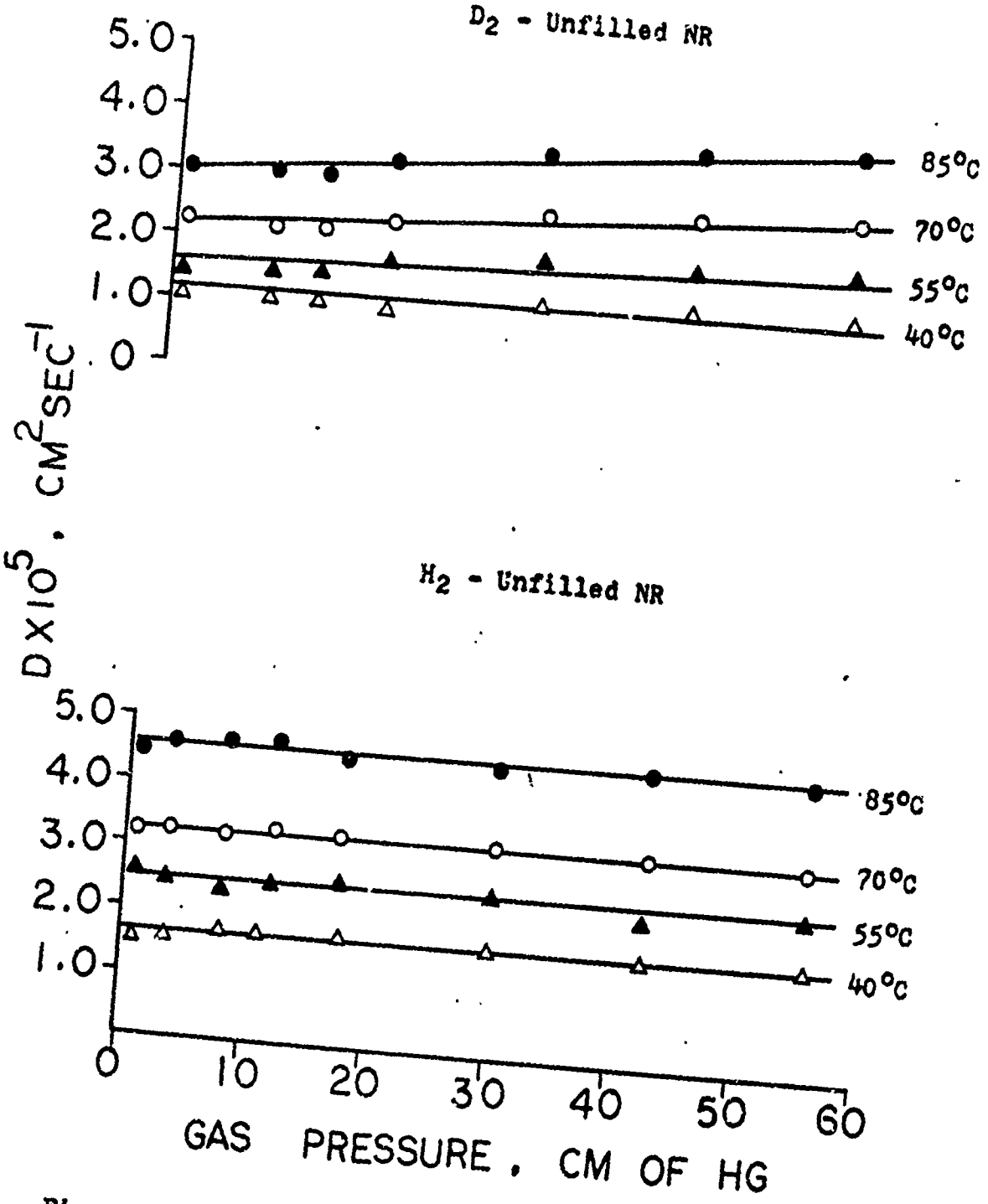

Fig. 13 - Difusivity isotherms versus gas pressure for unfilled natural rubber and penetrants, H_2 and D_2

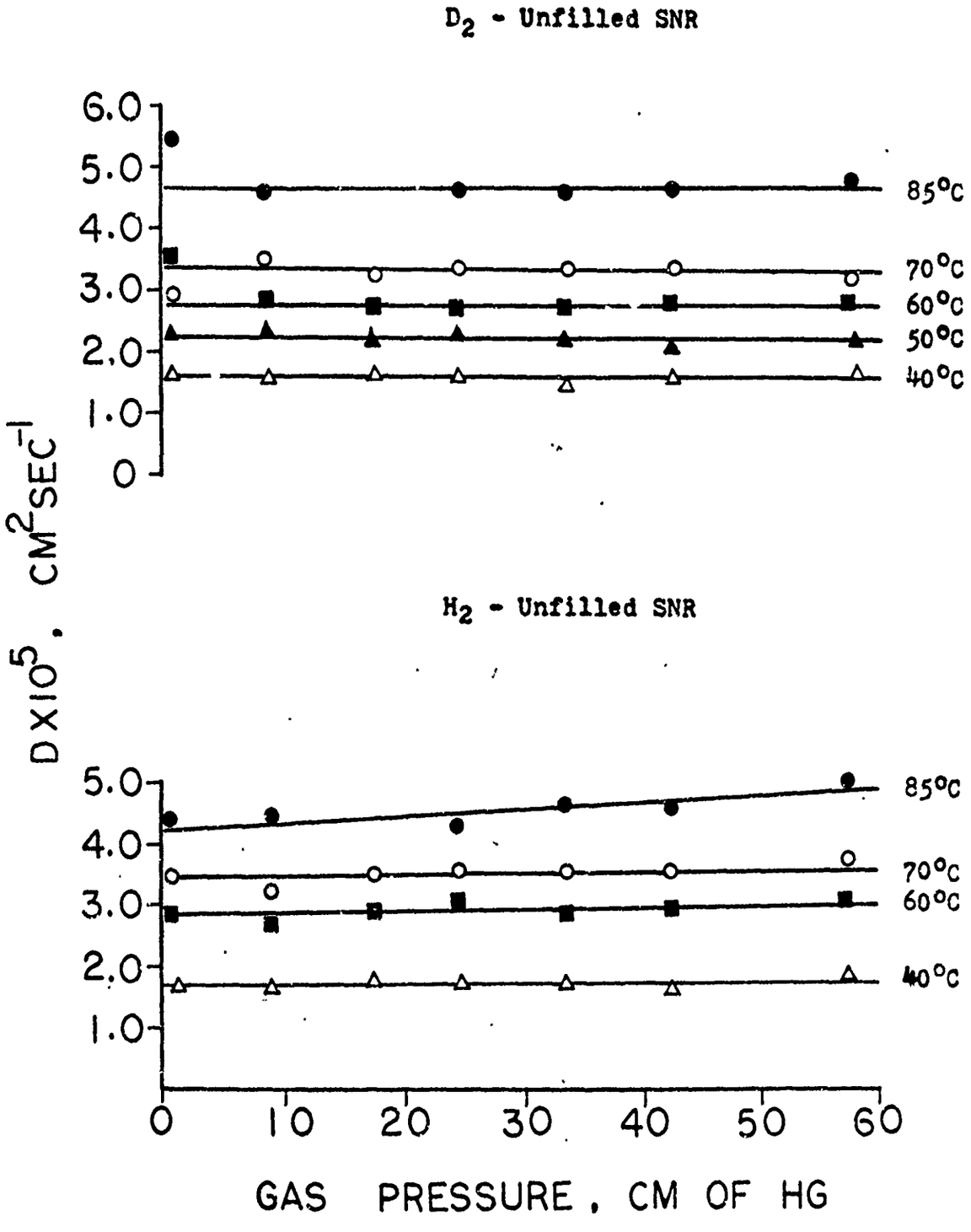

Fig. 14 - Diffusivity isotherms versus gas pressure for unfilled synthetic natural rubber and penetrants, H_2 and D_2.

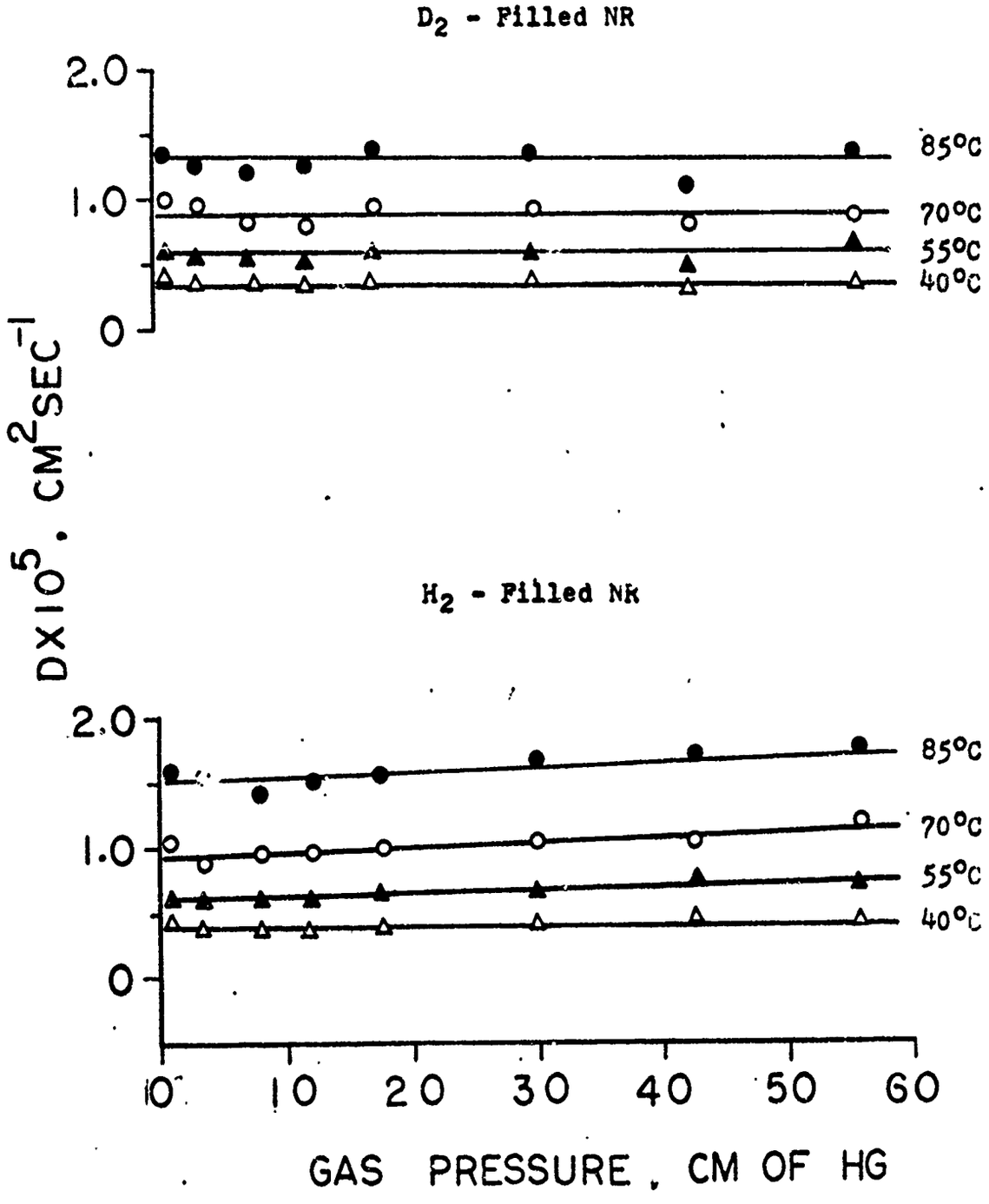

Fig. 15 - Diffusivity isotherms versus gas pressure for filled natural rubber and penetrants, H_2 and D_2.

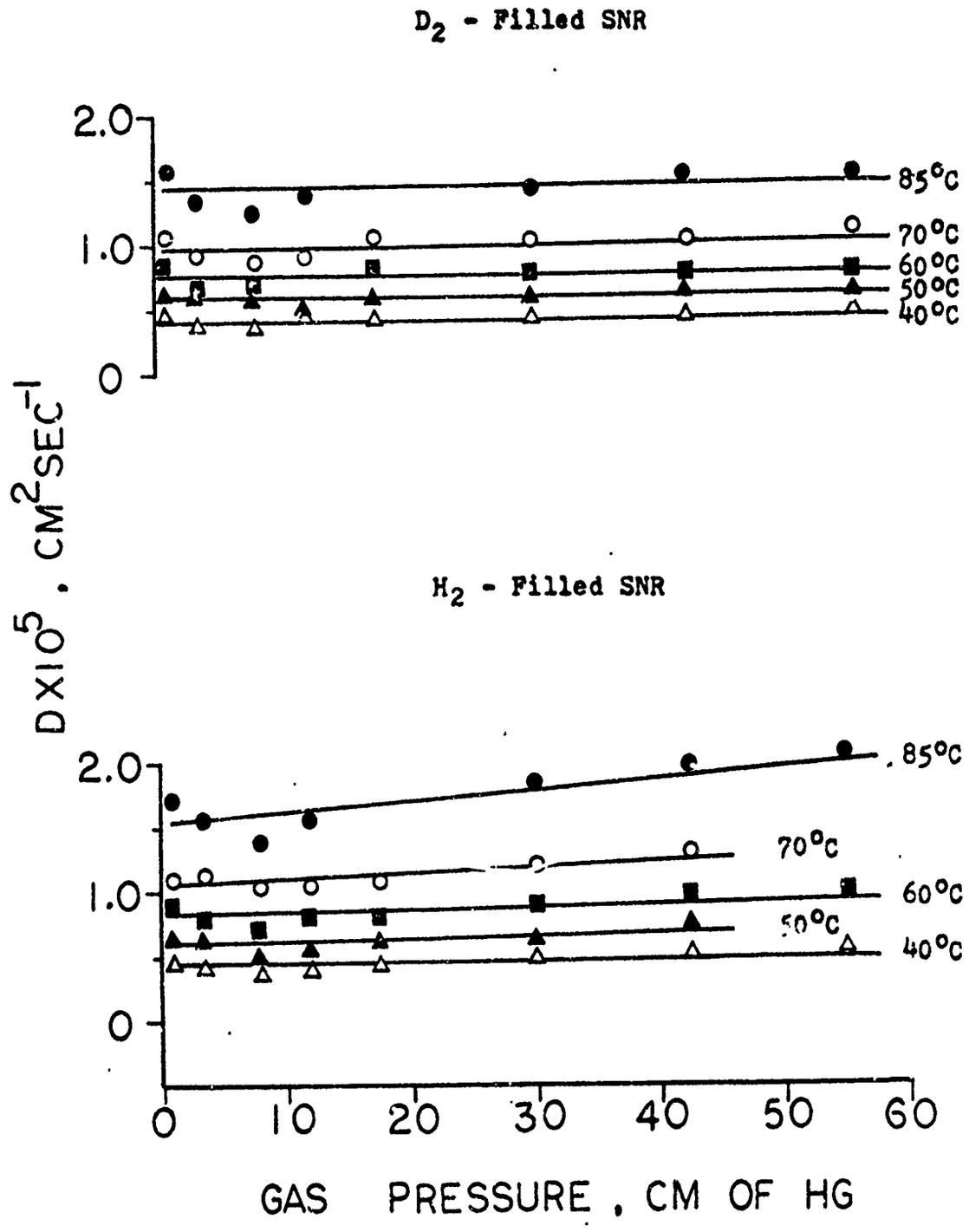

Fig. 16 - Diffusivity isotherms versus gas pressure for filled synthetic natural rubber and penetrants, H_2 and D_2

values of each isotherm are listed in Table 14.

Comparison of these values reveals three effects which influence the magnitude of the diffusivity (besides the temperature): the effects of the penetrant mass, that of the nature of the rubber, and the effect of the filler in the rubber. The first indicates that, in the same medium, hydrogen has a higher diffusivity than its isotope, deuterium; the second shows that this difference varies very much with the nature of the rubber; and the third effect indicates that, for the same penetrant, the diffusivity in the filled rubber is several times lower than in the unfilled rubber.

(1) Effect of the penetrant mass: An influence of mass is obvious if one considers the translational kinetic energy of a penetrant along the diffusion coordinate, yielding

$$E_k = \tfrac{1}{2} kT = \tfrac{1}{2} m_i v_i^2$$

This equation shows clearly that at the same temperature, the lighter penetrant should have a higher penetrating velocity. For H_2 and D_2 the mass ratio is 2, and therefore the diffusion ratio should be 1.4. For unfilled, and less so for filled, NR we see the ratios to be close to the ideal values, within the experimental error. For SNR, there is practically no difference between the diffusivities of H_2 and D_2. This is quite remarkable because the difference in mass must affect the diffusion mechanism. There must be a compensating mechanism that enhances the diffusion of D_2 in SNR, possibly connected with the lack of crystallinity in

TABLE 14

AVERAGE VALUE OF DIFFUSIVITIES FOR GAS PRESSURES IN THE RANGE OF 1 TO 55 cm Hg AT CONSTANT TEMPERATURE

Gas	t (°C)	Unfilled NR $\bar{D}$	Filled NR $\bar{D}$	Ratio ($\bar{D}_{unf.}/\bar{D}_{filled}$)
H_2	40	1.63	0.39	4.19
	55	2.45	0.65	3.78
	70	3.24	1.02	3.19
	85	4.57	1.61	2.85
D_2	40	1.18	0.35	3.37
	55	1.76	0.58	3.06
	70	2.51	0.88	2.84
	85	3.44	1.29	2.66

Gas	t (°C)	Unfilled SNR $\bar{D}$	Filled SNR $\bar{D}$	Ratio ($\bar{D}_{unf.}/\bar{D}_{filled}$)
H_2	40	1.71	0.45	3.78
	60	2.82	0.86	3.27
	70	3.51	1.12	3.12
	85	4.58	1.72	2.66
D_2	40	1.60	0.43	3.75
	50	2.18	0.57	3.82
	60	2.87	0.76	3.77
	70	3.35	0.99	3.37
	85	4.63	1.44	3.21

$\bar{D}$ in $cm^2/sec.$
Filler content is 0.16 volume fraction.

the latter, (see also Table 17).

(2) Effect of filler: Fillers contained in the rubber may be reinforcing or non-reinforcing and their particles may be spherical or non-spherical depending on the type. The most important groups are mineral fillers, fibrillar or lamellar fillers, reinforcing and non-reinforcing carbon blacks, and organic fillers such as resins, pigments or other rubber phases. The particular type of filler (carbon black) used here is a reinforcing one. Consequently, the filler particles will not only act as impermeable barriers but also affect the structure of the rubber in their vicinity by various types of rubber-filler attachments. If the surfaces of the particles are wetted by the rubber and thus induce a more or less dense distribution of rubber chain segments at the interface, the filler particles will certainly have the effect of reducing the overall chain flexibility. This is evidenced by data in Table 14. The ratio of the average diffusivity for the unfilled rubber to the filled ranges approximately from 2.6 to 4.2, and the ratio decreases as the temperature increases. The latter fact implies that the diffusivity increases faster with the temperature in the filled rubber than in the corresponding unfilled one, probably as the result of a desorption of the locally concentrated segments from the filler surfaces, thus making the filled rubber relatively more flexible.

Diffusivities measured by van Amerongen[30,31] for natural rubber containing various types of fillers are quoted in Table 15. Also of interest are the data of Ziegel[40].

TABLE 15

DIFFUSIVITY D ($cm^2 sec^{-1}$) AND SOLUBILITY S (cc gas $cm^{-3} atm^{-1}$) OF GASES IN NATURAL RUBBER COMPOUNDS CONTAINING VARIOUS TYPES OF FILLERS AT 25°C[30,31]

Data on S from Indirect and Direct Measurements

	Vol. fraction	H_2			N_2			O_2		
		$Dx10^6$	S(=Q/D)	$S_{dir.}$	$Dx10^6$	S(=Q/D)	$S_{dir.}$	$Dx10^6$	S(=Q/D)	$S_{dir.}$
No filler		10.0	0.038		1.1	0.058		1.65	0.109	
No filler at 43°C		18.5	0.042							
Mineral fillers										
Whiting	0.18				0.95	0.051		1.4	0.097	
Aluminum oxide	0.17				1.0	0.051		1.5	0.097	
Barium sulfate	0.18				0.94	0.052		1.4	0.099	
Hi-sil	0.22	4.1	0.061		0.63	0.060		0.62	0.18	
Durosil	0.18	4.4	0.064		0.88	0.050		0.90	0.13	
Aerosil	0.18	6.2	0.045		0.76	0.055		1.2	0.098	
Lamellar fillers										
Aluminum powder	0.18	3.9	0.032		0.40	0.050		0.57	0.095	
Mica powder	0.18	2.7	0.031		0.30	0.043		0.42	0.086	
Carbon blacks										
Thermax (MT)	0.22			0.036	0.96	0.048	0.048	1.4	0.094	0.088
P 33 (FT)	0.22	7.2	0.041	0.038	0.96	0.048	0.048	1.4	0.093	0.098
Statex K (VFF)	0.22	2.8	0.098	0.11	0.53	0.079	0.097	0.64	0.19	0.19
Vulcan 3 (HAF)	0.22	2.0	0.13	0.12	0.50	0.080	0.15	0.54	0.21	0.35
Spheron 9 (EPC)	0.22	2.5	0.11	0.13	0.11	0.38	0.46	0.19	0.64	0.61
Spheron 4 (HPC)	0.22	1.9	0.16	0.13	0.10	0.41	0.61	0.15	0.82	0.93

Comparing the uncorrected value for D of the unfilled samples, without adjusting for the difference in temperatures, we find $D = 1.63 \times 10^{-5}$ versus $D = 1.85 \times 10^{-5}$ from von Amerongen's data. This is in excellent agreement if one takes into account the three degrees difference in temperature, and the inevitable differences in rubber samples. Taking the filled samples, a comparison becomes more difficult. But we can see that, for the comparable carbon black, Amerongen finds the ratio of the unfilled to the filled samples to be also in the range of 4 to 5. Comparing with Ziegel, his value of 1.82×10^{-5} at 44°C for the unfilled SNR for deuterium is also in excellent agreement with our value of 1.60×10^{-5} at 40°C. For hydrogen there is also good agreement. As shown by Meares[41], these values of diffusivities are typical for hydrocarbon rubbers. The present values for the filler effect are also supported by other relevant data in the literture[42,43].

The present data differ, however, from Ziegel's in that they do not show the strong pressure dependence of the diffusion constant at low pressures. It is likely that in this range Ziegel's data exhibit a spurious trend because his thermocouple gauge was not as accurate as the one used here. From the gas pressure of about 10 cm Hg on, our and his data are quite comparable.

Concerning the magnitude of the filler effect, we see that permeation has been reduced much beyond the change in penetrable cross-section which is about 36% of the unfilled rubber. In fact, the change in D is greater than the factor of about 2

by which our volume fraction of filler would increase the rubber viscosity, or modulus, (assuming $D\eta$ = constant) in accordance with any of the existing equations for this effect, such as Mooney's[44], Guth's[45], Smallwood's[46], or Kerner's[47] equation. In other words, the reduction in diffusivity must be due to yet another factor besides the corresponding reduction in the mobility of the rubber between the filler particles. In the absence of a detailed theory of the change in diffusion due to the replacement of rubber by barrier particles, it would be difficult to estimate how much of this is due to the changes in bulk rubber mobility and how much due to the strain or compaction of the rubber adsorbed to the filler particles. The tortuosity of the diffusion path is also involved. The situation is actually similar to the diffusion through a partially crystalline polymer where the crystalline volume fraction acts like a filler. This will be discussed in later Sections.

2. Diffusivity as a Function of Temperature

The isobaric plots of diffusion coefficients for our four samples are shown in Figures 17 through 20. In all the plots the degree of divergence indicates the pressure dependence of D which again is seen to be small at low temperature, but increases at higher temperature.

The plots for the unfilled samples are linear in contrast to those of the filled rubbers. The linear isobaric plots (for the unfilled rubber) may be represented empirically by the following four equations:

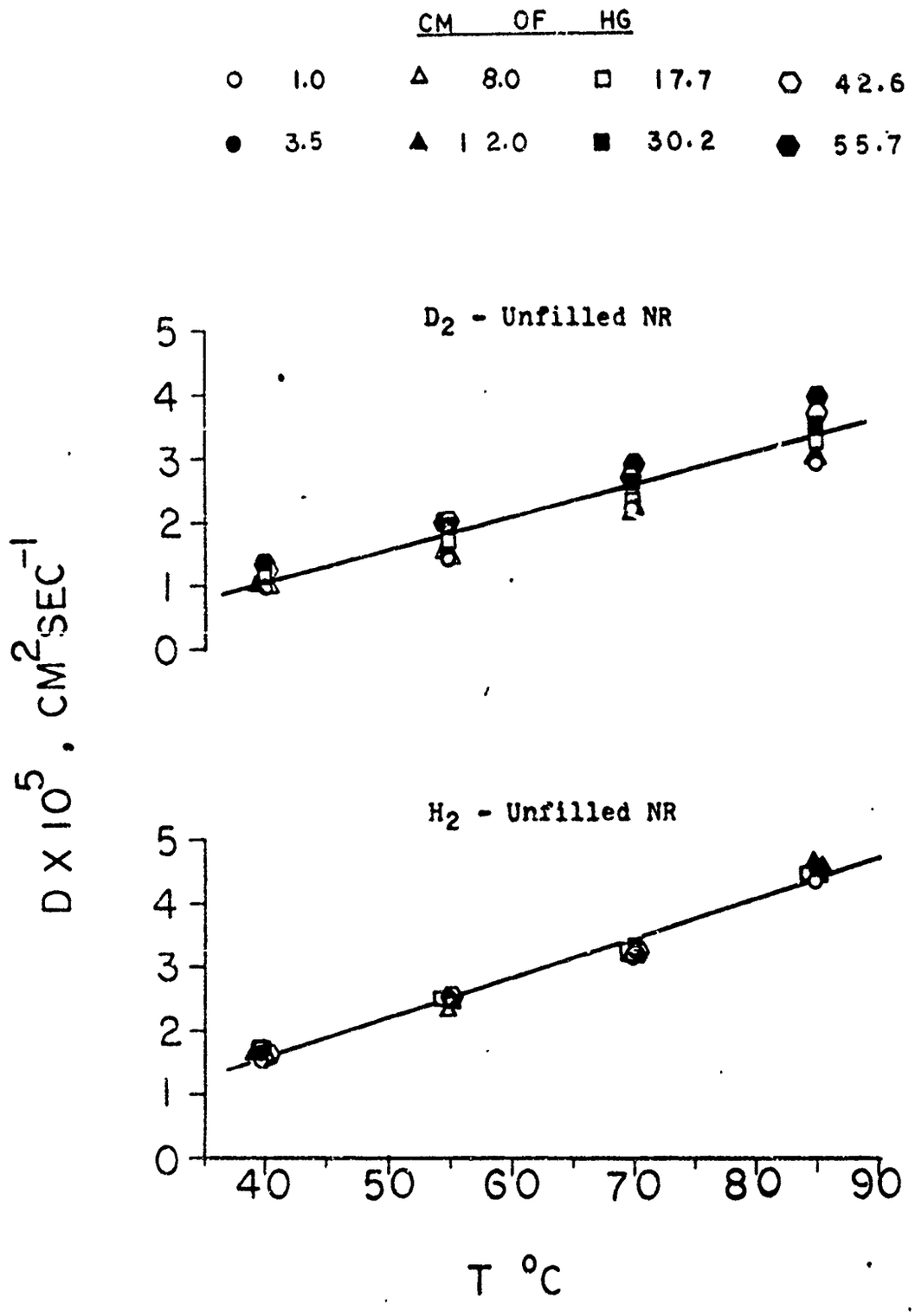

Fig. 17 - Diffusivity isobars versus temperature for unfilled natural rubber and penetrants, H_2 and D_2

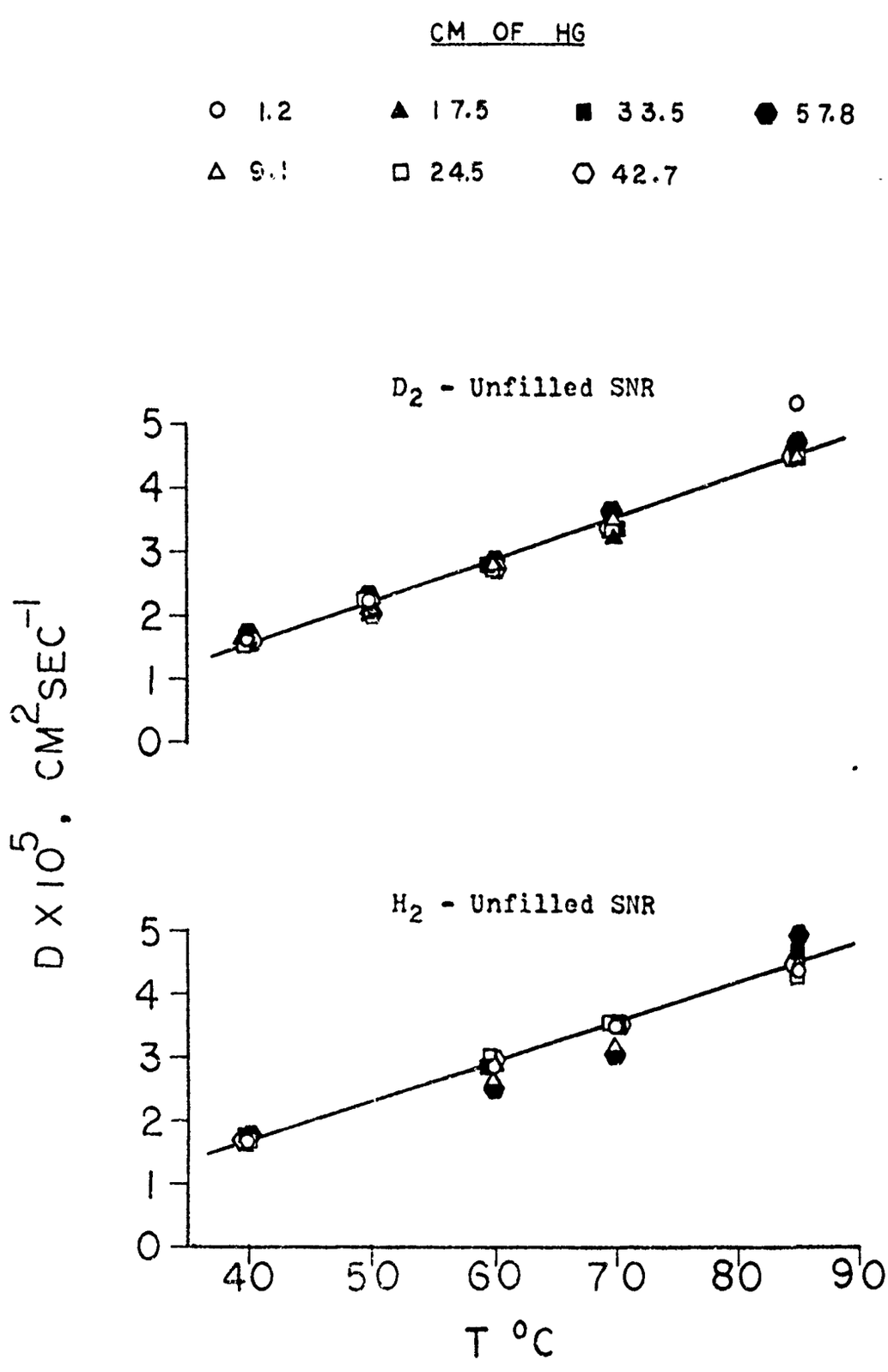

Fig. 18 - Diffusivity isobars versus temperature for unfilled synthetic natural rubber and penetrants H_2 and D_2.

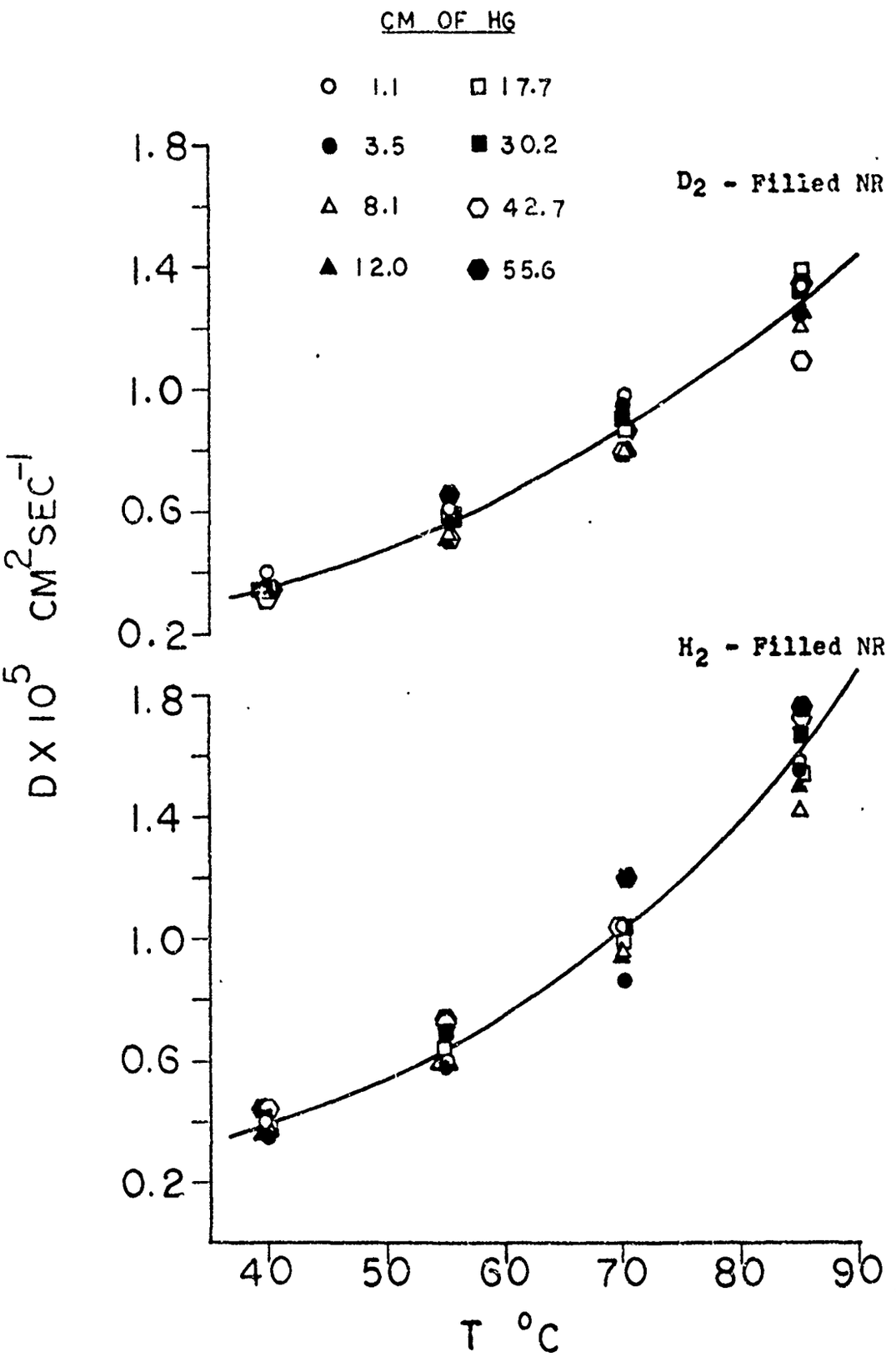

Fig. 19 - Diffusivity isobars versus temperature for filled natural rubber and penetrants, H_2 and D_2.

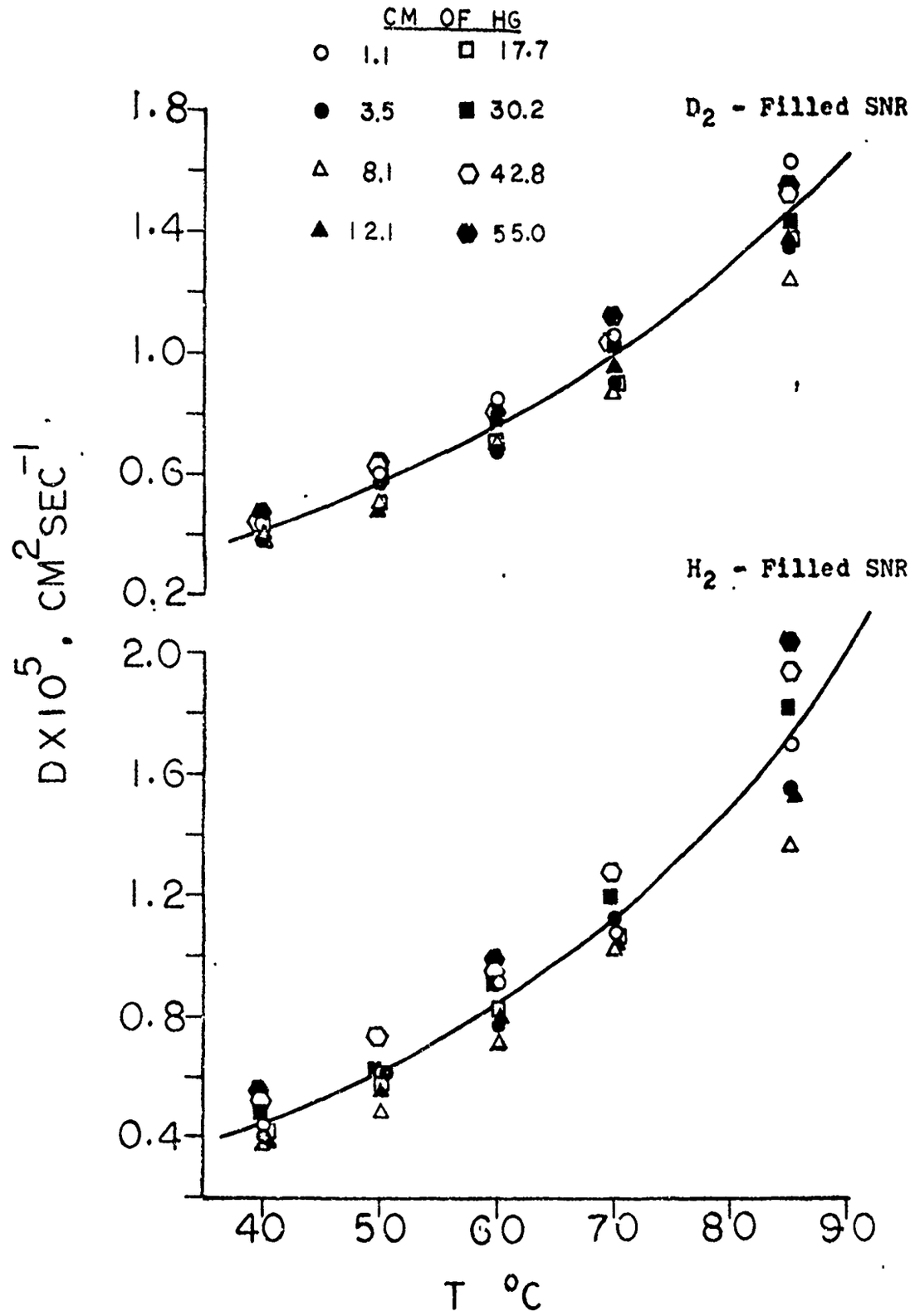

Fig. 20 - Diffusivity isobars versus temperature for filled synthetic natural rubber and penetrants, H_2 and D_2.

Penetrant-Rubber	Equation	"Cut-off" Temp. (t_1 °C)	Error
H_2-unfilled NR	$D = 6.17\ (t_2-t_1) \times 10^{-2}$	14.5	± 5.7%
D_2-unfilled NR	$D = 4.95\ (t_2-t_1) \times 10^{-2}$	17.5	± 5.5%
H_2-unfilled SNR	$D = 6.25\ (t_2-t_1) \times 10^{-2}$	13.7	± 6.8%
D_2-unfilled SNR	$D = 6.19\ (t_2-t_1) \times 10^{-2}$	14.5	± 5.7%

D in unit of $cm^2/sec \times 10^{-5}$

Here, t_1 denotes a practical "cut-off" temperature at which the diffusivity appears to vanish (in fact, becomes very small compared with values between 40 and 85°C). Using this linearized equation, the diffusivity at any temperature, t_2, can be calculated in this range with an error of no more than 6.8% compared with the average value listed in Table 14. However, diffusivities calculated for temperature higher than the experimental upper bound temperature of 85°C may be subject to greater errors.

The "linearity" of D with temperature in the unfilled samples expresses the fact that the diffusion mechanism resembles that of a diffusant following Einstein's law if moving through a medium whose viscosity changes little with the temperature: $D = kT/6\pi\eta r$. The real curvature of these plots is not only implied by the applicability of Arrhenius plots which will be discussed later, but becomes strongly pronounced in the filled samples, where rubber attachments and viscosities must change more strongly with temperature.

3. Solubility, S, as a Function of Gas Pressures

The solubilities listed in Tables 3, 4, 6, 7, 9, 10, 12 and 13 are plotted against the gas pressure for two temperatures, 40 and 85°C (the lower and upper bound temperature used in the study) as shown in Figures 21 to 24. It is interesting to note that in both unfilled rubbers, the two penetrants show the same trend of increasing solubility with temperature whereas in the filled rubbers the two isotope species show different trends in their solubilities. For hydrogen the solubility in the filled rubbers decreases as temperature increases, while for deuterium the trend is reversed and less regular.

These differences can be explained by the signs of their heats of solution. From the thermodynamic point of view, positive values of heats of solution, i.e., endothermic dissolution of the gas, cause rising solubilities with increasing temperatures. On the other hand, for negative heats of solution, or exothermic processes, the solubility should decrease as temperature increases. The mean heats of solution deduced for the respective penetrant-rubber systems listed in the following (quoted from Table 16 on page 125) are consistent with this, as shown below:

$\Delta\bar{H}_S$, kcal/mole

Gas \ Rubber	Unfilled		Filled	
	NR	SNR	NR	SNR
H_2	1.24	1.02	-0.28	-0.34
D_2	0.65	0.71	0.28	0.35

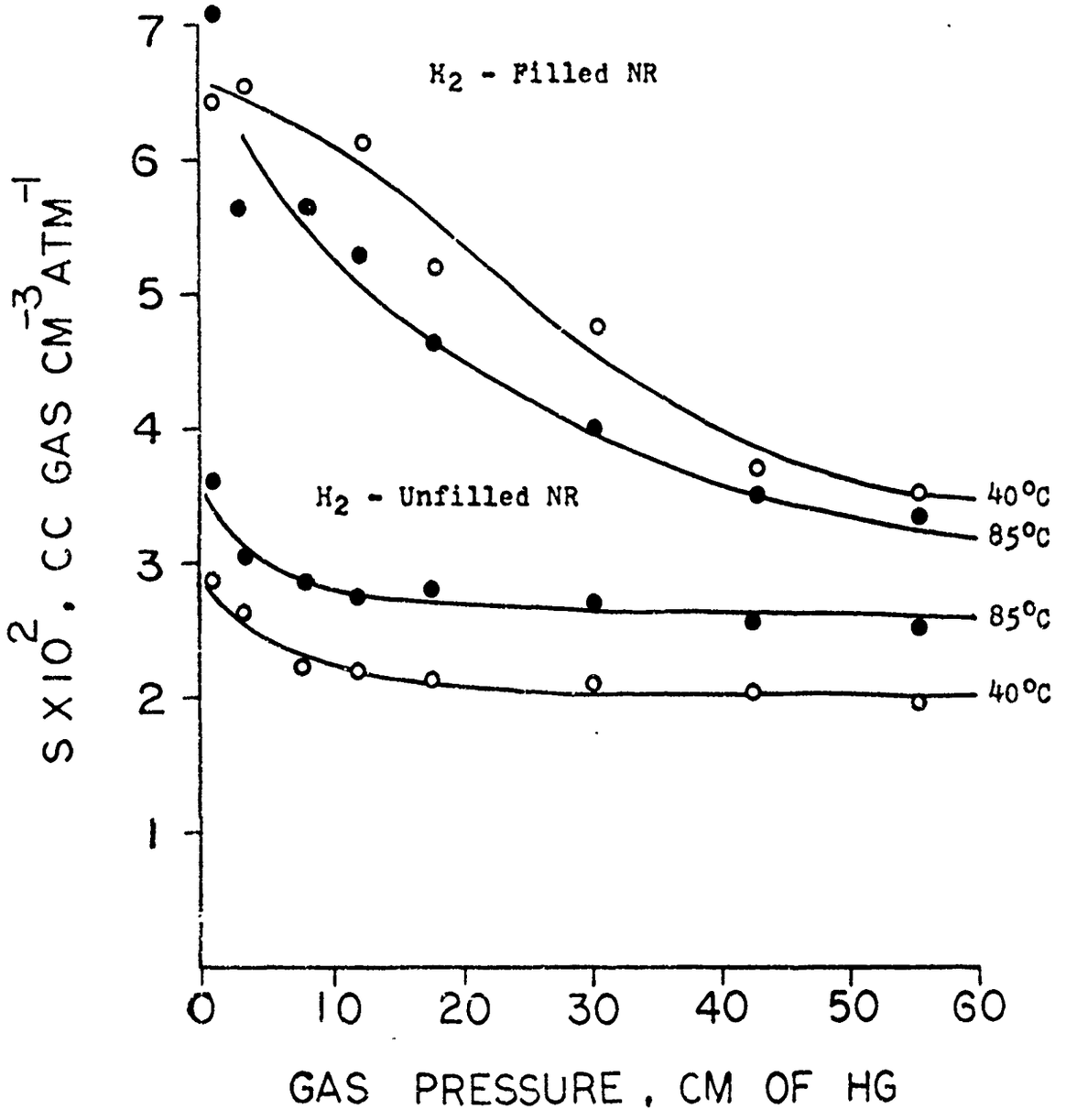

Fig. 21 - Solubility isotherms versus gas pressure for H_2 and natural rubber (filled or unfilled).

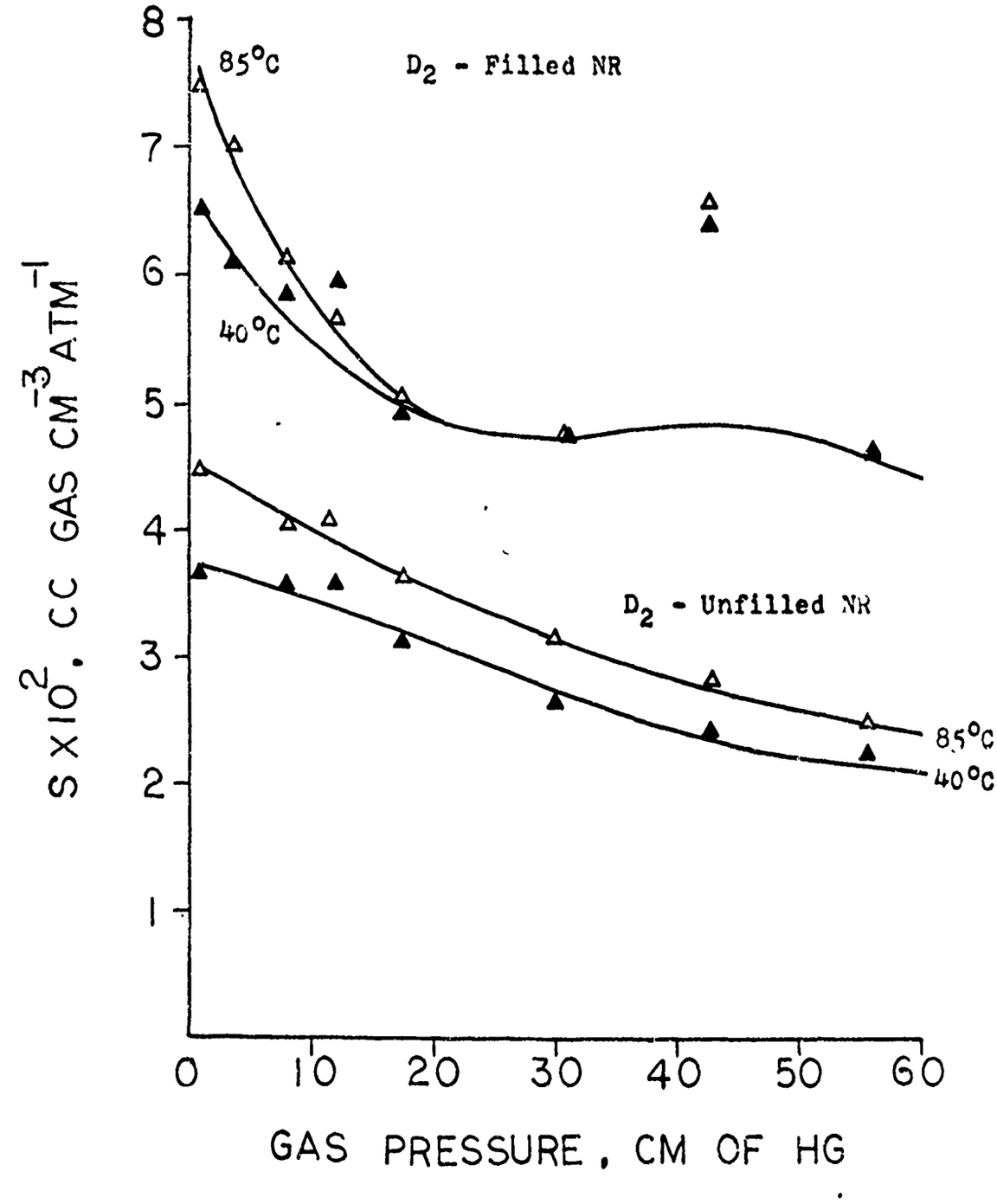

Fig. 22 - Solubility isotherms versus gas pressure for D_2 and natural rubber (filled or unfilled).

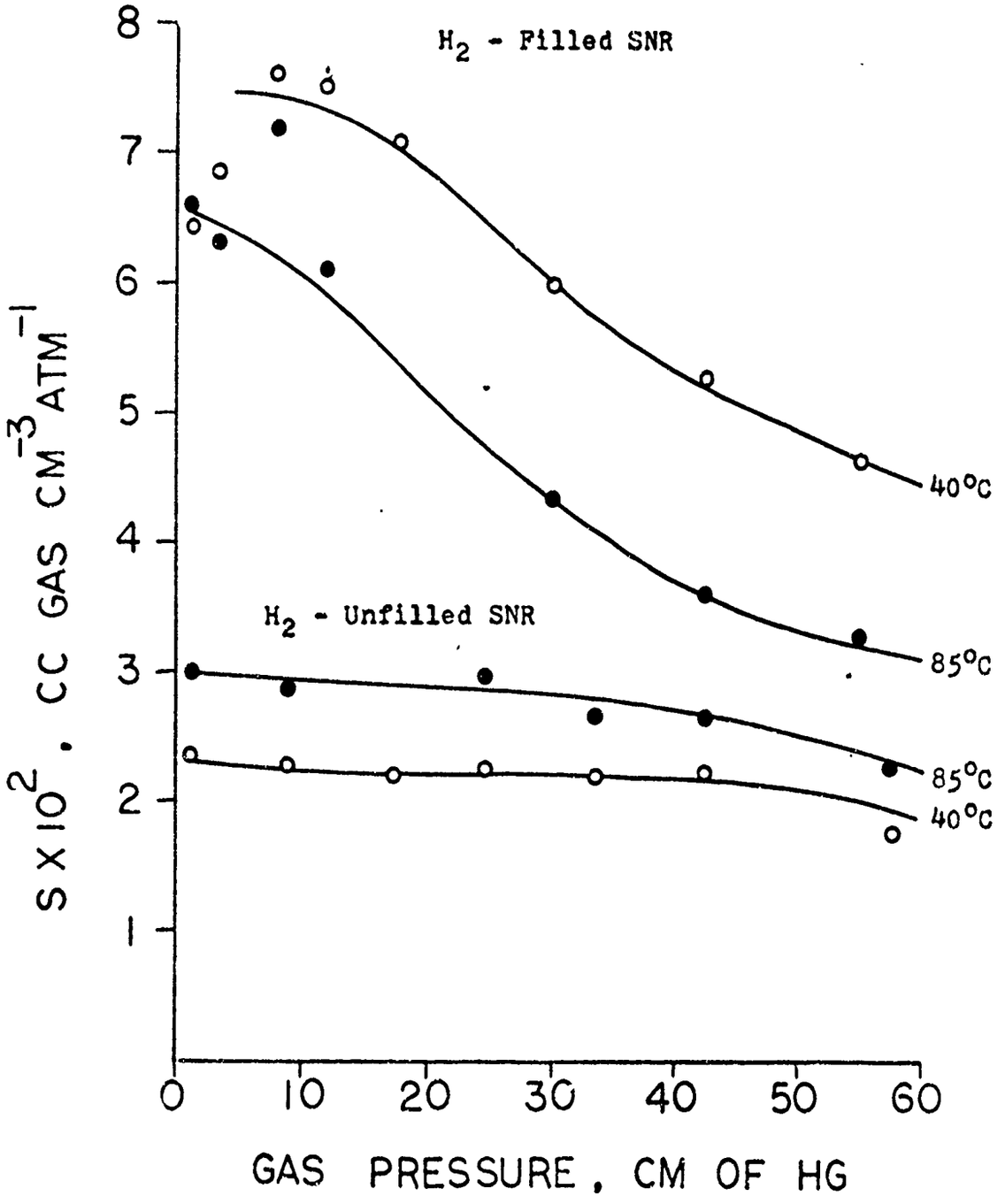

Fig. 23 - Solubility isotherms versus gas pressure for H_2 and synthetic natural rubber (filled or unfilled).

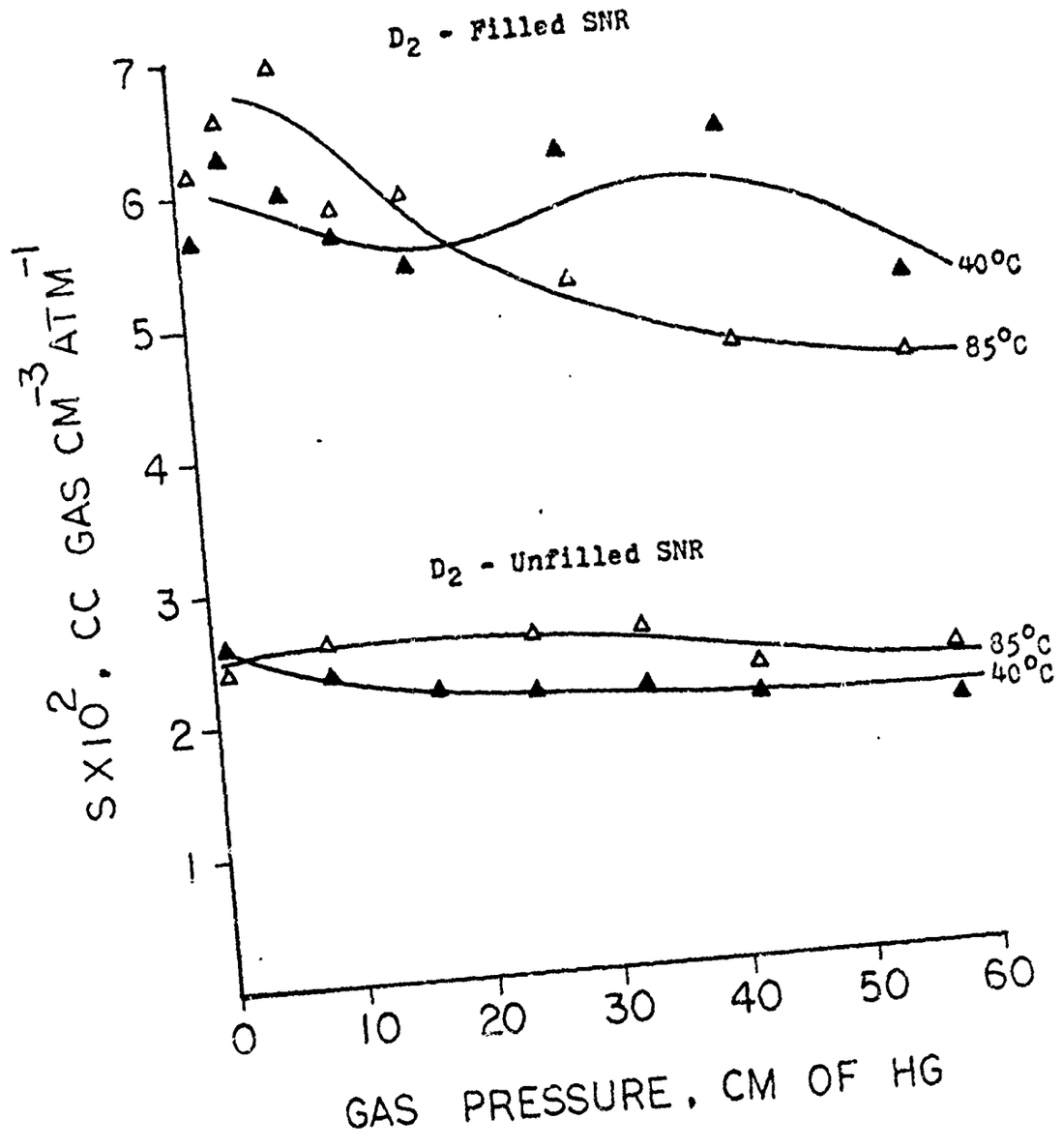

Fig. 24 - Solubility isotherms versus gas pressure for D_2 and the synthetic natural rubber (filled or unfilled).

In this Table, ΔH is the difference of the arithmetic mean of the activation energies for permeation and for diffusion for the pressure range investigated (see Section of activation energies on page 117). The value of ΔH_S for each gas pressure can also be calculated from

$$\Delta H_S = \frac{-R \, d \ln S}{(1/T)}$$

which is a more direct method. However, if this is done, the trends of ΔH_S are slightly clearer but the scatter of the values remains. Therefore, values of ΔH_S were calculated by the former method.

The solubility isotherms shown in these figures also illustrate the fact that the solubilities of the penetrants in the filled rubbers are much higher than in the unfilled rubbers. In general, the solubility, $S_{(rb+f)}$, of a gas in a rubber-filler system may be resolved into three factors, first S_{rb}, related to the solubility in the rubber, second, S_f, related to the gas adsorption by the filler and, third, S_{vac}, related to filling up (condensing in) vacuoles or small capillaries which may be present in the porous fillers, or may be created by high concentration of fillers in the rubber[58]

$$S_{(rb+f)} = \lambda_{rb} S_{rb} + \lambda_f S_f + \lambda_{vac} S_{vac}$$

where λ_{rb}, λ_f, and λ_{vac} are the volume fractions of rubber, filler and vacuoles respectively. In the special case of complete wetting of the surface of a non-porous filler by the rubber,

the above equation reduces to

$$S_{(rb+f)} = \lambda_{rb} S_{rb}$$

With rubber containing filler of say, 0.2 volume fraction, the solubility of the gas should, in this case, be 80% of that of the gum compound. For special mineral fillers such as whiting, aluminum oxide and barium sulfate and with the non-reinforcing carbon blacks, the experimentally determined solubilities by van Amerongen[30] are in fact only a little higher than this 80% value (see Table 15). If the filler particles contained in our filled rubber were non-adsorbing, the solubilities of the gas should be about 84% of that of the unfilled rubber since the volume fraction of the filler is 0.16. In fact, we find for our system that $S_{(rb+f)}$ is almost twice as much as S_{rb}. This is certainly due to the high adsorption power of the carbon black and also possibly due to the increase in free volume as a result of the strain introduced by the filler particles. The later effect, of course, should be small.

Figures 21 to 24 show interesting trends of solubilities. The solutions of H_2 gas in the filled rubbers are the only ones showing the negative ΔH_s values. These are undoubtedly due to the strong adsorption of hydrogen on the filler and thereby presents special cases. However, even these two (like the other six cases) show a general trend of increase in solubilities at low pressures.

One sees that S is reasonably constant, i.e., that Henry's law is fulfilled, for three of the unfilled rubber experiments. In the forth case, there is a downward trend of solubility with pressure which is probably exaggerated by experimental errors. In the filled rubbers, the solubility declines quite markedly with pressure, particularly, at the low pressures, which indicates complications beyond the ordinary solubility processes. This may derive from a superimposed effect, according to Gibbs' equation, if a gas acts as external pressure carrier besides dissolving in the material under pressure. Very likely we see a variation of this in the form of an effect of mechanical strain, intensified by the presence of fillers and vacuoles, as the rubber is compressed against the porous metal support in the diffusion cell.

The data found here for the solubility and the heat of adsorption allow an interesting calculation. Assuming an average surface area of the carbon (particle size 300 Å in diameter) of 120 m^2/g, and 9 $Å^2$ for the area required for each H_2 molecule, one can calculate that the amount of the carbon required for adsorption of one mole of H_2 gas is about 500 g. In view of the weight ratio of the rubber to the carbon in the filled rubber, there should be about 2.5 times as much

rubber required to adsorb one mole of H_2 gas. Instead, our solubility data at gas pressure of 30.2 cm Hg and 40°C reveal that only 8×10^{-6} g. of H_2 gas is adsorbed on 1 g. of carbon in the filled NR. In other words, 2.5×10^5 g. of carbon is needed to adsorb one mole of H_2 gas in our case. The adsorptive capacity of the carbon in the filled rubber is thus only 1/500 of that calculated for a theoretical monolayer. Undoubtedly, this is a result of a lower effective surface area of the carbon due to the fact that probably 90% or more of the carbon surface is occupied by the rubber.

The experimental heat of adsorption for H_2 on carbon is -1.52 kcal/mole which is obtained by taking the difference of ΔH_s for filled and for unfilled NR. The heat of internal adsorption for H_2 on rubber is estimated about -0.8 kcal/mole. This is reasonable since this energy must be smaller than the heat of adsorption on carbon and larger than the product of entropy loss and temperature due to the gas being adsorbed at low pressure and room temperature. This loss is about 600 cal/mole, i.e., RT. Therefore, the energy of hole formation is found to be 2.040 cal/mole (see the analysis of the heat of solution on page 126, where the heats of self condensation of gas in the rubber and on the carbon are stated to be negligibly small). This is about two fifth of the frequently derived molar cohesive energy of rubber and again reasonable.

The following consideration is also interesting. The heat of solution, ΔH_s for H_2 in unfilled NR is 1.24 kcal/mole. To occur spontaneously, the free energy of the solution must

be negative. According to Gibbs' equation, $\Delta F = \Delta H_s - T\Delta S$, the entropy ofmixing, ΔS, must be positive and the term, $T\Delta S$, must be greater than ΔH_s which is 1.24 kcal/mole, in order to have a negative ΔF. Again setting the entropy loss due to H_2 adsorbed on rubber to be -2.0 e.u/mole and $T = 300^{\circ}K$, there must be an entropy increase in the rubber of at least 6 e.u per mole of isoprene through H_2 adsorption. This "entropy of swelling" is large, but at least comparable to the entropy of fusion of NR, 3.5 e.u/mole, quoted in the literature[48].

4. Permeability, P

The values for P found have been given in Tables 3, 4, 6, 7, 9, 10, 12, and 13. Obviously, the magnitudes and trends of permeabilities agree with the discussion above on the factors that influence D and S, of which P is the product. However, one must remember that the permeabilities, as normalized flux rates, are the primary data since even the values of D are derived from the intercept of the flux rate on the time axis. Consequently, features of the membrane structure, or of the absorption behaviour of the gases, must receive here some attention.

Concerning the unfilled rubbers, Ziegel[40] e.g., noted a change in permeability of the samples with time. He attributed this, probably correctly, to aging and crystallization of the rubber membranes, facilitated by the changes in temperature and pressure, and the presence of the dissolved gas. Such time effects on permeabilities were not observed in

this study.

On the other hand, in dealing with the filled samples one must analyze the possible changes of rubber structure and diffusion pattern due to the presence of the reinforcing carbon black. Firstly, there is a change in the effective cross section for the diffusive passage of the gas which the filler reduces to 84% of the total membrane area. Secondly, we have to consider the fact that the gas molecule can not follow a direct diffusion path, but must bypass the filler particles, so that the effective travelling length through the membrane becomes greater. This so-called tortuosity factor has been repeatly discussed in the literature in connection with the flow of fluids through porous media. Although the permeation of gas through the membranes is a matter of diffusive rather than fluid mass transport, the generally accepted tortuosity factor of 1.6 for randomly packed beds[49] should apply, though as a maximum. Thus, the effective membrane thickness is greater by factor of 1.6, or the normal concentration gradient established in the membrane should be reduced by a factor of 1.6.

Thirdly, the mobility of the rubber segments located next to the filler particles must be reduced, bringing the segmental viscosity closer to that prevailing in the glassy state. The observation that temperature has such a large effect on the diffusivity of the filled rubbers could be explained on this basis.

Finally, the increased solubility of the gases in the filled samples, as well as the overall more negative

enthalpy of solution, suggests higher concentrations of the gases in and around the filler particles. Consequently, there may be another mechanism of diffusion besides the assumed migration of the gas molecules from segmental site to site by adsorption and desorption steps on the rubber This latter mechanism neglects another likely aspect, namely that rubber segments themselves also diffuse. In doing so they enhance gas transport by moving out of the way of gas particles, thereby opening suitable cavities for the gas to diffuse into, at an energy expense which is different from that of the activated desorption assumed in this thesis. This new mechanism would allow the gas molecules to diffuse into the dense gas zone in and around the filler particles, to become adsorbed there, while a gas particle at the opposite side of the filler is given off. This involves a fluid type of transport in the adsorbed atmosphere of the filler which, if this movement is effective, would decrease the obstructive power of the filler. There may be yet other factors at work, but we want to restrict the discussion to these obvious ones.

The combined effects of change in effective membrane cross section through the filler and of rubber adsorption on the carbon may be described as follows: We accepted the relation $P = SD$, as a result of Fick's first law, $Q = -D\frac{\partial c}{\partial x}$, and of Henry's law, $c = Sp$, under the assumption of constant D (see derivation on page 6). However, since the cross section is changed from unity to an area reduced by to 84%, and since the length of the diffusion path is increased by 60%, one sees

that the permeability, P, for the filled rubbers must be reduced to one half of that for the unfilled rubber for these geometrical reasons alone. Introducing, then, the effect of fillers on the segmental mobility and the consequently increased viscosity, as discussed in the section of diffusivity, we first arrive at a diffusion rate ratio between the unfilled and filled samples of 0.55. However, the time lag itself must also be affected by tortuosity so that the diffusion factor would be further reduced by 1.6, or by $(1.6)^2$ as maintained by some theories[50]. Applying these factors, leads to the diffusion ratios as listed in Table 14.

It follows from this analysis that our values for solubilities, S, in the filled samples are also affected. The true solubility should be the quotient of the true permeability divided by the true diffusivity. The true permeability is in reality larger than that measured if one takes the tortuosity and the change in the cross section of the specimen into account. Similarly, the true diffusivity should be corrected for the tortuosity (or the true length of the diffusion path). If all these corrections are made, the true solubility calculated would be smaller than the apparent value (i.e., calculated from the uncorrected values of P and D) by a factor of 1.35. No doubt, this argument can be refined or revised by a different model of filler action. For the present, we have calculated the solubility directly from the experimental permeabilities and diffusivities which are uncorrected for the tortuosity. Having thus preserved

the primary data they can be later recalculated in accordance with a more complete theoretical study of filler action. Similarly, the quantities of H_2 adsorbed on carbon which we have derived with the aid of solubilities might have to be revised later. But even without this correction, the essence of the conclusions drawn here remains correct.

The temperature dependencies of the permeabilities and diffusivities can be expressed by the Arrhenius equation. Values at different temperatures, T_2, can be calculated from a value of T_1 and the activation energies by the following relationships:

$$\log P_2 = \log P_1 + \frac{E_p}{4.6}\left(\frac{1}{T_1} - \frac{1}{T_2}\right)$$

$$\log D_2 = \log D_2 + \frac{E_d}{4.6}\left(\frac{1}{T_1} - \frac{1}{T_2}\right)$$

where P_1, P_2 and D_1, D_2 are the permeabilities and diffusivities at temperatures T_1 and T_2 ^{o}K respectively, and E_d and E_p are the activation energies in calories per mole, see Figures 25 and 26, which are presented as examples.

The temperature dependencies of the diffusivity and permeability are usually such that P and D decrease uniformly with decreasing temperatures. However, in some temperature-pressure regions, the permeabilities deviate markedly from the otherwise almost linear relation between log D and 1/T as the temperature decreases. Figures 27 and 28 show that this occurs, for H_2 and D_2, only in filled SNR in contrast to the linear

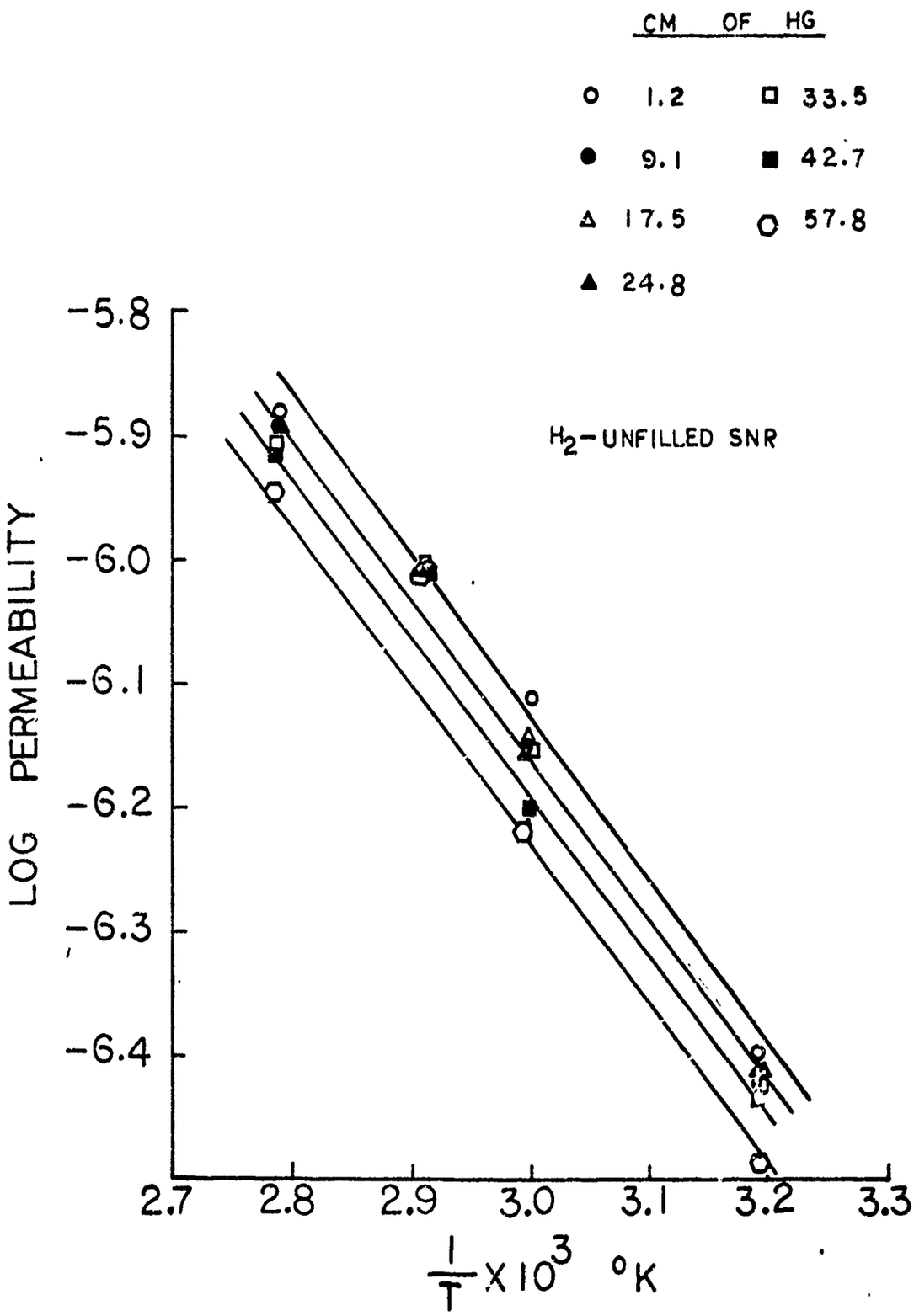

Fig. 25 - Arrhenius plot of permeability isobars for H_2 and unfilled synthetic natural rubber.

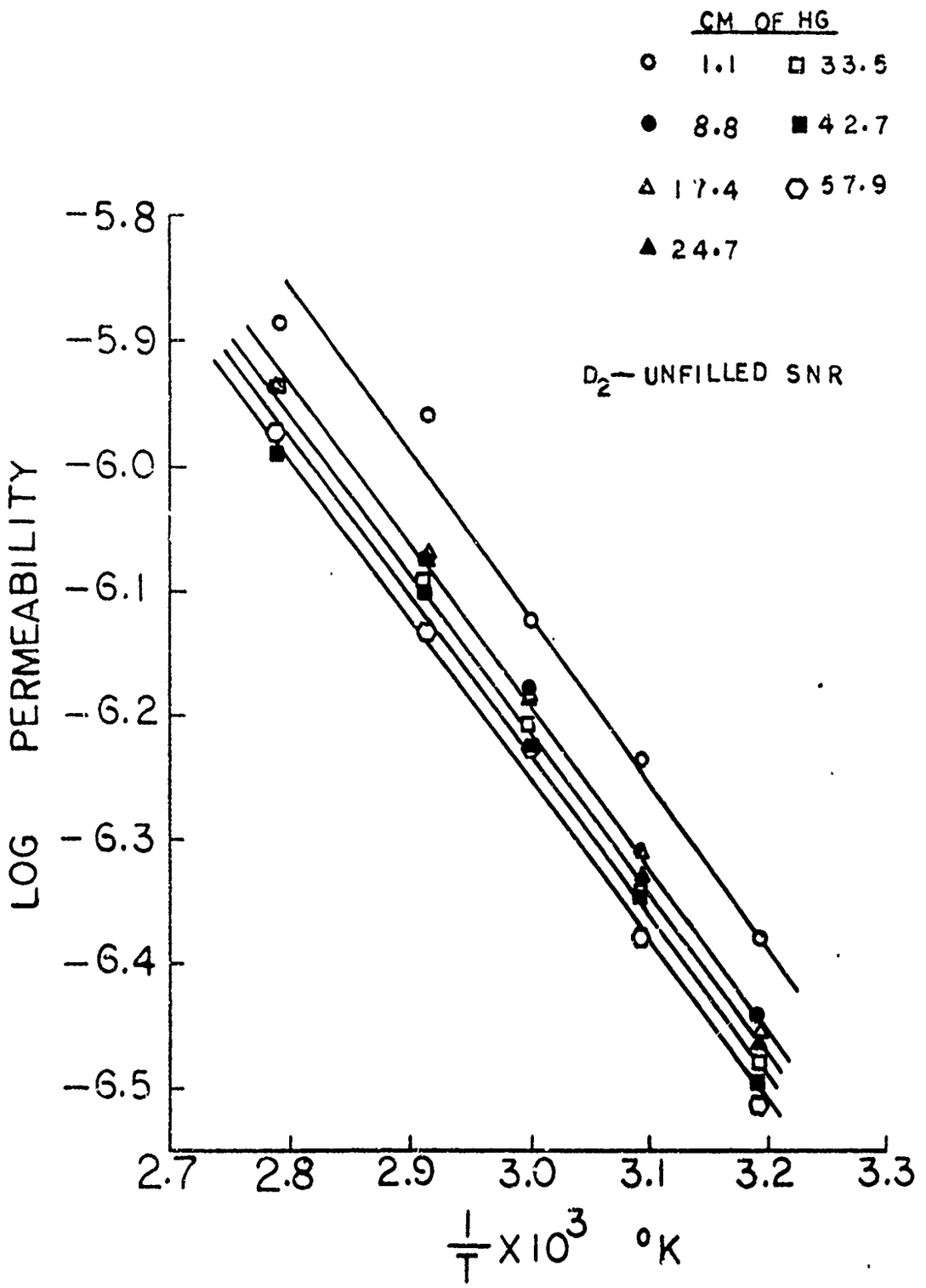

Fig. 26 - Arrhenius plot of permeability isobars for D_2 and unfilled synthetic natural rubber.

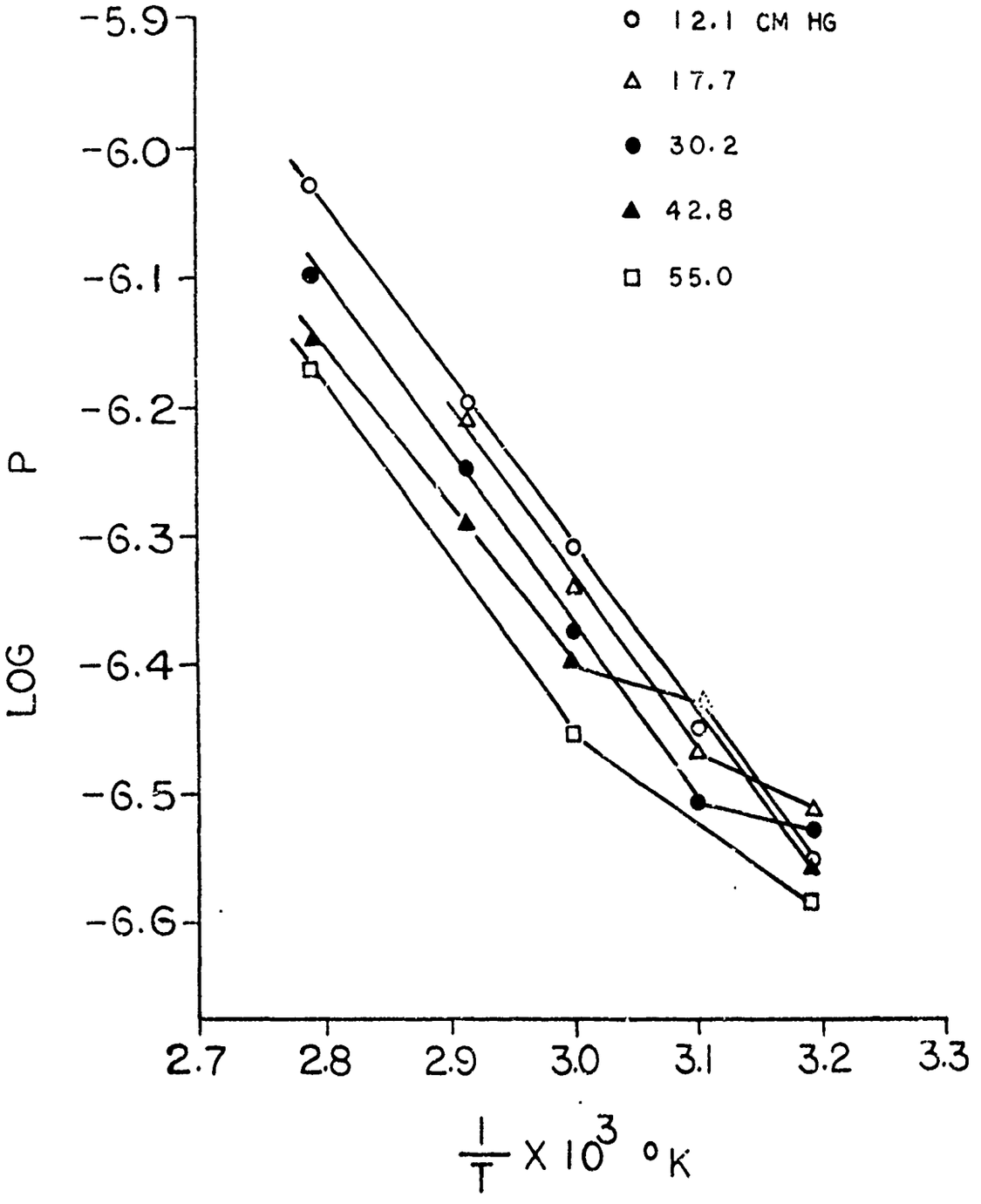

Fig. 27 - Arrhenius plot of permeability isobars for H_2 and filled synthetic natural rubber.

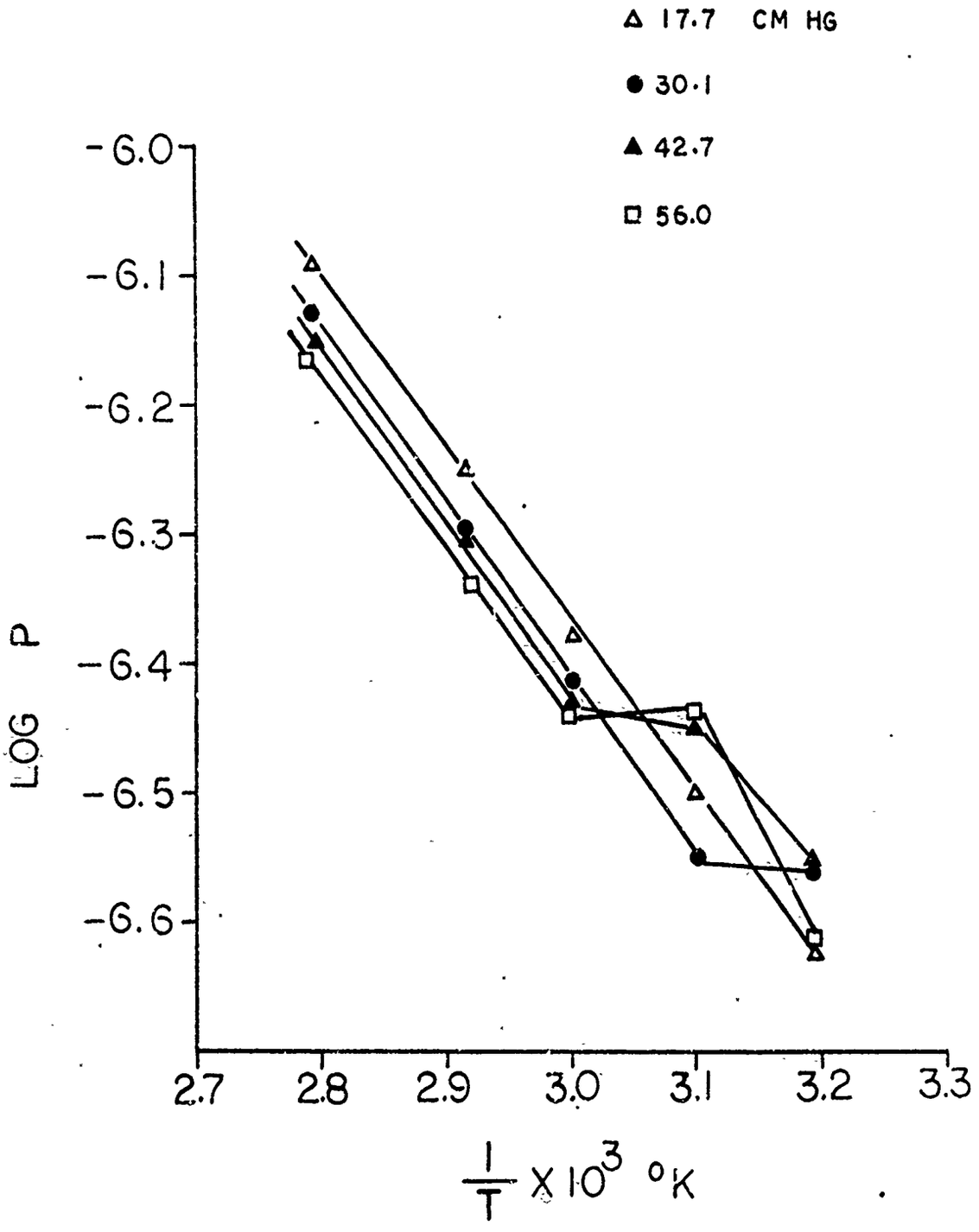

Fig. 28 - Arrhenius plot of permeability isobars for D_2 and filled synthetic natural rubber.

plots at sufficiently low prossures. These deviations are puzzling and possibly experimental, though similar observations were made by Sobolev[50] in his study of the polyethylene-methyl bromide system, and alike trends exist in our S-P curves, see Figures 21 to 24.

The presence of crystallinity causes a delay of diffusion, similar to that of caused by filler[50,52]. A number of measurements have been made and theories have been postulated based on the general physics of heterogeneous systems containing dispersed particles[53,54]. The experiments showed that the reduction in diffusion was a function of the nature of the gas, so that a simple model of permeable and impermeable domains is not sufficient[55]. The tortuosity factor, was also introduced, but still the agreement with the model remained unsatisfactory. We included into the mechanism also the effects of the presence of the rigid domains on the viscosity of the metrix and thereby obtained an improved agreement, at least for our case. However, our data are not good enough to decide whether one should use the tortuosity factor to the first or second power, as also debated in the literature[56].

B. Activation Energies for Diffusion and Permeation, E_d and E_p and the Heats of Solution, ΔH_s

The activation energies for permeation and for diffusion were obtained from the Arrhenius equations,

$$\log P = \log P_o - \frac{E_p}{2.303\ R}\frac{1}{T}$$

$$\log D = \log D_o - \frac{E_d}{2.303\ R}\frac{1}{T}$$

at various pressures for the four samples. They are listed in Tables 3, 12, 21 and 30, and two sample plots are shown in Figures 29 and 30. Plots of the activation energies against gas pressures are shown in Figures 30 to 34. It is seen that the activation energies are independent of the gas pressure, although the values of E_p for filled rubbers scatter and may hide minor trends. The arithmetic means of the activation energies for various gas pressures, $\bar{E}_p$ and $\bar{E}_d$, for all samples are listed in Table 16, along with the heats of solution, ΔH_s, which are the differences of these mean values.

For both unfilled rubbers, the activation energy required for diffusion of D_2 gas is about 350 cal/mole greater than that of for H_2 gas. In the filled rubbers, the case is reversed, and the activation energy for diffusion of H_2 gas is about 550 cal/mole higher than D_2 gas. Although these difference are small on an absolute scale, the least square analysis of the points for the above equations (see Appendix II) demonstrates the reality and order of magnitude of the data.

In order to comment on these findings, it should be remembered that as shown in Table 16, the heats of solution are all positive except for hydrogen in the filled rubbers.

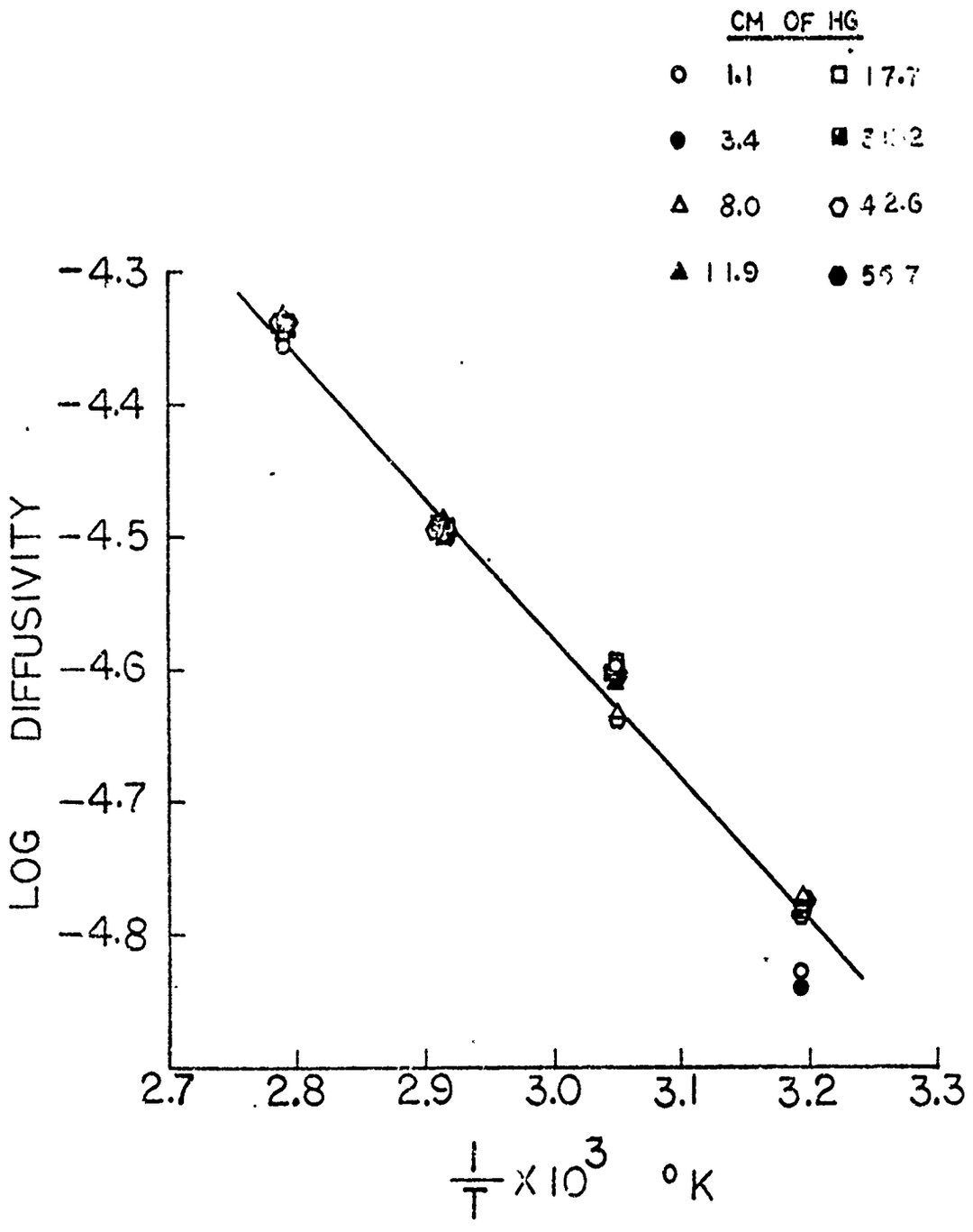

Fig. 29 - Arrhenius plot of diffusivity isobars for H_2 and unfilled natural rubber.

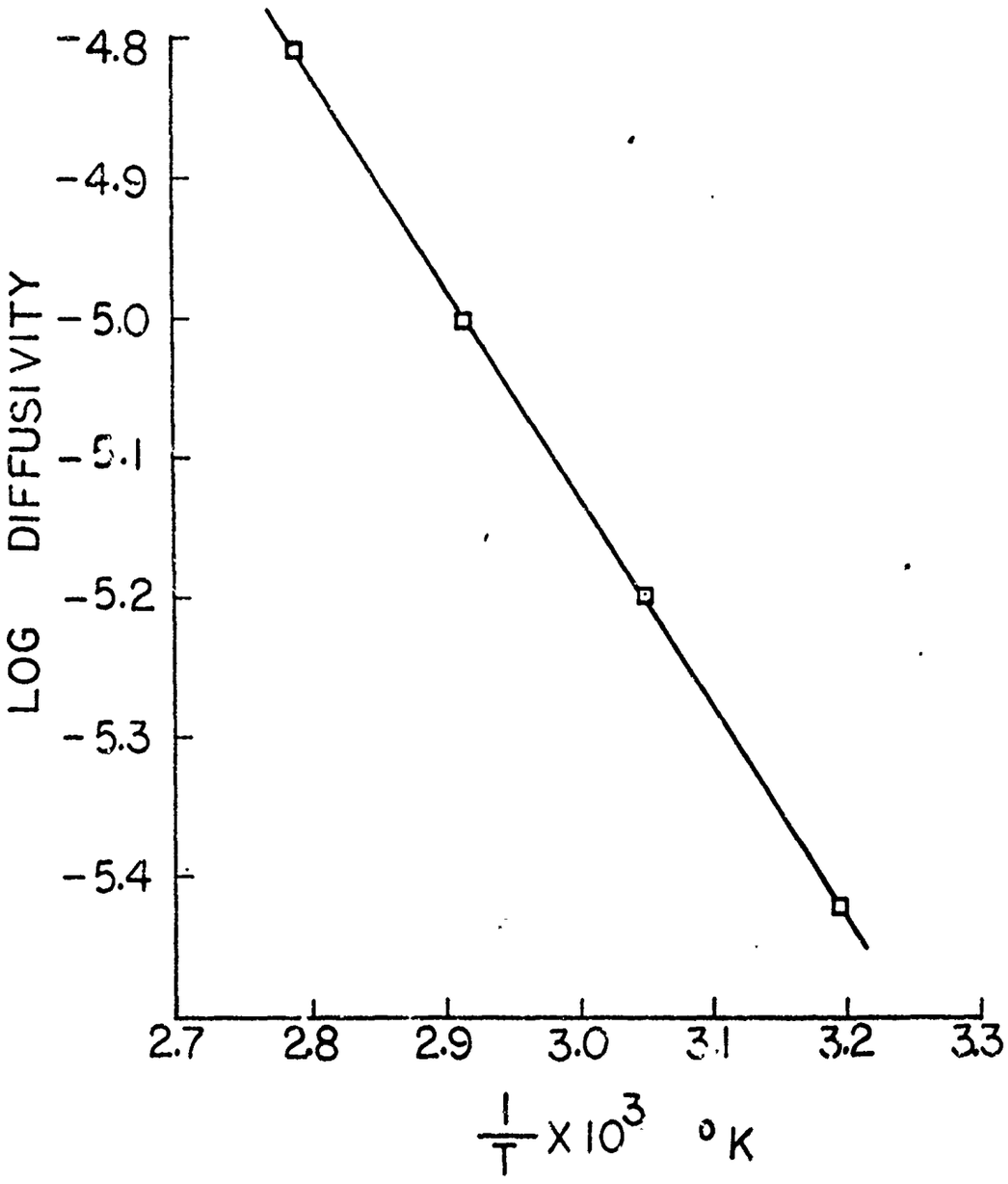

Fig. 30 - Arrhenius plot of diffusivity for H_2 and filled natural rubber at gas pressure of 17.7 cm Hg.

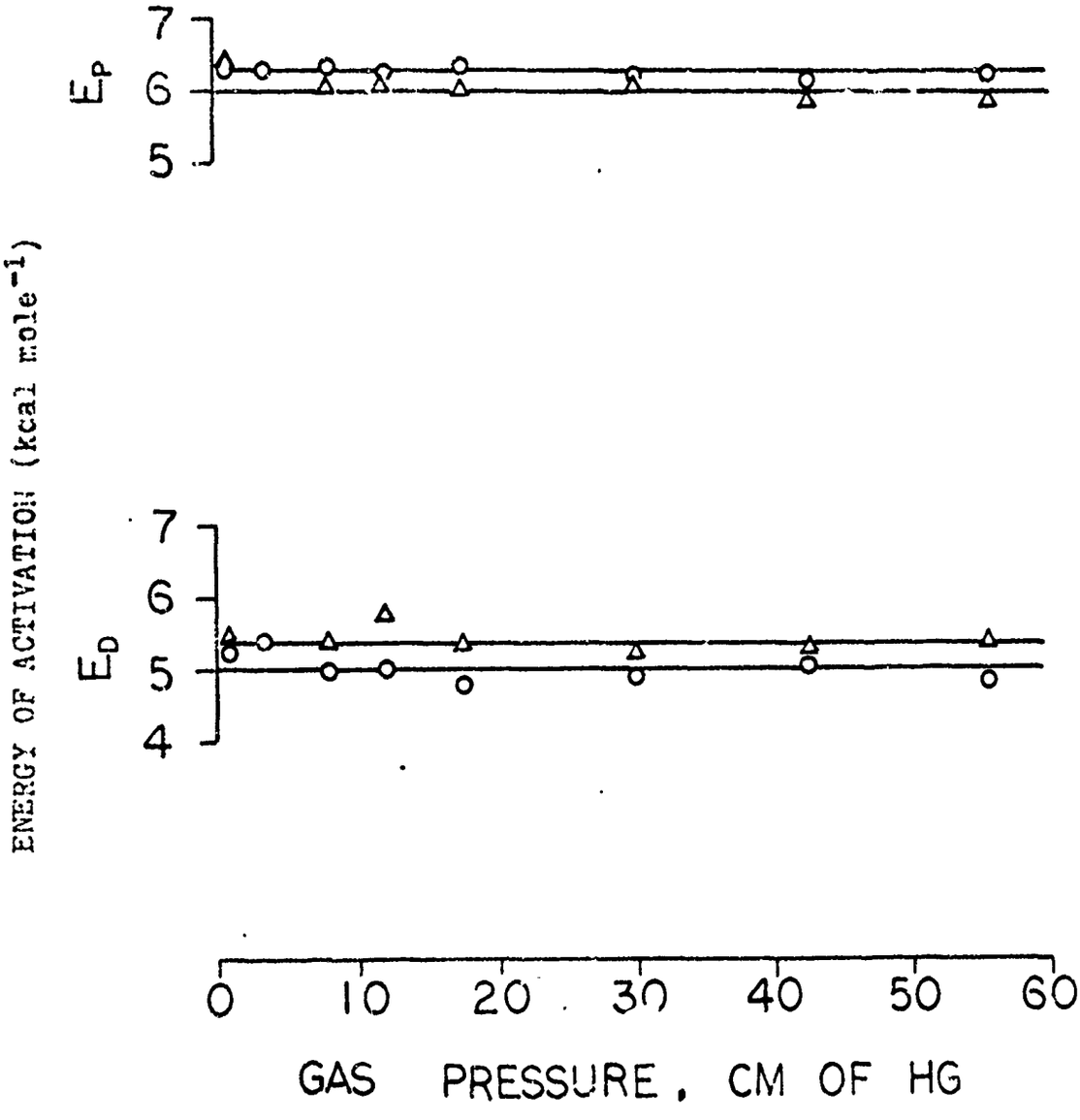

Fig. 31 - Energy of activation for permeation and for diffusion, E_p and E_d, versus gas pressure for H_2 and D_2 in unfilled natural rubber.

▲ denotes D_2 o denotes H_2

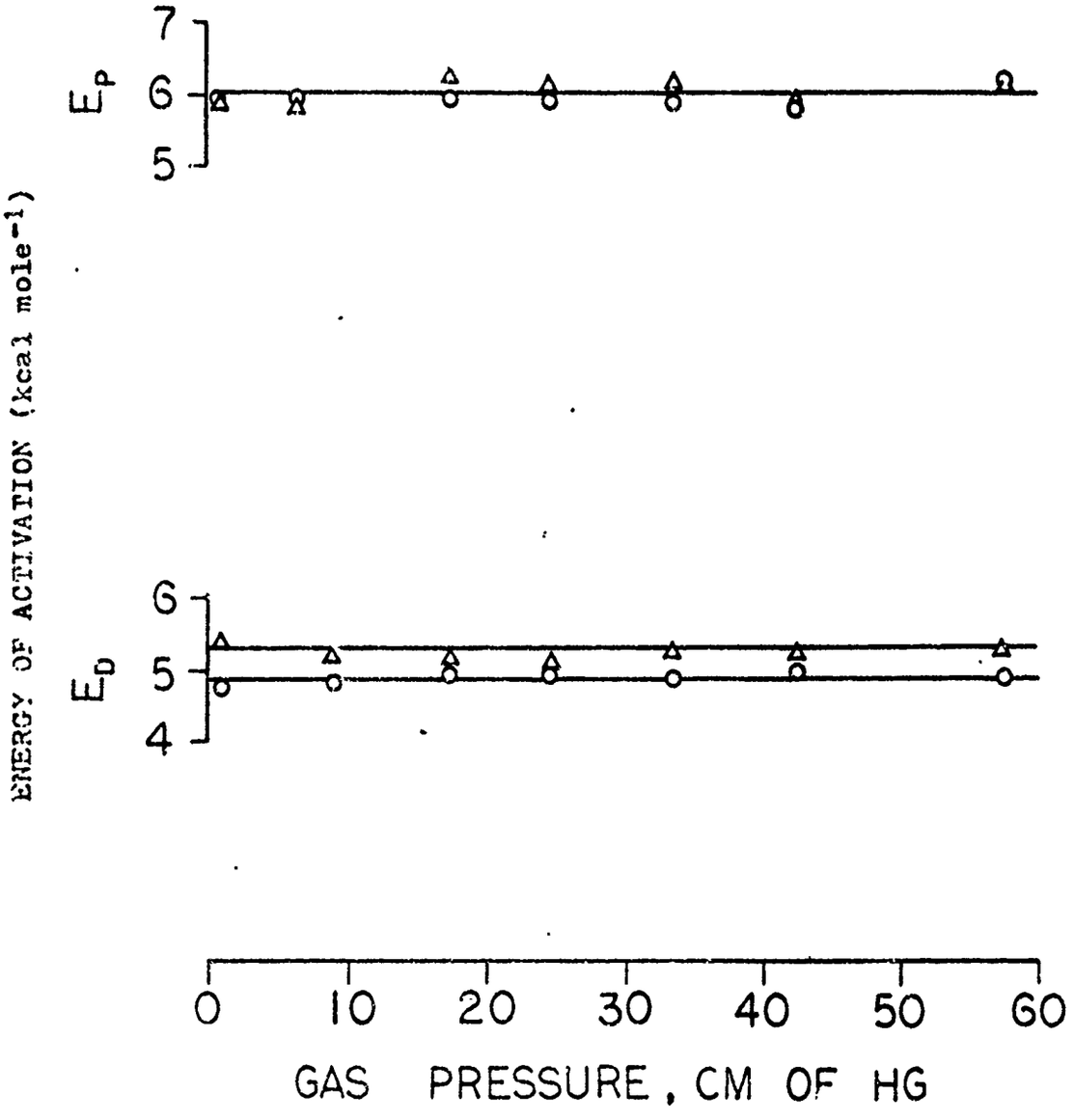

Fig. 32 - Energy of activation for permeation and for diffusion, E_p and E_d, versus gas pressure for H_2 and D_2 in unfilled synthetic natural rubber.

Δ denotes D_2 O denotes H_2

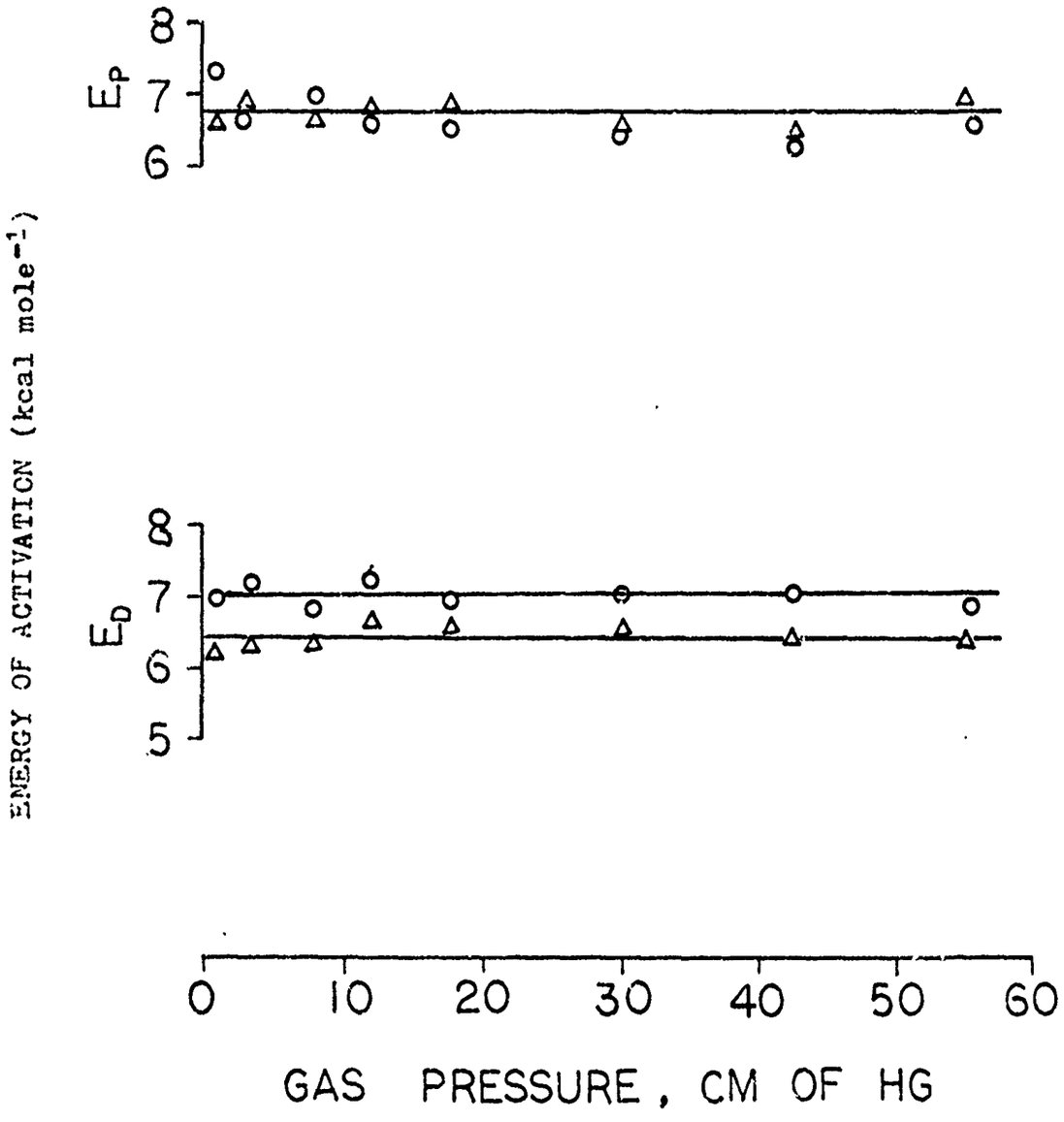

Fig. 33 - Energy of activation for permeation and for diffusion, E_p and E_d, versus gas pressure for H_2 and D_2 in filled natural rubber.

Δ denotes D_2 o denotes H_2

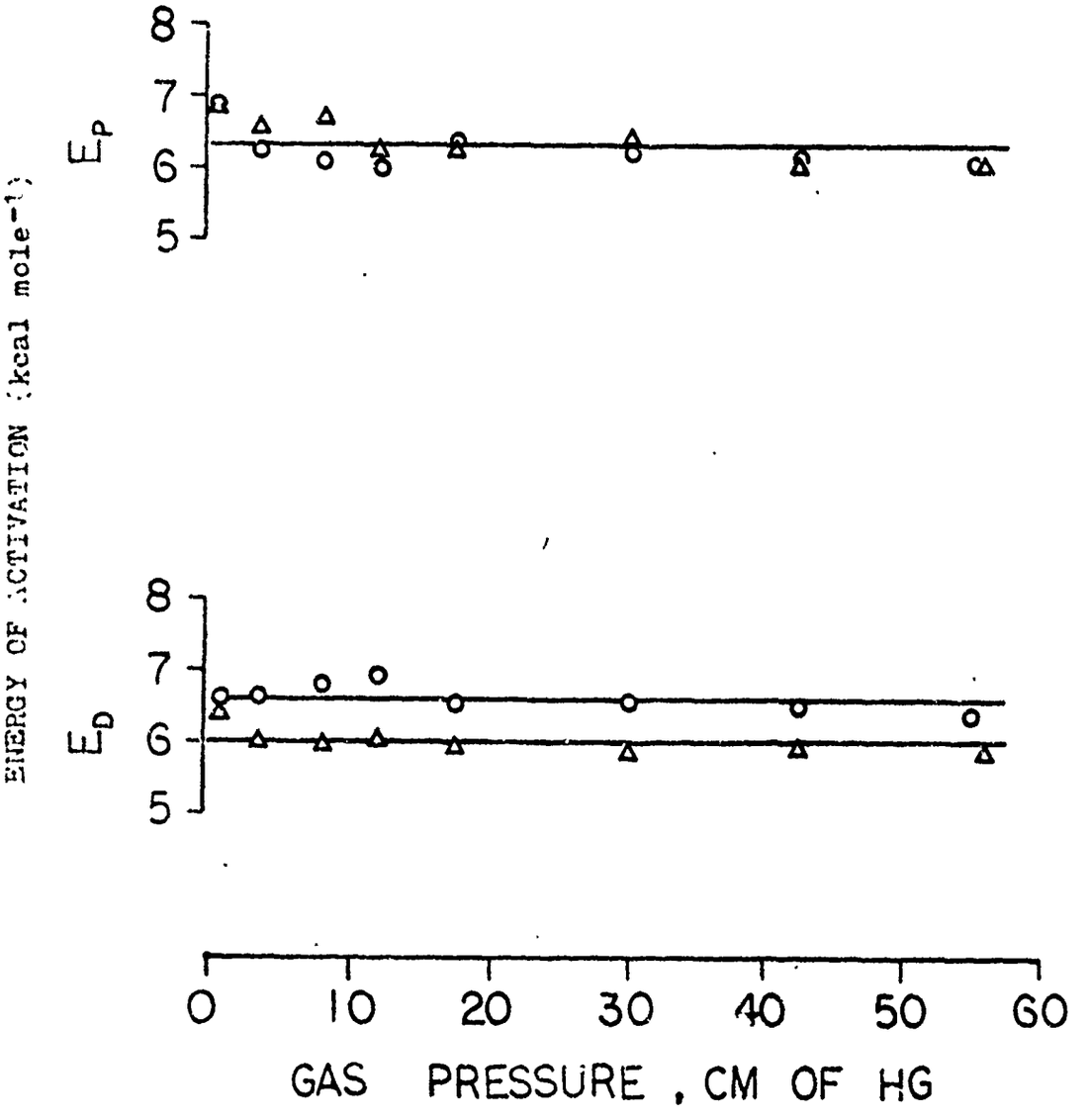

Fig. 34 - Energy of activation for permeation and for diffusion, E_p and E_d, versus gas pressure for H_2 and D_2 in filled synthetic natural rubber.

Δ denotes D_2 O denotes H_2

TABLE 16

AVERAGE ACTIVATION ENERGIES* FOR PERMEATION AND DIFFUSION, $\bar{E}_p$ AND $\bar{E}_d$, AND HEATS OF SOLUTION, ΔH_s

Gas	Unfilled NR			Filled NR		
	$\bar{E}_d$	$\bar{E}_p$	$\Delta\bar{H}_s$	$\bar{E}_d$	$\bar{E}_p$	$\Delta\bar{H}_s$
D_2	5.36	6.01	0.65	6.45	6.73	0.28
H_2	5.03	6.27	1.24	7.03	6.75	-0.28
δ	0.33		-0.59	-0.58		0.56

Gas	Unfilled SNR			Filled SNR		
	$\bar{E}_d$	$\bar{E}_p$	$\Delta\bar{H}_s$	$\bar{E}_d$	$\bar{E}_p$	$\Delta\bar{H}_s$
D_2	5.32	6.03	0.71	6.03	6.38	0.35
H_2	4.93	5.95	1.02	6.60	6.26	-0.34
δ	0.39		-0.31	-0.57		0.69

* Arithmetic mean in units of kcal/mole.

$\Delta\bar{H}_s = \bar{E}_p - \bar{E}_d$

δ is the difference of the $\bar{E}_d$'s or the $\Delta\bar{H}_s$'s for D_2 and for H_2, i.e., the difference between the numbers within these columns.

Standard deviations for $\bar{E}_d$ and $\bar{E}_p$ are listed in Appendix II on page 144.

The heat of solution (mixing or absorption), ΔH_s, in the unfilled rubber samples includes (see the discussion above on the contributions to the gas solubility, S_{rb}, in rubber) the heat of hole formation in the rubber, ΔH_h, the heat of condensation of the gases, and the heat of internal adsorption of the gas to the rubber chains, ΔH_c and ΔH_{ads}, i.e.,

$$\Delta H_s = \Delta H_h + \Delta H_c + \Delta H_{ads}$$

The last two terms in the equation are always negative, but the middle term ΔH_c is quite small in the case of these gases. The heat of mixing of gases with rubber, ΔH_s, may then be negative or possitive depending on the heat of the hole formation.

For the filled rubbers, there are two additional terms to the heat of solution, namely, the heat of adsorption on the filler and the heat of gas condensation on, or within, the filler (absorption). Therefore,

$$\Delta H_s' = \Delta H_s + \Delta H_{ads.\ on\ filler} + \Delta H_{cond.\ inside\ filler}$$

The last two terms of the equation are strongly negative.

The positive ΔH_s listed in Table 16 implies that the energy for providing the volume for the gas in the rubber is the preponderent term. The fact that the heat of solution for H_2 in filled rubbers is negative comes from the strong adsorption of H_2 on carbon ($\Delta H_{ads.\ on\ filler} \simeq -1500$ cal/mole). On the other hand, the small positive heat of solution for D_2 in the filled

rubber reflects the fact that, although D_2 is also more strongly adsorbed on the filler than on the rubber chains, the forces are not quite as strong as for H_2; in other words, the potential well for D_2 on the carbon is less deep. As a result, deuterium requires a lower activation energy to escape from the filler, and thus from the filled rubber as a whole, than H_2 does. The energy diagram is shown in Fig. 35.

In light of the amounts of energy involved, about 1500 cal/mole both penetrants are physically adsorbed on rubber and filler. For physical adsorption usually only a few hundred to a few thousand calories per mole are involved, due to the operation of van der Waals' forces. Chemi-sorption would reveal itself by much stronger binding forces.

C. Free Volume of Unfilled Rubber

Using Frisch's model, as described in Section I page 22, the average dimension of the unit free volume or free volume increment, V_f, in the rubber can be estimated by the following equation,

$$V_f^{1/3} = \frac{18.8}{(-\delta \Delta H_s)^{\frac{1}{2}}} + \sigma$$

Here, $\delta \Delta H_s$, is the difference of the heat of solution for D_2 and H_2 gas in the same medium, i.e., $\delta\Delta H_s = (\Delta H_s)_{D_2} - (\Delta H_s)_{H_2}$, and, σ is the molecular diameter of the isotopic species. The quantum mechanically corrected Lennard-Jones potential diameter of hydrogen (also for deuterium) is 2.93 A^{o}[15].

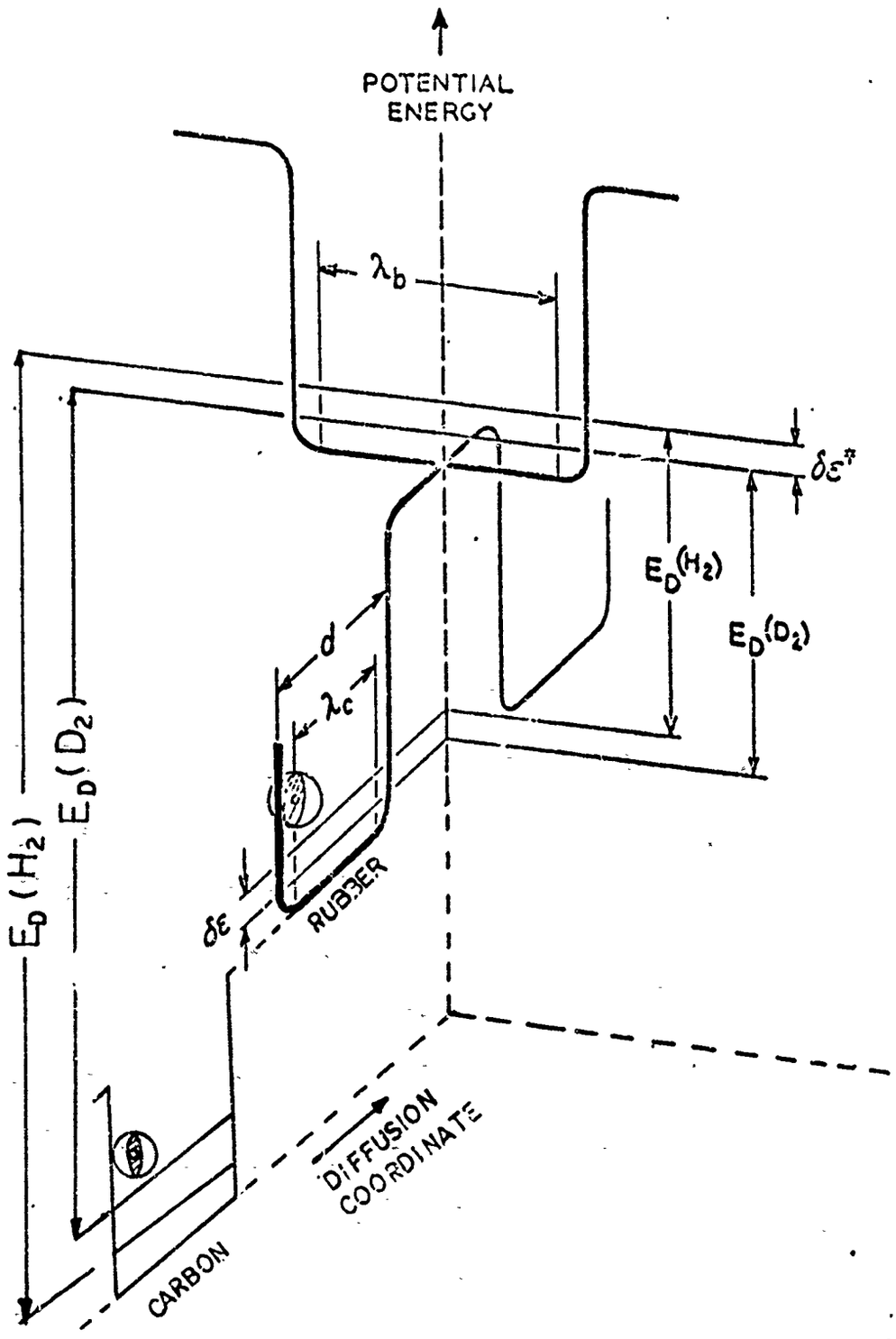

Fig. 35 - Potential energy diagram for gas on rubber or on Carbon Black

Using the average value of ΔH_s listed in Table 16, one finds that the average unit free volumes for the unfilled natural and synthetic rubber are about 51 and 64 $Å^3$ respectively (see Table 17).

TABLE 17

AVERAGE UNIT FREE VOLUME OF UNFILLED NR AND SNR

Sample	$(\Delta H_s)_{D_2}$ (cal/mole)	$(\Delta H_s)_{H_2}$ (cal/mole)	$\delta\Delta H_s$ (cal/mole)	$V_f^{1/3}$ (Å)	V_f^3 ($Å^3$)
NR	650.0	1,240	-590.0	3.7	50.9
SNR	710.0	1,020	-310.0	4.0	63.9

Thus, the average unit free volume in NR is about 20% smaller than the free volume in the SNR, which explains the higher permeation rate in SNR for the penetrants. The molecular basis for this is the absence of crystallinity of SNR which lacks the crystalline nuclei of the natural rubber latex particles, i.e., SNR is truly amorphous, but NR can be considered as lightly filled by its own crystallites.

If one attempts to calculate the free volumes of the filled rubbers from the apparent values of ΔH_s, this is found to be impossible. The reason is that Frisch's theory does not apply to this case in that the theory requires $\delta\Delta H_s$ to be negative in order to get a positive root to satisfy

the equation for $V_f^{1/3}$. We see (Table 16) that for the filled rubber $\delta\Delta H_s$ becomes positive which in a literal interpretation would signify that H_2 is bonded more strongly to the rubber than D_2, a physical unreality. This dilemma can be resolved by assuming that the adsorption of H_2 onto the carbon, where π-complex bonds can be formed, is much stronger than that of D_2. If, one assumes further that the reversal in the heats of adsorption is entirely due to the presence of carbon and that the solubilities for H_2 and D_2 remain the same in the matrix of the filled as in the pure rubber, then the heats of solution in rubber and thus the incremental free volumes would be the same for the filled and unfilled samples. The intriguing point remains that, if the polarizability difference between H_2 and D_2 played a part in the adsorption on carbon, and if this were true for the heats of adsorption on the rubber, then the heats of solutions would be affected not only by the isotope effect but also by binding specificities; thus the outcome of the free volume calculations could be changed. Of course, the resulting error should be very small.

D. Jump Distance of Gas in Rubber

The jump distance of the gas in the rubber can be calculated by Eyring's equation (combined from equation (33) and the Arrhenius equation),

$$\lambda = \left[\left(2\pi m/kT \right)^{\frac{1}{2}} D_o V_f^{1/3} \right]^{\frac{1}{2}}$$

Using the average values of D_o and $V_f^{1/3}$ listed in Tables 2, 5, and 17, the culculated jump distances, λ, for the two gases in the unfilled rubber are shown in Table 18,

TABLE 18

JUMP DISTANCES FOR HYDROGEN AND DEUTERIUM GAS IN UNFILLED RUBBERS AT 40°C

Rubber	Gas	$\bar{D}_o \times 10^2$ (cm^2/sec)	$\bar{V}_f^{1/3}$ (Å)	λ (Å)
NR	H_2	5.49	3.7	21.1
	D_2	6.00	3.7	26.2
SNR	H_2	4.95	4.0	20.8
	D_2	7.74	4.0	30.9

The jump distances should be larger for D_2 because of its greater mass. This trend is further reinforced by the basic diffusion constant, D_o, which is also larger for D_2. As a result, the jump distances of D_2 are about 40 to 50% higher than those of H_2. On the other hand, we have seen in Table 14 that the difference in diffusivities for the two gases in SNR is surprisingly small. This cannot be explained by the larger λ values of D_2, so that there must be also other factors. For example, the tortuosity of NR due to its crystallites which are absent in SNR may affect the diffusivities

of gases of different mass differently. Further, if D_2 were markedly less adsorbed within the non-crystallized SNR than it is in NR, while the adsorption of H_2 in the two rubbers is less affected, the lack of difference in diffusivity would become more understandable.

E. Conclusion

Referring to the Introduction, this investigation intended to find, by way of permeation studies, details of structural difference between NR and SNR and differences resulting from filling with carbon black. In particular, the study aimed at testing and applying Frisch's theory and at obtaining further information on the unit size of the free volume in rubbers.

The results show that the permeabilities are greater and the diffusion is faster in SNR which also has the greater solubility for H_2 and D_2. This agrees with the notion[57] that SNR is more amorphous than NR.

The measurements of D and P of H_2 and D_2 permitted then to calculate the free volumes and jump distances. The results are physically acceptable and in line with the data of Frisch and Rogers[1], and Ziegel and Eirich[40]. Though the differences are small, SNR shows the larger values for the free volume and jump distances. Since the trends and consistency of the data support their statistical significance (see Ziegel), the findings here amount again to a confirmation of Frisch's theory.

The results obtained on the filled samples permit interesting conclusion when the values of P, D and S are further analyzed. One finds that one can relate the data to those of the unfilled samples if one takes the following factors into account: the blockage of part of the cross section by the filler, the imposed tortuosity of the diffusion path, and the increase in viscosity of the rubber due to the presence of the filler particles. Introducing the corresponding corrections brought reasonable agreement between experimental results on filled and unfilled samples even though the corrections applied can not be tested because suitable theories have not yet been developed.

The solubilities for H_2 and D_2 were found to be low in both rubbers and the same is true for the adsorption on the carbon. Thus, the later is probably completely wetted by the rubber. As a consequence, the diffusion of H_2 through filled rubber is not likely to be modified by the adsorption of H_2 on the carbon.

Even so, gas adsorption on the carbon is about equal to the absorption in the rubber. Therefore, the heats of solution are more negative in the filled rubbers. Interestingly, ΔH_s for H_2 is much more negative than that for D_2 so that the difference in overall heat of solution between H_2 and D_2 in unfilled rubber is not only wiped out, but also becomes positive for the filled rubbers. Consequently, the free volume increments could not be determined in the filled samples, but it is reasonable to assume that the free volume

is lowered in the filled rubber since the diffusion process is impeded beyond reasonable assumptions about a diminished cross section and increased tortuosity.

Comparison of the heats of solution between the filled and unfilled rubbers, and of the heats of adsorption on the carbon derived therefrom, permits to estimate the heat of adsorption on the rubber. Substracting these two adsorption heats from the overall heat of solution allows to estimate the enthalpies and entropies of hole formation to accomodate H_2 gas. This energy corresponds to that of separating rubber molecules during a swelling process where H_2 is the "solvent". It is then peculiar that, although at our pressure only about one H_2 molecule dissolves per several thousands cavities (which explains the concentration independent of the diffusion), the heat of solution is positive so that a volume expansion must take place in the rubber. This could be explained by assuming that the existing cavities are too small to accomodate the gas molecules, which is unlikely in view of the magnitude of $V_f^{1/3}$. It is more likely that the intrusion of H_2 creates some changes in the molecular conformations which are akin to melting.

Inasmuch as filled rubber has a heterogeneous or composite structure, it is evident that the method applied here could also be used more generally for studies of composite materials.

V. BIBLIOGRAPHY

1. Frisch, H. L. and Rogers, C. E., J. Chem. Phys., 40, 2293 (1964).

2. Daynes, H., Proc. R. Soc. 97A, 286 (1920).

3. Barrer, R. M., "Diffusion in and through Solids" Cambridge University, London (1941).

4. Frisch, H. L., J. Phys. Chem. 61, 93 (1957).

5. Rogers, W. A., Buritz, R. S., and Alpert, D., J. Appl. Phys. 25, 868 (1954).

6. Meares, P., J. Appl. Polym. Sci., 9, 917 (1965).

7. Garret, T. A., and Park, G. S., J. Polym. Sci., C., 16, 601 (1966).

8. Crank, J. "Mathematics of Diffusion", PP. 87, 66, O.U.P., Oxford, 1956.

9. Prager, S., and Long, F. A., J. Amer. Chem. Soc., 73, 4072 (1951).

10. DiBenedetto, A. T., and Paul, D. R., J. Polyme. Sci., A2, 1001 (1964).

11. Frenkel, J., "Kinetic Theory of Liquids", Oxford University Press, Oxford, 1946.

12. Bueche, F., "Physical Properties of Polymers", Interscience Publishers, New York, 1962.

13. Glasstone, S., Laidler, K. J., and Eyring, H., "The Theory of Rate Processes", McGraw-Hill Book Co., Inc., New York, 1941.

14. Stern, A. E., Irish, E. M. and Eyring, H., J. Phys. Chem., 44, 981 (1940).

15. Davis, J. C. "Advanced Physical Chemistry", The Ronald Press Co., New York, 1965.

16. Hirschfelder, J. O., Curtiss, C. F., and Bird, R. B., "Molecular Theory of Gases and Liquids" John Wiley & Sons, Inc., New York, 1954.

17. van Amerongen, G. J., J. Appl. Phys., 17, 972 (1946).

18. Kumins, C. A., and Roteman, J., J. Polym. Sci., 55, 683 (1961).

19. van Amerongen, G. J., Rubber Chem. Technol., 24, 109 (1951).

20. Frensdor, H. K., J. Polym. Sci., Part A., 2, 341 (1964).

21. Auerback, L., Miller, W. R., Kuryla, W. C., and Gehman, S. D., J. Polym. Sci., 28, 129 (1958).

22. Barrer, R. M. and Skirrow, G., J. Polym. Sci., 3, 549, 564 (1948).

23. Michaels, A. S., and Parker, R. B., J. Polym. Sci., 41, 53 (1959).

24. Meares, P., J. Am. Chem. Soc., 76, 3415 (1954).

25. Stannett, V., and Williams, J. L., J. Polym. Sci., c10, 45 (1966).

26. Deeg, G., and Frosh, G. J., Mod. Plas. 22, 155 (1944).

27. Doty, P. M., Aiken, W. H., and Mark, H., Ind. Engng Chem. Analyt. Edn., 6, 686 (1944).

28. Doty, P. M., J. Chem. Phys., 14, 244 (1946).

29. Kumins, C. A., Roole, C. J., and Rotemen, J. J. Phys. Chem. Wash., 61, 1290 (1957).

30. van Amerongen, G. J., Rubb. Chem. Technol., 28, 821 (1955).

31. van Amerongen, G. J., Rubb. Chem. Technol. 37, 1067 (1964).

32. Barrer, R. M., Trans. Faraday Soc., 35, 628 (1939).

33. Flory, P. J., "Principles of Polymer Chemistry", Cornell University Press, New York, 1953.

34. Miller, M. L., "The Structure of Polymers", Reinhold Publishing Co., 1966.

35. Flory, P. J., and Rehner, J., J. Chem. Phys., 11, 521 (1943).

36. Flory, P. J., J. Chem. Phys., 18, 108 (1950).

37. Huggins, M. L., J. Chem. Phys., 9, 440 (1941).

38. Meissner, G., Klier, I., and Kucharick, S., J. Polym. Sci., c, No. 16, 793 (1967).

39. Grove, R., Thesis (M. S., Chem.), Polytechnic Institute of Brooklyn (1966).

40. Ziegel, K. D., Dissertation (Ph.D. Chem.), Polytechnic Institute of Brooklyn (1966).

41. Meares, P., "Polymers: Structure and Bulk Properties" Chap. 12, van Nostrand, 1965.

42. Carpenter, A. S., and Twiss, D. F., Ind. Eng. Chem. Anal. Ed. 12, 99 (1940); Rubber Chem. Technol. 13, 326 (1940).

43. Barrer, R. M., Barrie, J. A., and Rogers, M. G., J. Polym. Sci. A, 1, 2665 (1963).

44. Mooney, M., J. Colloid Sci., 6, 162 (1951).

45. Guth, E., and Gold, O., Phys. Rev. 53, 322 (1938).

46. Smallwood, H., J. Appl. Phys., 15, 758 (1944).

47. Kerner, E. H., Proc. Phys. Soc., London, 69B, 808 (1956).

48. Tobolsky, A. V., "Properties and Structure of Polymers" P. 65, John and Wiley, 1960.

49. Carman, P. C., Trans. J. Soc. Chem. Ind., 57 225 (1938)

50. Meares, P.,"Polymers: Structure and Bulk Properties" van Nostrand (1965), P. 340.

51. Sobolev, E., Meyer, J. A., Stannet, V., and Szwarc, M., Ind. Eng. Chem., 49, 441 (1957).

52. Lasoski, S. W. and Cobbs, W. H., J. Polymer Sci., 36 21 (1959).

53. Klute, C. H., J. Appl. Polym. Sci., 1, 340 (1959); J. Polym. Sci., 41, 307 (1959).

54. Carman, P. C., "Flow of Gases Through Media", Butterworths, London (1956), P. 45.

55. Jeschke, C. H., J. Appl. Polym. Sci., 1, 340 (1959); J. Polym. Sci., 41, 307 (1959).

56. Brandt, W. W., J. Polym. Sci., 41, 415 (1959).

57. Glaser, Z. R., and Eirich, F. R., "Thermo-mechanics and Structure of Elastomers", Polytechnic Institute of Brooklyn, 1969.

58. Vieth et. al., G. Colloid Sci., 20, 9 (65); 22, 454 (66)

APPENDIX I

SAMPLE CALCULATION OF PERMEABILITY, P, DIFFUSIVITY D, AND SOLUBILITY, S

The application of equations (42) and (43) to calculate P and D is illustrated in the following example. Let us examine the Q_t versus t plot as shown in Fig. 12 for the permeation of D_2 gas at 70°C through unfilled natural rubber of thickness 0.2101 cm under a gas pressure of 17.60 cm of Hg. The slope of the linear portion of the plot is

$$b = 3.2786 \text{ micron/min.}$$

and the value of the intercept, "a", is calculated from the slope, b, and a value of t_k with its corresponding value of pressure p_k as indicated in the figure. Therefore,

$$a = p_k - bt_k = 60 - 3.2786 \times 23.4$$

$$= 60 - 76.72$$

$$= -16.72$$

Substituting this value together with

P_o = 0.02 micron (initially measured residual pressure)

L = 0.2101 cm

into equation (42), one obtains,

$$D = \frac{L^2 \times b}{360\ (P_o - a)} = \frac{(0.2101)^2 \times 3.2786}{360[0.02 - (-16.72)]}$$

$$= 2.40 \times 10^{-5}\ cm^2/sec.$$

The slope b in Fig. 12 also represents the steady state flux Q_s in units of micron per minute. Assuming ideal gas behaviour, the number of moles of gas transported per second is

$$Q_s = \frac{b \times 10^{-4}}{76 \times 60} \times \frac{V_1}{RT}\ \text{moles/sec}$$

where T is the temperature of the gas collector. Q_s is customarily expressed in units of standard cc of gas defined as cc of gas at 25°C and one atmosphere pressure. Therefore,

$$Q_s = \frac{b \times 10^{-4}}{76 \times 60} \times \frac{V_1 \times 298}{T}$$

$$= \frac{b \times 10^{-4} \times 298 \times V_1}{76 \times 60 \times T}\ \text{Std. cc/sec}$$

Substituting this value of Q_s into equation (43), one obtains the permeability,

$$P = \frac{L}{(\Delta p/76) \times A} \times \frac{b \times 10^{-4} \times V_1}{76 \times 60} \times \frac{298}{T}$$

$$= 8.51 \times 10^{-7}\ \text{Std. cc gas sec}^{-1}\text{cm}^{-1}\text{atm}^{-1}$$

where $\Delta p = 17.6$ cm Hg

$L = 0.2101$ cm

$b = 3.2786$ micron/min

$V_1 = 37.9$ cc

$A = 2.85$ cm^2

$T = 298^{\circ}K$ (when the collector is at the room temperature)

Finally, according to equation (11), the solubility,

$$S = P/D = 3.55 \text{ cc gas cm}^{-3} \text{ atm}^{-1}$$

APPENDIX II

A. SAMPLE CALCULATION OF ENERGIES OF ACTIVATION FOR PERMEATION AND DIFFUSION(E_p and E_d), AND HEAT OF SOLUTION(ΔH_s) BY THE LEAST SQUARE METHOD

B. STANDARD DEVIATION FOR $\overline{E}_d$ AND $\overline{E}_p$

A. The logarithmic form of Arrhenius equation for diffusion and for permeation is as the follows (quoted from P. 53)

$$\log D = \log D_o - \frac{E_d}{2.303\ R}\ \frac{1}{T}$$

and

$$\log P = \log P_o - \frac{E_d}{2.303\ R}\ \frac{1}{T}$$

Both above equations can be simply represented by a straight line equation as

$$y = a + bx \qquad (46)$$

where $y = \log D$ or $\log P$

$a = \log D_o$ or $\log P_o$

$b = E_d/2.303\ R$ or $E_p/2.303\ R$

$x = 1/T$

For a set of experimental data, the deviation of each datum point from a best straight line, ϵ_i, can be expressed by

$$\epsilon_i = y_i - a - bx_i$$

Summation of the square of each deviation, obtains

$$\epsilon^2 = \sum_{i=1}^{n} \epsilon_i^{\,2} = \sum_{i=1}^{n} (y_i - a - bx_i)^2$$

$$= (y_1 - a - bx_1)^2 + (y_2 - a - bx_2)^2 + \cdots\cdots$$

$$= (y_1^2 + y_2^2 + \cdots) + b^2(x_1^2 + x_2^2 + \cdots)$$

$$- 2a\,(y_1 + y_2 + \cdots) - 2b\,(x_1y_1 + x_2y_2 + \cdots)$$

$$+ 2ab\,(x_1 + x_2 + \cdots) + na^2$$

minimize ϵ^2 with respect to "a" and "b" respectively, giving

$$\frac{\partial \epsilon^2}{\partial a} = -2\,(y_1 + y_1 + \cdots) + 2b\,(x_1 + x_2 + \cdots) + 2na = 0$$

or
$$na = b\,\Sigma x_i = \Sigma y_i \qquad (47)$$

$$\frac{\partial \epsilon^2}{\partial b} = 2b\,(x_1^2 + x_2^2 + \cdots) - 2\,(x_1y_1 + x_2y_2 + \cdots)$$

$$+ 2a\,(x_1 + x_2 + \cdots) = 0$$

or
$$a\sum_{i=1}^{n} x_i + b\sum_{i=1}^{n} x_i^2 = \sum_{i=1}^{n} x_iy_i \qquad (48)$$

Solving for "a" and "b" from above two equations, results

$$a = \frac{\bar{y}\sum_{i=1}^{n} x_i^2 - \bar{x}\sum_{i=1}^{n} x_iy_i}{\sum_{i=1}^{n} x_i^2 - \bar{x}\sum_{i=1}^{n} x_i} \qquad (49)$$

$$b = \frac{\sum_{i=1}^{n} x_i y_i - \bar{y}\sum_{i=1}^{n} x_i}{\sum_{i=1}^{n} x_i^2 - \bar{x}\sum_{i=1}^{n} x_i} \qquad (50)$$

where $\bar{x} = \sum_{i=1}^{n} x_i / n$ and $\bar{y} = \sum_{i=1}^{n} y_i / n$

and hence, the slope, "b", and the intercept, "a" of the straight line can be separately calculated by equations (49) and (50) for a set of data. Further according to equation (46), values of D_o, E_d and E_p are readily calculated for each gas pressure.

To illustrate this, the permeation data of Table 2 on P. 55 for H_2 gas transport through the unfilled natural rubber at gas pressure of 1.1 cm Hg are quoted to calculate E_d, D_o and E_p as the following:

Temp. (^oC)	D x 10^5 (cm^2/sec)	$x_i = 1/T$	y_i = log D
40	1.49	3.2×10^{-3}	-4.8269
55	2.54	3.05×10^{-3}	-4.5960
70	3.18	2.92×10^{-3}	-4.4981
85	4.43	2.79×10^{-3}	-4.3537

Applying equations (49), (50) and (46), one obtains,

$$a = \log D_o = -1.148$$

or $$D_o = 7.1 \times 10^{-2} \quad cm^2/sec$$

$$b = -1.145 \times 10^3$$

and $$E_d = 5.24 \text{ kcal/mole}$$

Similar calculation for energy of activation for permeation E_p arrives at

$$E_p = 6.34 \text{ kcal/mole}$$

Finally, the heat of solution, ΔH_s is

$$\Delta H_s = E_p - E_d = 1.10 \text{ kcal/mole}$$

B. STANDARD DEVIATIONS FOR $\bar{E}_d$ AND $\bar{E}_p$

$$S = \left(\frac{\sum_{i=1}^{n} (\bar{x} - x_i)^2}{n-1} \right)^{\frac{1}{2}}$$

	Unfilled NR		Filled NR	
	$\bar{E}_d$	$\bar{E}_p$	$\bar{E}_d$	$\bar{E}_p$
D_2	5.36 ± 0.21	6.01 ± 0.19	6.45 ± 0.17	6.73 ± 0.20
H_2	5.03 ± 0.17	6.27 ± 0.06	7.03 ± 0.15	6.75 ± 0.28

	Unfilled SNR		Filled SNR	
	$\bar{E}_d$	$\bar{E}_p$	$\bar{E}_d$	$\bar{E}_p$
D_2	5.32 ± 0.22	6.03 ± 0.20	6.03 ± 0.19	6.38 ± 0.30
H_2	4.93 ± 0.10	5.95 ± 0.13	6.60 ± 0.16	6.26 ± 0.26

Security Classification

DOCUMENT CONTROL DATA - R & D

Security classification of title, body of abstract and indexing annotation must be entered when the overall report is classified)

1. ORIGINATING ACTIVITY (Corporate author) Polytechnic Institute of Brooklyn	2a. REPORT SECURITY CLASSIFICATION Unclassified 2b. GROUP

3. REPORT TITLE

Permeability of Gases Through Filled and Unfilled Rubber Membranes

4. DESCRIPTIVE NOTES (Type of report and inclusive dates)

Research Report

5. AUTHOR(S) (First name, middle initial, last name)

G. Y. Lei and F. R. Eirich

6. REPORT DATE October 1970	7a. TOTAL NO. OF PAGES 167	7b. NO. OF REFS 58
8a. CONTRACT OR GRANT NO N00014-67-A-0438-0100 b. PROJECT NO. NR-064-457 c. d.	9a. ORIGINATOR'S REPORT NUMBER(S) Pibal Report No. 70-44 9b. OTHER REPORT NO(S) (Any other numbers that may be assigned this report)	

10. DISTRIBUTION STATEMENT

ONR and DDC

Distribution of this document is unlimited

11. SUPPLEMENTARY NOTES	12. SPONSORING MILITARY ACTIVITY Office of Naval Research Washington, D. C.

13. ABSTRACT

This is a study, by way of gas permeation experiments, of the structural differences between synthetic poly-cis 1,4-isoprene (SNR) and natural rubber (NR), and the differences arising from filling these rubbers with carbon black.

The permeation rates of H_2 and D_2 through filled and unfilled NR and SNR, measured by the time-lag method as a function of temperature and pressure, yield the permeability coefficient, P, diffusion coefficient, D, and the solubility, S. From these the energies of activation for permeation and for diffusion and the heats of solution were calculated. H_2 is found to have the larger permeability and diffusivity, the permeabilities or diffusivities which are largely independent of the gas pressure are markedly reduced by the filler, and the solubilities in the filled rubbers are almost double that of the unfilled samples. The heats of solution, ΔH_s, are positive for both gases in the unfilled samples, but in the filled samples ΔH_s is positive for D_2, and negative for H_2. These signs of ΔH_s are consistent with their solubilities.

Utilizing H. Frisch's theory of isotope effects in activated diffusion, the unit free volume in the unfilled rubbers calculated from $\delta\Delta H_s$ was found to be 51 and 64 Å for NR and SNR. The free volumes of the filled samples could not be calculated, since ΔH_s was positive in these cases. All data differences between the filled and unfilled samples can be qualitatively accounted for by a reduction of the diffusive cross section of the imposed tortuosity of the diffusion path, and by the increase in the viscosity of the rubber due to the filler.

DD FORM NOV 1473

Unclassified
Security Classification

Security Classification

14 KEY WORDS	LINK A		LINK B		LINK C	
	ROLE	WT	ROLE	WT	ROLE	WT
carbon black filler						
deuterium permeation						
diffusion activation energies						
diffusivity of gases						
gas permeation						
heats of solution of H_2 and D_2 in rubbers						
hydrogen permeation						
natural rubber						
rubber free volume						
rubber membranes						
synthetic natural rubber						
time-lag method of permeation						

unclassified
Security Classification